ELECTRO-OPTICAL STUDIES ON METAL PHTHALOCYANINES

Thesis submitted to
the Cochin University of Science and Technology
in partial fulfilment of the requirements
for the degree of
DOCTOR OF PHILOSOPHY

by

NARAYANAN P.

DEPARTMENT OF APPLIED CHEMISTRY
COCHIN UNIVERSITY OF SCIENCE AND TECHNOLOGY
COCHIN - 682 022

SEPTEMBER 1992

DECLARATION

I hereby declare that the work presented in this thesis is based on the original work done by me under the guidance of Dr.V.N.Sivasankara Pillai, Professor, Department of Applied Chemistry, Cochin University of Science and Technology and no part of the thesis is included in any other thesis submitted previously for the award of any degree.

Cochin - 682 022
23rd Sept., 1992

NARAYANAN, P.

CERTIFICATE

Certified that the work presented in this thesis is based on the original work done by Mr.Narayanan, P under my guidance in the Department of Applied Chemistry, Cochin University of Science and Technology and no part of the thesis is included in any other thesis submitted previously for the award of any degree.

Dr.V.N.Sivasankara Pillai
Professor
Dept.of Applied Chemistry
Cochin University of Science
and Technology

Cochin - 682 022
23rd Sept., 1992

ACKNOWLEDGEMENT

With great pleasure, I express my gratitude and obligation to Dr.V.N.Sivasankara Pillai, Professor, Department of Applied Chemistry for his kind guidance and constant encouragement throughout the period of this research.

The help rendered by Prof.(Dr.)P.Madhavan Pillai, Head of the Department of Applied Chemistry, is gratefully acknowledged. I sincerely thank Prof.(Dr.)Paul A.Vatakencherry and Prof.(Dr.)K.L.Sebastian, the former Heads of the Department for their encouragement. The whole hearted support extended by the faculty members of the department is also gratefully acknowledged. I take this opportunity to thank the administrative and technical staff of the Department of Applied Chemistry and the staff of the University Science Instrumentation Centre for their timely help and co-operation.

I sincerely appreciate all the assistance given to me by my colleagues--Dr.P.S.Harikumar, Mr.K.C.Philip, Mr.Jayan Thomas, Ms.K.Usha and Ms.C.R.Seena. I thank all the Research Scholars of the department for the invaluable help given to me during my work.

I am thankful to Shri K.R.Prasad, Senior General Manager, IRE Ltd., Udyogamandal, Shri T.K.S.Murthy, Shri V.M.Karve, Shri A.S.K.Menon, Shri T.V.Swaminathan and to Dr.V.R.Nair for providing me the necessary facilities and for their encouragement. I also extend my thanks to all the members of R.E.Division, IRE Ltd., Udyogamandal for their encouragement.

I take this opportunity to thank Dr.N.C.Santhakumari, Professor, N.S.S.College, Changanacherry for her valuable encouragement.

The financial assistance received from STEC, Kerala in the form of fellowship in the initial phase of this work is gratefully acknowledged. I thank RSIC, IIT Madras and School of Chemical Sciences, Mahatma Gandhi University, Kottayam for recording some of the spectra.

I would like to extend my gratitude to Mrs.P.A.Bharathy and Mr.K.P.Sibiraj for the neat typing of this thesis.

Finally, I am very much indebted to my beloved parents, brothers and sisters for their affection, patience, interest and encouragement.

NARAYANAN, P.

PREFACE

The metal derivatives of tetrabenzo(b,g,l,q)-5,10,15,20-tetraazaporphyrins, usually referred to as phthalocyanines (MPcs) constitute a class of compounds unique in many respects. Apart from their structural similarity with biologically significant compounds like chlorophyll and haemoglobin, they have unusual chemical, thermal, electrical and optical properties. They already find use as active elements in sensors, electrochromic and liquid crystal displays, optical memory recording media, and as photodynamic therapeutic agents.

The major disadvantage restricting their bulk application is the lack of processability due to limited solubility in common solvents. Structural modification of the phthalocyanine macrocycle with appropriate substituents can partly circumvent this limitation. Incorporation of substituted MPcs into preformed matrices is usually achieved by diffusion from solution. The diffusion characteristics of MPcs doped into matrices depend on their association in solution. These characteristics, in turn, depend on the nature of the substituents.

The work presented in this thesis deals with two aspects of phthalocyanine chemistry. The first aspect concerns with the association of n-dodecanoyl and n-octadecanoyl amides of nickel, cobalt and copper phthalocyanines and the sulfonamides of cobalt phthalocyanines in solvents as probed by UV-vis spectrophotometry. The results help to draw vital conclusions regarding the bulk preparation of MPc-doped polymer thin films for applications like light shielding and optical recording.

The second aspect deals with the electrical and electrochemical characteristics of iodine-doped MPcs. Doping with iodine gives stable adducts with non-integral oxidation state on the metal phthalocyanine. The electrical conductivity and conduction mechanism in iodine-doped phthalocyanines have been investigated by AC and DC conductivity and dielectric constant. The stability and enhanced conductivity of iodine-doped MPcs make them candidate materials for cathodes in all-solid batteries. This aspect has been studied using a galvanic cell of the type,

$$Ag_{(s)}|AgI_{(s)}|M(Pc)I_{(s)}$$

It is hoped that the results presented in this thesis unveil some more aspects of the materials science of metal phthalocyanines and open up possibilities for further work on their applications.

CONTENTS

* * *

CHAPTER - I

METAL PHTHALOCYANINES - AN OVERVIEW

1.1 INTRODUCTION

Organic quasi-one-dimensional conductors have become the focus of many investigations in the search for functional materials for electronic application and solar energy conversion. Of such materials, metal phthalocyanines (MPcs) have many attractive features like thermal and chemical stability, possibility of incorporating substituents to get the desired processability, and high molar absorptivity for optical radiation. The ability of derivatives with tailored structure to form liquid crystalline phases[1] and Langmuir-Blodgett[2] films open up new avenues for their applications.

Eventhough phthalocyanines were known in the turn of this century, their commercial potential was realised only in 1930's. The extensive work of Linstead and co-workers[3] on the structure and synthesis of phthalocyanines shed new light on their uniqueness. Intense scientific excitement was aroused in the 70's and continues unabatedly due to newer revelations on the properties of this class of compounds.

Some of the unique properties of MPcs are:

(i) They are easily crystallized and sublimed resulting in materials of a purity (10^{14} to 10^{16} traps/cm^3) exceptional in organic chemistry.

(ii) They show excellent thermal and chemical stability. In air MPcs do not undergo any degradation upto 400°C and in vacuum most of these complexes do not decompose below 900°C.[4] Strong non-oxidising acids (eg., conc. H_2SO_4), or strong bases do not attack them. Only strong oxidizing agents like chromic acid and conc. HNO_3 degrade them.[4]

(iii) They show remarkable optical properties. The conjugated π system containing 18 electrons in the macrocyclic ring, leads to very intense absorption bands at 400-700 nm with a molar absorptivity of the order of $2x10^5$ l mol^{-1} cm^{-1} in solution.

(iv) They provide an astonishingly versatile chemical system. Elements from group I_A to V_B can combine with phthalocyanine and more than 70 different MPcs are known. The nature of the sequestered metal ion has a profound influence on the physico-chemical properties of MPc. The redox behaviour of the

macrocyclic ring or the nature of its photochemically excited state may be altered drastically by changing the central metal atom.

(v) By varying substituents on the ring the range of properties of the MPcs can be expanded further. An infinite number of structural variations is possible with MPcs as the theme.

1.2 STRUCTURE OF PHTHALOCYANINES

The molecular structure of a metal phthalocyanine can be represented as in Fig.1.1.

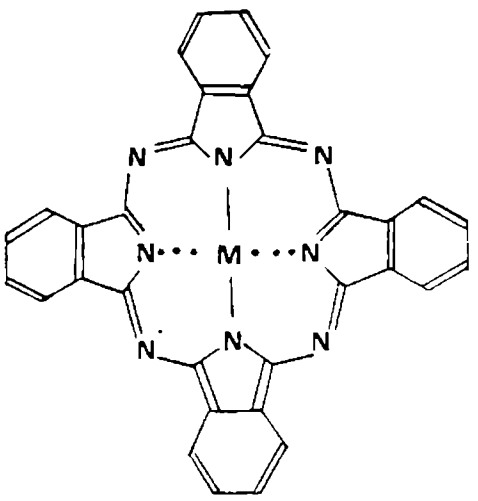

Fig.1.1: Molecular structure of metal phthalocyanine (MPc)

The unique molecular structure stems from conjugation of π electrons over the entire inner 16-membered cycle known as macroring. The planar configuration of the macroring, the possibility of substitution of the H atoms in the pyrrole rings (positions 1-8) and the C-H bridges, so called meso positions (α-δ), distribution of the electronic substitution effects throughout the molecule, and finally, the presence of proton-donor imino groups in the centre of the macroring contribute to the uniqueness of the properties of phthalocyanines.

The H atoms of the porphyrin imino groups when substituted by metals give rise to additional donor-acceptor properties. This determines the biological activity of many of them. The metal atom that has entered into coordination with porphyrin changes the properties of all atomic groups in the porphyrin molecule.

This effect is most pronounced on the electronic energy levels of the molecules and manifests itself in the electronic spectrum. The substitution of aza bridges (-N=) for four methine bridges (-CH=) in the porphyrin macroring, whereby a tetra azaporphyrin or porphyrazine macroring (phthalocyanine) is formed, results not only in entirely

different electronic spectrum but also in more pronounced aromaticity.

Phthalocyanines have four pyrrole units in the macrocycle and are structurally similar to porphyrins. The compounds usually referred to under the phthalocyanine class consist of metal derivatives of phthalocyanine. In metal phthalocyanines, the metal atom supplies one electron each to the nitrogen atoms of the isoindole groups and these isoindole nitrogen atoms in turn supply an electron to the metal atom, forming a covalent bond. A metal phthalocyanine molecule, therefore, contains four six-membered chelate rings. The unusual stability of these metal complexes can be explained on the basis of the coordination of the central metal atom.

1.3 SYNTHESIS OF PHTHALOCYANINES

1.3.1 General Methods

The methods of synthesis originally described by **Linstead**[3] are still the most widely used ones for preparing **metal phthalocyanines.** A specific feature of the synthesis **of phthalocyanine** complexes is that they are seldom **obtained from an** available phthalocyanine ligand. More often the complex is formed from molecular fragments of

phthalocyanine, namely phthalonitrile, phthalimide, phthalic anhydride, diimino isoindoline and other derivatives of o-phthalic acid in presence of a metal ion source- chloride, acetate or oxide of metals, or free metals.

The methods available for the synthesis of phthalocyanines can be classified into four groups:

1. reaction of phthalonitrile with a metal or metal salt in a high boiling liquid like nitrobenzene or quinoline.

2. reaction of phthalic acid or phthalic anhydride or phthalimide with urea and a metal salt in presence of a catalyst.

3. reaction of o-cyanobenzamide with a metal, and

4. reaction of phthalocyanine or labile metal phthalocyanine with a metal salt forming a more stable phthalocyanine.

1.3.1(a) Method 1

In this procedure a mixture of phthalonitrile and metal chloride in the mole ratio 4:1 is treated at

180-190°C for two hours in quinoline or nitrobenzene. Cobalt, nickel, chromium, iron, vanadyl, chloroaluminium, lead and titanium phthalocyanines have been synthesized by this method.[5,6] The reaction may be written as,

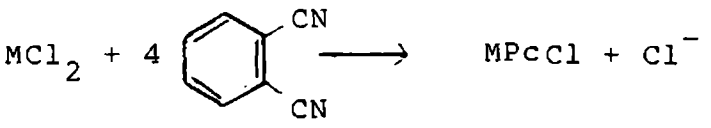

This reaction takes place in the presence of urea or quinoline. The decomposition products of urea, and quinoline act as acceptors for the halogen atoms which enter the phthalocyanine molecule to an appreciable extent when an acceptor is not present.

1.3.1(b) Method 2

A stoichiometric mixture of phthalic anhydride, urea, a metal salt and a catalyst is heated at 170-200°C for 4 h in a solvent such as nitrobenzene or chlorobenzene. Copper, cobalt, nickel, iron and tin phthalocyanines have been prepared by this procedure.

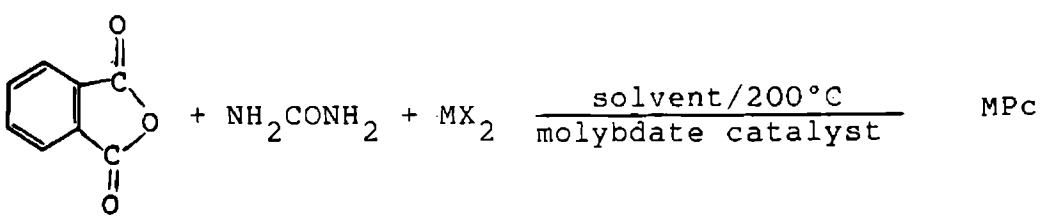

1.3.1(c) Method 3

In this procedure o-cyanobenzamide and a metal salt are heated to 250°C for 4 to 6 h. The product is freed of phthalimide by heating with concentrated sodium hydroxide. After filtration, washing and drying, the product is freed from excess metal by the floatation of the pigment in a suitable solvent or by chemical means. Iron, nickel, cobalt, magnesium and copper phthalocyanines have been prepared by this method.

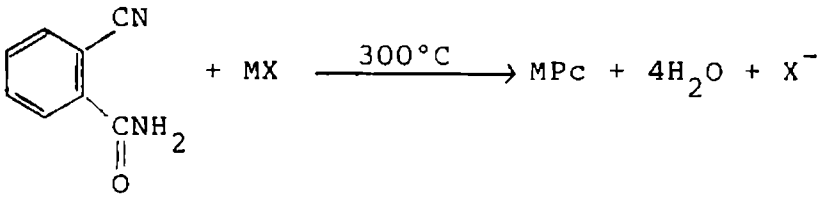

An analogous condensation route with o-cyanobenzamide has also been used to prepare MPc with metal in the higher oxidation state.

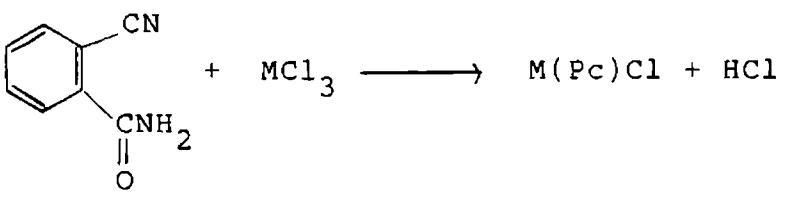

Phthalocyanines of Al(III), Si(IV), Ru(III) and Rh(III) have been synthesized by this method.

1.3.1(d) Method 4

This method involves boiling phthalocyanine and a metal in quinoline or benzophenone and is usually employed to prepare more stable metal derivatives from dilithium phthalocyanine. The dilithium complex is particularly useful because of its solubility in alcohol. Copper phthalocyanine is immediately precipitated when an alcoholic solution of dilithium phthalocyanine and anhydrous cupric chloride are mixed. Phthalocyanines of silver, mercury, calcium, zinc, lead, manganese and cobalt have been prepared by this procedure.

A number of rare-earth metal phthalocyanines have been synthesized from dilithium phthalocyanine by double decomposition in liquid Lewis-base type organic compounds such as DMF or DMSO as the reaction medium. This method is especially suited for the preparation of phthalocyanine complexes of uranium, lead, thorium, lanthanum, gadolinium, samarium, holmium, erbium, europium, thulium, lutetium, ytterbium and halfnium. These complexes are most often dimeric with the metal "sandwiched" between the two phthalocyanine rings. Lanthanide ions are normally in the +3 state, the dimer is therefore a neutral molecular

radical. The first of such dimeric metal phthalocyanine was described in 1936 by Linstead et al.[5]

1.3.2 Electrosynthesis of phthalocyanines

A procedure for the electrosynthesis of MPc has recently been reported.[7] 1,2-Dicyanobenzene is electrolysed at -1.6 V (vs. SCE) in a two compartment cell. Phthalocyanine is formed in the cathodic region. The MPc is probably formed by a mechanism involving the anion radical of 1,2-dicyanobenzene.

Phthalocyanine thin films can be prepared on substrates by electrolytic micelle disruption (EMD) method.[8]

Phthalocyanine powder is dispersed in an aqueous solution containing (11-ferrocenyl)undecyltridecaethylene glycol ether (FPEG) and LiBr. The solution is sonicated and then stirred for a couple of days with occasional sonication. The resulting solution after centrifugation is subjected to electrolysis. Such films show properties comparable with those of vacuum deposited films.

1.3.3 Synthesis of substituted phthalocyanines

Metal phthalocyanines of transition metals are insoluble in common organic solvents such as chloroform, methanol and carbon tetrachloride. The sixteen peripheral hydrogen atoms on the four benzene rings can be substituted by a variety of atoms and groups.

The solubility of MPcs in nonpolar solvents is increased by introducing peripheral substituents ($-CF_3$, $-CH_2OEt$, $-CH_2O\emptyset$) on the aromatic ring.[9] Tetra, -nitro, -chloro, -amino MPcs have been prepared from substituted phthalimides in the presence of urea and ammonium molybdate in nitrobenzene at 180-190°C.[10]

Water soluble MPcs may be obtained in the same way using 4-sulfophthalic acid.[11] Rosch et al.[12] have prepared a group of phthalocyanine sulfonic acids by the reaction of a benzene-o-dicarboxylic acid, urea and metal salt at elevated temperatures.[13]

Weber and Busch[11] have reported the synthesis of transition metal derivatives of 4,4',4",4"'-tetrasulfophthalocyanine and measured the magnetic moments of these substances in the solid state and in solution.

Hanack et al.[14] reported the synthesis of peripherally substituted metal phthalocyanines, $(C_8H_{17}OCH_2)_8PcM$ with M = Co, Ni and Pb. The macrocycle $(C_8H_{17}OCH_2)_8PcCo$ is reacted with sodium cyanide under oxidative condition to give the cyano bridged compound $[(C_8H_{19}OCH_2)_8PcCoCN]_n$. All of these substituted phthalocyanines show liquid crystalline properties with phase transition between 53° and 94°C.

1.3.4 Synthesis of bridged phthalocyanines

μ-Bridged dimeric phthalocyanines are also known. The first dimeric species of this type PcM-L-MPc was synthesized by Linstead et al.[5] a complex of the formula Pc-Al-O-AlPc with a μ-oxo-bridge linked to $PcAl^{III}$ subunits.

Numerous dimeric, trimeric and tetrameric systems have since been described. $(PcMn)_2O,2Py$,[15-17] $[PcGeO_2]_2X$,[18] $[PcAlOSiPcOAlPc]X$,[19] $[PcSiO]_3X$,[18] $[PcSiO]_4X$,[20] where X stands for various oxysilane derivatives. The μ-oxo-manganese(III) derivative is obtained by heating MnPc in pyridine in the presence of air.[15]

The silicon oligomers are obtained in a two step reaction:

$$PcSiCl_2 \xrightarrow{OH^-} PcSi(OH)_2 + 2\ Cl^-$$

$$PcSi(OH)_2 + Pc(SiOH)\ [OSi(Me)(-OSiMe_3)_2] \xrightarrow{300°C} [PcSiO]_n$$

$$n = 2\text{-}5.$$

The oligomers are soluble in most organic solvents. They are purified by column chromatography over alumina using petroleum ether-benzene mixture as eluent.[18] Polymers of empirical formula [PcSiO]X,[21] [PcGeO]X,[22-24] are synthesized by heating the dihydroxy monomer $PcM(OH)_2$ in vacuum at 300-400°C. $PcM(OH)_2$ may also be heated in nitrobenzene at 175°C in which case the degree of polymerisation is approximately 11, as compared with 100 for polymerisation under vacuum. Silicon polymers are exceptionally stable, they are unaffected by heat treatments in aqueous HF at 100°C, NaOH or conc. H_2SO_4.[25-27]

Other bridging ligands may also be used to link the phthalocyanine subunits. Examples are [PcFe ]X.[28,29] The fluro derivatives are obtained by

treating the corresponding hydroxo compound with HF. High purity polymers are obtained by vacuum sublimation (10^{-3} Torr; M = Al, 540°C; M = Ga, 430°C).

1.3.5 Synthesis of polymeric phthalocyanines

Two dimensional polymers have also been prepared. 1,2,4,5 tetracyanobenzene is the privileged starting material for this purpose. Poly phthalocyanines have been known for many years. The materials, however, were very poorly characterized. Improved methods of synthesis have been reported recently.[30] A gas phase reaction between the tetracyanobenzene and metal substrates (Cu, Ni, Co, Fe, Ti) has also been described.[31] It is claimed that such a procedure directly gives a polymeric phthalocyanine coating on the metal.

1.3.6 Synthesis of superphthalocyanines

Complexes containing more than four subunits of phthalonitrile per atom of metal have been synthesized. Such "superphthalocyanines" containing six phthalonitrile moieties have been prepared by heating phthalonitrile at 160-170°C with the corresponding metal salt (Cu^{2+} Co^{2+} Ni^{2+}).[32,33] A pentameric uranyl superphthalocyanine

complex has also been described.[34,35] The equitorial coordination of UO_2^{2+} is achieved by five nitrogen atoms. The macrocyclic ligand is severely distorted from planarity. The uranyl superphthalocyanine reacts with transition metal salts:

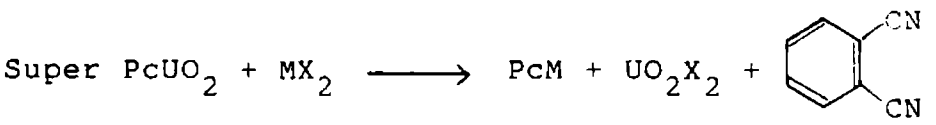

Super $PcUO_2$ shows strong absorption band in the NIR region (log ϵ = 4.82 at 914 nm) which is considerably shifted away from metal phthalocyanine (614 nm for Pc_2U).[10]

Other dicyano aromatic derivatives may be used instead of phthalonitrile. Naphthalocyanine has been synthesized from dicyanonaphthalene and iron dipivaloyl methane.[36]

1.4 PURIFICATION OF METAL PHTHALOCYANINES

Every method described for the synthesis of phthalocyanine cited in section 1.3 results in the contamination of the product with unreacted materials and by-products. The phthalocyanine formed itself is a mixture of oligomers. Common purification technique such as acid, alkali or solvent washing is used for the initial purifica-

tion of the product. This is usually followed by specialized purification techniques like vacuum sublimation and chromatography to further purify the crude phthalocyanine.

Phthalocyanines produced from phthalic acid derivatives both in melt and in solvent may contain impurities such as phthalimide, phthalonitrile, salts of metals and free phthalocyanine. To remove the impurities phthalocyanines are boiled alternatively with acid and alkali solutions.[3,37] However, treatment with acids is possible only in the case of a stable group of phthalocyanines.

In the case of labile metal phthalocyanines satisfactory purification is achieved by multiple extraction of impurities with acetone or benzene in a soxhlet apparatus. The phthalocyanine is further purified by vacuum sublimation (10^{-3} mm Hg, 300-500°C). In recent years methods of fractional and multiple sublimation of MPc have been developed, which yield excellent results in combination with reprecipitation from H_2SO_4.

Labile phthalocyanine complexes are practically impossible to obtain in a pure form. They contain a large amount of H_2Pc impurities which are not completely removed during sublimation of MPc.

The rare-earth phthalocyanines are found to be a mixture of complexes having different compositions. Neodymium, praseodymium, erbium, lutetium and lanthanum phthalocyanines give mono and diphthalocyanines. The rare-earth phthalocyanines can be purified by chromatographic techniques. Walton *et al.*[38] purified lutetium and ytterbium diphthalocyanines by chromatography over alumina using methanol as eluent.

Substituted phthalocyanines are also purified by column chromatography. Tetraoctadecylamino metal phthalocyanines were purified by column chromatography over silica gel using chloroform/methanol mixture as eluent.

To isolate polymeric phthalocyanines from a melt and to purify them, reprecipitation from their solutions in conc. H_2SO_4 is carried out. This method is applicable to complexes of both linear and crosslinked structure with a low degree of polymerisation. Certain complexes of linear

phthalocyanine polymers become soluble in DMF, they can be purified by fractional precipitation with chloroform or water.

1.5 PHYSICO-CHEMICAL CHARACTERISTICS OF PHTHALOCYANINES

1.5.1 Structure and morphology

The structure of most of the MPcs has been determined from X-ray diffraction data.[39-41] Three polymorphic forms are known. They are designated as α, β and X. Large size mono crystals are, in most cases of the β-type. They are generally grown by sublimation under vacuum in a stream of nitrogen (7 Torr) at a temperature of 400-500°C.

The phthalocyanine of Mn, Be, Fe, Co, Ni, Cu and H_2 are isomorphous, they differ only slightly in the angle between the b-axis and the perpendicular of the phthalocyanine ring.[42] PtPc and CrPc are monocrystals belonging to the α-crystalline form.[41,43,44] MPcs form polycrystalline films of the α-type[45-49] when evaporated under vacuum (10^{-5} Torr to 10^{-6} Torr). H_2Pc sublimed in high vacuum on to a substrate cooled to liquid-nitrogen temperature gives amorphous films.[50]

The crystallization to the α-form occurs between 50°C and 140°C, and this phase is stable upto 207°C where the β-form is formed. The α-crystalline form is directly obtained if the MPc is sublimed at a pressure less than 50 Torr on to a substrate held at room temperature.[48]

X-ray diffraction studies are used to distinguish the polymorphs of phthalocyanine.[51] The typical parameters observed for CuPc are given in Table 1.1.[52]

Table 1.1: Cell dimensions and constants from X-ray analysis of copper phthalocyanines

	α-CuPc	β-CuPc
a, A	17.367	19.6
c, A	12.790	14.6
Space group	C_4^1-P_4/M	C_2^5 h PZ1/a
Molecules per cell	6	2
Density	1.49 g cm^{-3}	1.61 g cm^{-3}

The infrared spectra of the α and β-forms are significantly different allowing the determination of the kinetics of the α to β transition. The nature of the complexed metal as well as the state of purity also has effect on $\alpha \rightarrow \beta$ transition.[53,54]

MPcs undergo $\alpha \rightarrow \beta$ transition on heating and this transformation is accompanied by change in its electrical conductivity. The electrical conductivity in MPc can be further enhanced by doping. The iodine doping also results in enhanced electrocatalytic activity.[55]

Precise determinations of the bond length in MPcs have been achieved by low temperature X-ray diffraction[42] and neutron diffraction.[56,57] This method also enables the estimation of the extent of π-delocalisation. The C-N bonds of the bridging nitrogen atoms are 0.07 Å shorter than those of the isoindole moieties. The C-C bonds of the aromatic rings vary from 1.391 A to 1.405 Å. These data show that the extent of π delocalisation in the whole of the phthalocyanine ring is very high.

The molecular structure of two of the μ-oxodimers has been determined. In $[PcMn]_2O$ the two phthalocyanine

rings are parallel and staggered by 49° with respect to each other.[16] The manganese is in the +3 state. The Mn-O-Mn angle is 178°, the Mn-O distance is slightly shorter (1.71 Å) than would be predicted for a single covalent bond. [$PcSiO_3$] also shows a linear PcSi-O-SiPc arrangement with an interplanar spacing of 3.324 Å.[58,59]

The structural features of various dimeric phthalocyanines obtained with 4 f and 5 f elements have been determined.[10,60] The metal ion is sandwiched between the two phthalocyanine rings, it is simultaneously coordinated to both central nitrogens of the two subunits. In Pc_2Nd^{III}, the eight Nd-N distances vary from 2.39 to 2.49 A. One of the phthalocyanine macrocycle is slightly deformed towards the neodymium ion while the other is planar. The existence of an extra-acidic hydrogen has been postulated. The two phthalocyanine rings are oriented in a staggered configuration. Pc_2U and Pc_2Sn show the same sandwich-type structure. In Pc_2U, the distance between the two planes defined by four pyrrole nitrogen atom is 2.8 Å.[61,62] The macrocyclic rings are not planar. The uranium ion is equidistant from all the pyrrole nitrogen atoms. The U-N distance is 2.43 Å. The phthalocyanine ring is staggered by 37°.

Besides the solid phases described, substituted MPcs may form liquid crystalline phases[63] or may form aggregates in solution.[64-67] The tetrasulfonic acid derivatives of MPcs are soluble in water and form aggregates if the concentration exceeds $\sim 10^{-5}$ M. Dimerisation constants are in the range 10^{5}-10^{7} l mol^{-1}. The size of the aggregates is not known with certainty in many cases. But the largest particle contains approximately 20 Pc molecules.[68] Tetra octadecylsulfonamidophthalocyanines form aggregates in non-polar solvents.

The foregoing account of the methods of synthesis, purification and structural characteristics of MPcs casts some light on the uniqueness of these materials and the complexity associated with investigations in this area.

1.6 SPECTROSCOPIC PROPERTIES

The complexation of a transition metal ion by a phthalocyanine macrocycle involves the coordination of nitrogen lonepairs directed towards the centre of the ring with the central metal atom to form in-plane σ-orbitals. Interaction of the metal orbitals with nitrogen π-orbitals arises perpendicular to the plane of overlap. The macrocyclic ligand, through the σ-orbitals, is a donor of

electrons to the metal ion. The π-orbitals of the ligand may act as π-donor or acceptor. Besides, the pyrrolic nitrogen orbitals, which ensures coordination to the central metal, the π-orbitals of the ligand form a conjugated system.

Experimentally, the absorption spectra of the metal phthalocyanines are composed of two very intense bands ($\log \alpha a \sim 5$) in the 300-400 nm region (Soret band) and in the 650-700 nm region (Q band). Because of the high extinction coefficients (αa), films as thin as 30 Å are visible to the naked eye.[71,72] The peak around 700 nm is split into a doublet in the case of PcH_2. Most MPcs show three other bands in the UV region. They are labelled N(36,400 cm^{-1}, 275 nm), L(40,800 cm^{-1}, 245 nm) and C(47,600 cm^{-1}, 210 nm). The N band is the most sensitive to substitution of the central metal atom.[73]

Various models have been used to rationalize the optical properties of MPcs. The simplest one relies on the free-electron gas model, the π electrons are assumed to freely move in a closed ring shaped path.[71,74,75] The energy difference between the highest occupied state and the lowest empty state is given by,

$$E = \frac{8\ mc}{h} \left(\frac{I_{cp}^2}{N_{\pi}} + 1\right)$$

where C is the velocity of light, I_{cp} is circumfrence path and N_{π} is number of π electrons involved.

More satisfactory are the various molecular orbital treatments.[76-78] Ab initio calculations,[79,80] extended Huckel (EH) calculations and Pariser-Parr-Pople (PPP)-type calculations.[81,82] All these procedures have been carried out in the case of porphyrin complexes. Only extended Huckel[77,78] and PPP calculations[83,84] have been performed for MPcs. The two main absorption bands of the MPcs are both ascribed as $\pi-\pi^*$ transition from a_{1u} to e_g for the Q band and from a_{2u} to e_g for the Soret band. Both PPP and EH calculations give the same results for the nature of the transitions.

For MgPc and ZnPc, the Q band at 660 nm is a relatively pure a_{1u} (π) e_g (π^*) transitions. In the near UV region, NiPc shows unusual absorption bands, they arise from $d\rightarrow\pi^*$ transitions. This assignment is in agreement with a model relating the redox potentials of the complexes with the observed charge-transfer bands.[85]

Important spectroscopic changes are induced on going from solid into solution. The relatively narrow Q band is transformed into a broad peak showing a splitting.[86,87] According to Davydov theory[88] the amount of splitting is a measure of the interaction energy between molecules having different site symmetries. The Davydov splitting varies from 1350 cm^{-1} for H_2Pc to 2220 cm^{-1} for ZnPc.[86] The Davydov splitting is observed both for the Q and B (Soret) bands but not for the N band corresponding to higher energies.[89] The transformation of the α-form to the β-form also induces large differences in the transimission spectra.[90]

Luminescence properties of MPcs have been extensively studied by Russian workers.[91-95] The spin multiplicity of the excited state is determined by the nature of the central metal atom and its effect on the magnitude of the spin-orbit coupling.[96-98] Light closed shell metal phthalocyanines exhibit high fluorscence yields (0.03 to 0.7) and are only weakly phosphorecent. Metal phthalocyanines are, however, considerably more fluorescent than their porphyrin counterpart.[99]

The total luminescence yield of MPcs increases with increasing nuclear charge within a group (PdPc: PtPc:

RhPcCl, IrPcCl). NiPc and CoPc do not show any luminescence. This has been attributed to the presence of low-lying energy states arising from metal d electrons. In NiPc and CoPc, the metal state lies below the triplet state of the macrocyclic ligand providing radiationless paths to the ground state.[98]

1.7 MAGNETIC PROPERTIES

The magnetic susceptibility measurements on metal phthalocyanines give information relating to their structure and the nature of bonding of the central metal atom with the surrounding isoindole nitrogen atoms.

Many transition metal phthalocyanines are paramagnetic owing to the presence of unpaired electrons in the d-orbitals. Klemm[100,101] studied the magnetic properties of vanadyl, manganous, ferrous, cobaltous, nickel and copper phthalocyanines. The results are in good agreement with the magnetic behaviour predicted on the basis of electronic configuration.

The magnetic susceptibility of NiPc, CoPc, CuPc were studied by Havemann et al.[102] The magnetic susceptibility of the iodo derivatives and their temperature dependence have also been reported.[103]

The static magnetic susceptibility of Co(Pc)I measured at 293 K is 5.00×10^{-4} emu mol^{-1} which is equivalent to 0.4 spins/macrocycle when $S = \frac{1}{2}$ and $g = 2$. This value is 2.5 times larger than that for Ni(Pc)I. The reduced susceptibility demonstrates a strong interaction between cobalt atoms and is consistent with assignment of the site of oxidation as the metal (Co^{3+} is diamagnetic) rather than the ring. The magnetic susceptibility value for the Cu(Pc)I is 1.38×10^{-3} emu $mole^{-1}$. This value corresponds to approximately 1.1 unpaired electron spin ($S = \frac{1}{2}$, $g = 2$) per metallomacrocycle and support the view that oxidation does not occur at the Cu^{2+} metal sites.

1.8 ELECTRICAL PROPERTIES

The semiconducting potentialities of MPcs were recognized and much study has been devoted to their electrical properties. The first systematic measurements were carried out in the late forties by Eley[104] and Vartanyan.[105] The primary goal of their studies was to determine the thermal activation energy for conduction from the temperature dependence of conductivity. In most cases an exponential relationship,

$$\sigma = \sigma_0 \exp\left(-\frac{\Delta E}{2KT}\right)$$

(where σ_o is the intrinsic conductivity, ΔE is the energy gap of the semiconductor and k is Boltzman constant) was found.

The term ΔE represents, the activation energy for the liberation of charge carriers from traps, or for the ionization of levels within the band gap. A relationship between ΔE and the energy of the absorption band in the visible region had been found.[87,106,107]

1.9 REDOX PROPERTIES

Gaseous ionization potentials corresponding to the equilibrium $(MPc)_g \rightleftharpoons (M^+Pc)_g + e^-$ have been determined by electron impact measurements.[108] The gaseous ionization potentials are remarkably independent of the nature of the central metal atom. The surface ionization potential shows pronounced variation.

The solvent dependence in the redox potential of phthalocyanines has also been reported.[109] The redox potentials determined in solution by cyclic voltammetry or polarography are strongly dependent upon the nature of the central metal.

It has been found that metal phthalocyanines are more easily reduced than the porphyrin homologue by approximately $\sim$0.4 V. The substitution of the H atoms on the benzene ring by sulfonate groups shifts the reduction potentials more positive by over 0.1 V.

Oxidation of MPcs may occur by removing electrons either from the π-orbitals of the macrocyclic ring or from the metal.

$$MPc \overset{-e^-}{\rightleftharpoons} M^+Pc \text{ (oxidation of the metal)}$$

$$MPc \overset{-e^-}{\rightleftharpoons} MPc^+ \text{ (oxidation of the ring)}$$

ESR studies have demonstrated that both cases are possible, depending on M. In FePc and CoPc the oxidation occurs first at the metal centre. For CuPc, ZnPc and H_2Pc the macrocyclic ring is oxidised first and for NiPc both metal and ring are oxidized simultaneously.[110]

MPcs can accept upto four electrons in the redox process.[111,112] The electrons are added to the lowest empty antibonding π-orbital of the macrocycle,[113] but it is the metal which is preferentially reduced in the case of CoPc,[111-117] FePc,[111,112] and MnPc.[112]

Chemical reagents may be used to oxidize or reduce MPc. CoPc reacts with iodine to give Co(Pc)I though NiPc is not oxidized under the same condition.[112,118] The dilithium salt of benzophenone reacts with MPcs in THF to yield the anion $(MPc)^{n-}$ with n varying from 1 to 4.[119-122] Although reduced MPcs are fairly stable in solution under an inert atmosphere, oxidized MPcs are relatively unstable and cannot be kept in solution over long periods of time at room temperature. CrPc, FePc, CoPc, and ZnPc react at 60-80°C with $SOCl_2$ in nitrobenzene to yield the corresponding cation radicals. NiPc, VOPc and H_2Pc are unaffected by this treatment.[118,123] The reactivity of MPcs towards NO follows the same trend as the reactivity towards $SOCl_2$.[124] MPcs when treated with strong acids form mixture of products. FePc reacts with HCl at 100°C to give several derivatives including PcFeHCl and PcFeCl.[118]

1.9.1 Doping of MPc by O_2

O_2 is an almost unavoidable dopant for molecular semiconductors. The redox properties of O_2 in solution are well known.[125,126] The superoxo species $O_2^{\cdot-}$ is formed by the monoelectronic reduction process.

$$O_2 + \bar{e} \rightleftharpoons O_2^{\cdot-} \qquad E_{1/2} = 0.75 \text{ V vs. SCE}$$

$O_2^{\cdot-}$ in the presence of protons or other acceptors, can dismutate into O_2 and O_2^{2-}

$$O_2^{\cdot-} + H^+ \rightleftharpoons HO_2$$

$$2HO_2 \rightleftharpoons H_2O_2 + O_2$$

$O_2^{\cdot-}$ may be further reduced into the peroxo species

$$O_2^{\cdot-} + \bar{e} + H^+ \rightleftharpoons HO_2^- \qquad E_{1/2} = 2.0 \text{ V vs. SCE}$$

The equilibrium when oxygen is doped into the lattice of MPc involves monoelectronic transfer from MPc to O_2.

$$MPcO_2 \rightleftharpoons M^+PcO_2^{\cdot-}$$

O_2 is, however, only a weak monoelectronic oxidant in solution and it will not be able to oxidize MPcs. This may be drastically different in the solid state. The binding of O_2 by MPc will favour the electron transfer between them. An analogous chlorophyll-O_2 complex has been detected in the solid state.[127]

The nature of the central metal ion does influence the MPc-O_2 association constant. Temperature-programmed desorption studies have shown that CuPc and FePc reversbly absorb O_2 while, under the same conditions, H_2Pc does not interact with oxygen. The molecule of O_2 is, therefore, probably directly bound to the central metal ion and the magnitude of binding constant is related to the ability of M to coordinate ligands in the axial position.

1.9.2 Doping of MPc by other doping agents

Many doping agents have been reported which can bring about the oxidation or reduction of metal phthalocyanines. The oxidation potentials of most of the MPcs lie between +0.6 and +1.0 V vs. SCE. For significant charge transfer between the dopant and the MPc to occur the reduction potential of the dopant E^{red}_{dopant} must be such that,

$$E^{red}_{dopant} \text{ ——— } E^{ox}_{MPc} \geqslant 0.25 \text{ V}$$

Most of the common oxidants like halogens, benzoquinone and anthraquinone derivatives satisfy this condition.[128,129]

The influence of halogens on the conductivity of single crystals,[130] or thin film[131] of MPc has long been recognized. These films of MPc may be doped by I_2 as vapour or in solution. The corresponding conductivities are in the range 0.06-4.2 $\Omega^{-1}cm^{-1}$ depending on M.[132,133] The thermal activation energies are approximately 50-fold less than those for the undoped complexes.

Bridged polymers of formula $[PcMF]_n$ (M = Al, Ga, Cr) have been doped with I_2 and Br_2.[134-136] Adducts of different stoichiometry $[PcMFI_y]X$ with y ranging from 0 to 3.4 have been isolated. Doping of μ-oxo-bridged polymeric systems has also been achieved.[58,137] Their conductivity is increased by more than nine orders of magnitude by bromination or iodination.

Quinone derivatives and related compounds may also be used as dopants since they have suitable redox potentials. However, the incorporation of compounds such as bromanil, chloranil or TCNQ into solid phases of MPcs does not change the overall conductivity of the material to any significant extent.[24,138]

MPcs may be "autodoped" by using mixtures of two different metal phthalocyanines.[139,140] CuPc and NiPc form

only acceptor levels within the band gap of host H_2Pc crystals. CdPc and FePc act only as donors. The mixture of FePc and MPc is made by dissolving H_2Pc and the appropriate MPc in con. H_2SO_4 and reprecipitating the mixture by pouring the solution into ice water. Mixed MPcs thin films have also been obtained by cosublimation of two MPcs under high vacuum.[141]

1.10 APPLICATIONS OF METAL PHTHALOCYANINES

1.10.1 Pigments and dyes

Although numerous phthalocyanines have been prepared, only copper phthalocyanine, copper polychlorophthalocyanine, and their derivatives have found widespread use as colorants in pigments and dye systems. Eventhough the shade range of these MPcs is rather limited and covers only the blue-green section of the spectrum, their excellent fastness, cleanliness, and intensity of colour have led to many applications. Numerous formulations of textile printing inks have used MPc pigments usually in the form of an aqueous dispersion, paste or a pulp containing 10-20% pigment[142] in the field of spin-dyeing. In these applications their excellent stability to acids, alkalies and solvents make the Pcs materials of choice.

The polysulfonamide derivatives of CuPc have been used to formulate improved inks for ball point pens.[142,144] Both copper phthalocyanine sodium sulfonate and leuco-CuPc[143,144] have been used in photographic processes to produce colored prints. For special applications metal surface can be coated by directly forming the MPcs on them.[145]

Phthalocyanines have been used to colour rubber, polystyrene foams, polyamides, vinyl chloride polymers and other polymeric materials.[146,147]

1.10.2 Analytical reagent

Copper phthalocyanine in concentrated sulphuric acid has been used as a reagent for the detection of oxidizing agents such as NO_2^-, NO_3^- ClO_3^- BrO_3^- IO_3^- $Cr_2O_7^{2-}$ CuPc is used as a redox indicator in the cerimetric determination of iron(II) and ferrocyanide.[148] It was found that copper 4,4'4",4"'-tetrasulfophthalocyanine (CuTSPc) is a suitable indicator for the titration of iron(II) in 0.5-2.5 M HCl or H_2SO_4 or $Fe(CN)_6^{4-}$ in 0.5 M H_2SO_4 with a 0.01 N to 0.001 N Ce^{4+} CuTSPc is stable towards con. HCl, con. H_2SO_4 and syrupy H_3PO_4. A 0.1% solution of CuTSPc is used as the indicator.

1.10.3 Catalysts

Certain MPcs, particularly ferrous and chloroferric complexes, catalyze the decomposition of hydrogen peroxide. MPcs catalyze the oxidation of many organic compounds.[149-151] Cobalt, nickel and iron-Pcs catalyze the oxidation of ∝-pinene to verbenone. NiPc catalyzes the autoxidation of saturated ketones at 120-130°C to ∝-diketones and aldehyde. The aerobic oxidation of unsaturated fatty acids catalyzed by Fe and CoPc has been reported.[152]

Fe and CuPc catalyze the isomerisation of dimethyl maleate to dimethyl fumarate in the vapour phase at 300°C.[153] ∝-Tetralin is catalytically oxidized in the presence of magnesium, zinc or iron phthalocyanine to ∝-tetralone, the reaction being chemiluminescent.[154-156] Fe, Co and CuPc and their derivatives have been used as rubber emulsification catalysts. When CoTSPc is attached to poly(vinyl alcohol) it can catalyze the auto-oxidation of thiols.[157]

The catalytic activity[158] of sheet-like poly(metal phthalocyanine) is found to be superior to that of the solid monomeric complexes.

1.10.4 Electrocatalysts

The electrocatalysis of cathodic oxygen reduction by macrocyclic organic N_4-complexes such as porphyrins and Pc has received much attention. This is due to the promising features of these compounds as practical electrocatalyst, and also due to their similarity to compounds found in the biological systems responsible for the transport and reduction of oxygen. Electrochemically incorporated CoTSPc polyaniline-modified glassy carbon electrode shows very good catalytic activity for dioxygen reduction.[159] The electroreduction of dioxygen on iron tetracarboxy phthalocyanine covalently linked to polystyrene has also been reported.[160]

1.10.5 Chemically modified electrodes

Carbon paste electrodes chemically modified with phthalocyanine have been reported.[161] The modified electrodes decrease the overpotential for the oxidation of thiols,[162] hydrazine,[163] α-ketoacids and oxalic acid. A glassy carbon electrode modified with CoPc[161] can be efficiently used as a liquid chromatographic detector for the clinical assay of oxalic acid, glucose and α-ketoacids in blood and urine.

1.10.6 Liquid crystals

Phthalocyanine molecules substituted with long, flexible chains exhibit discotic mesophases.[164] One of the interesting aspects of phthalocyanines used as discogenic materials is their ability to form stable complexes with a wide variety of metal ions. The introduction of ramification in the molecular structure lowers the transition temperatures so as to permit the formation of discotic mesophases at room temperature.

1.10.7 Electrochromic display devices

Liquid crystal displays with non-emissive electro-optic displays are now widely developed. New materials showing a large range of coloured states, a life time longer than 10^7 switching cycles and a response time down to 20 ms are still of great interest. The electrochromic phenomenon involves the change of light absorbing or light scattering property of a material, induced by an external voltage bias. Various electrochromic systems have been investigated, from purely inorganic materials like WO_3 and V_2O_3, to the more recent organic conducting polymers such as polypyrrole and polythiophone. Rare-earth diphthalocyanines[165] sublimed onto conducting glass can be used as

electrochromic displays due to high thermal and chemical stabilities together with the range of colour changes taking place for the small applied voltage (± 1.0 V). These electrochromic materials are also useful for full-colour imaging and graphic and alphanumeric displays.

1.10.8 Photovoltaic and photogalvanic devices

Phthalocyanines show photoconductivity. The photoconductive and photovoltaic properties of Pcs have been extensively studied for use in electrophotographic systems, diodes, laser printers, photovoltaic cells and photoelectrochemical devices.[166,167]

CoTSPc can be covalently bound to the surface of titanium dioxide particles Upon irradiation with light having energy exceeding the band gap energy of TiO_2 (0.80 eV), Co(II)TSPc is reduced to Co(I)TSPc. This photochemical reduction is reversable in presence of dioxygen. The photochemical stability and the high quantum yield for O_2 reduction makes this newly developed material a potent and stable oxidation catalyst.

1.10.9 Optical recording devices

For pit-formation by laser marking[168] in optical write-once media, metallic or semimetallic materials such

as tellurium alloys are commonly used. Organic dyes such as phthalocyanines have many advantages like high data storage density, low heat conductivity, low manufacturing cost due to spin-coatability, high recording sensitivity due to the low melting point of the suitably substituted material, stability to moisture and low toxicity.

1.10.10 Batteries

Phthalocyanines and their charge transfer complexes have been used as cathode materials in batteries[169] especially in fuel cells, air-cathode batteries and solid electrolyte cells.

1.10.11 Gas sensors

Devices based on MPcs such as PbPc show useful response towards NO_2. A thin film PbPc can detect NO_2 produced by short firing in coal mines.[170] Pc based devices offer much promise as resistance modulating sensors for toxic gases. They are thus complementary to metal oxide devices which are most useful in the detection of flamable gases. Lanthanide diphthalocyanine complexes have also been used as detectors for acidic and basic gases.[171]

REFERENCES

1. Guillon, P.; Weber, A.; Skoulis, C.; Piechocki; Simon. J. Mol. Cryst. Liq. Cryst. **1985**, 130, 323.

2. Arthur W. Snow; Lynn Jarvis, N. J. Am. Chem. Soc. **1984**, 106, 4706.

3. Linstead, R.P. J. Chem. Soc. **1934**, 1016 and 1031.

4. Lawton, E.A. J. Phys. Chem. **1958**, 62, 384.

5. Barret, P.A.; Dent, C.E.; Linstead, R.P. J. Chem. Soc. **1936**, 1719.

6. Kroenke, W.J.; Kenney, M.E. J. Inorg. Chem. **1964**, 3, 25.

7. Yang, C.H.; Lin, S.F.; Chen, H.L.; Chang, C.T. Inorg. Chem. **1980**, 19, 3541.

8. Katsuyoshi, H.; Tetsuo, S. J. Am. Chem. Soc. **1987**, 109, 5881.

9. Pawlowski, G.; Hanack, M. Synthesis **1980**, 287.

10. Kasuga, K.; Tsutsui, M. Corrd. Chem. Rev. 1980, 32, 67.

11. Weber, H.; Busch, D.H. Inorg. Chem. 1965, 4, 469.

12. Bernauer, K.; Fallab, S. Helv. Chim. Acta 1961, 44, 1287.

13. Rollmann, L.D.; Iwamoto, R.T. J. Am. Chem. Soc. 1968, 90, 1455.

14. Michael Hanack, Lehmann, A.B.H. Synthesis 1980, 703.

15. Vogt Jr, L.H.; Zalkin, A.; Templeton, D.H. Science 1966, 151, 569.

16. Vogt Jr, L.H.; Zalkin, A.; Templeton, D.H. Inorg. Chem. 1967, 6, 1725.

17. Elvidge, J.A.; Lever, A.B.P. Proc. Chem. Soc. 1959, 195.

18. Janson, T.R.; Kane, A.R.; Sullivan, J.T.; Knox, K.; Kenney, M.E. J. Am. Chem. Soc. 1969, 91, 5210.

19. Owen, J.E.; Kenney, M.E. Inorg. Chem. 1962, 1, 334.

20. Mooney, J.R.; Chog, C.K.; Knox, K.; Kenney, M.E. J. Am. Chem. Soc. 1975, 97, 3033.

21. Joyner, R.D.; Kenney, M.E. Inorg. Chem. 1962, 1, 717.

22. Joyner, R.D.; Kenney, M.E. J. Am. Chem. Soc. 1960, 82, 5790.

23. Kroenke, W.J.; Sutton, L.E.; Joyner, R.D. Kenney, M.E. Inorg. Chem. 1963, 2, 1064.

24. Dirk, C.W.; Mintz, E.A.; Schoch Jr, K.F.; Marks, T. J. Macromol. Sci. Chem. 1981, A16, 275.

25. Kuznesof, P.M.; Nohr, R.S.; Wynne, K.J.; Kenney, M.E. J. Macromol. Sci. Chem. 1981, A16, 299.

26. Colaitis, D. Compt. Rend. 1956, 242, 1026.

27. Colaitis, D. Bull. Soc. Chim. France, 1962, 23.

28. Schneider, O.; Hanack, M. Angew. Chem. Int. Ed. 1980, 19, 392.

29. Metz, J.; Hanack, M.; Nouveau. J. de Chimie. 1981, 5, 541.

30. Wohrle, D.; Wahl, B. Tetrahedron Lett. 1979, 227.

31. Bannehr, R.; Haeger, N.; Meyer, G.; Wohrle, D. Macromol. Chem. 1981, 182, 1633.

32. Banmann, T.; Binert, B. German Pat. 83939, U.S. Pat. 2768867.

33. Barnhart, G.; Skiles, B.T. U.S. Pat. 2772284.

34. Dag, V.W.; Marks, T.J.; Wachter, W.A. J. Am. Chem. Soc. 1975, 97, 4519.

35. Friedel, M.K.; Hoskins, B.F.; Martus, R.L.; Mason, S.A. J.C.S. Chem. Commun. 1970, 400.

36. Magner, G.; Savy, M.; Scarbeck, G. J. Electrochem. Soc. 1980, 127, 1076.

37. Byrne, G.; Linstead, R.; Lowe,A. J. Chem. Soc. 1934, 1017.

38. Walton, D.; Eley, B.; Elliott, G. J. Electrochem. Soc. 1981, 128, 2479.

39. Robertson, J.M.; Linstead, R.P.; Dent, C.E. Nature 1935, 135, 506.

40. Robertson, J.M. J. Chem. Soc. 1935, 615.

41. Robertson, J.M.; Woodword, I.J. J. Chem. Soc. 1937, 219; 1940, 36.

42. Mason, R.; Williams, G.A.; Fielding, P.E. J.C.S. Dalton Trans. 1979, 676.

43. Ercolani, C.; Neri, C.; Porta, P. Inorg. Chim. Acta. 1967, 1, 415.

44. Brown, C.J. J. Chem. Soc. 1968, A 2494.

45. Susich, G. Anal. Chem. 1950, 22, 425.

46. Tarantino, F.R.; Stubbs, D.H.; Cooke, T.F.; Melsheimer, L.A. Am. Ink. Maker 1950, 29, 35 and 425.

47. Ebert Jr, A.A.; Gottlieb, H.B. J. Am. Chem. Soc. 1952, 74, 2806.

48. Karasek, F.W.; Decius, J.C. J. Am. Chem. Soc. 1952, 74, 4716.

49. Shigimitsu, M. Bull. Chem. Soc. Jpn. 1959, 32, 607.

50. Mindorff, M.S.; Brodie, D.E. Can. J. Phys. 1981, 59, 249.

51. Kendall, D.N. Anal. Chem. 1953, 25, 382.

52. Shigemitsu, M. Bull. Chem. Soc. Jpn. 1959, 32, 502.

53. Wihksne, K.; Newkirk, A.E. J. Chem. Phys. 1961, 34, 2184.

54. Harrison, S.E.; Ludewig, K.H. J. Chem. Phys. 1966, 45, 343.

55. Harikumar, P.S.; Sivasankara Pillai, V.N. J. Mat. Sci. Lett. 1989, 8, 969.

56. Williams, G.A.; Figgis, B.N., Mason, R.; Mason, S.A.; Fielding, P.E. J.C.S. Dalton Trans. 1980, 1688.

57. Figgis, B.N.; Williams, G.A.; Forsyth, J.B.; Mason, R. J. C.S. Dalton Trnas. 1981, 1837.

58. Schoch Jr, K.F.; Kundalkar, B.R.; Marks, T.J. J. Am. Chem. Soc. 1979, 101, 7071.

59. Swift, D.R. Ph.D. Dissertation. Case Western Reserve University, Cleveland, Ohio, 1970.

60. Kasuga, K.; Tsutsui, M.; Pettersen, R.C.; Tabsumi, K.; Van Opdenbosh, N.; Meyer, E.F. J. Am. Chem. Soc. 1980, 102, 4835.

61. Bennet, W.E.; Broberg, D.E.; Baenziger, N.C. Inorg. Chem. 1973, 12, 930.

62. Gieren, A.; Hoppe. W. J.C.S. Chem. Commun. 1971, 413.

63. Piechocki, C.; Simon, J.; Skoulios, A.; Guillon, D.; Weber, P. J. Am. Chem. Soc. 1982, 104, 5245.

64. Schelly, Z.A.; Harward, D.J.; Hemmes, P.; Eyring, E.M. J. Phys. Chem. 1970, 74, 3040.

65. Farina, F.D.; Halko, D.J. Swinehart, J.H. J. Phys. Chem. 1972, 76, 2343.

66. Kratky, O.; Oelschlaeger, H. J. Colloid Int. Sci. 1969, 31, 490.

67. Gruen, L.C.; Blagrove, R.J. Aust. J. Chem. 1973, 26, 319.

68. De Bolfo, J.A.; Smith, T.D.; Boas, J.F.; Pilbrow, J.R. J.C.S. Faraday Trans. 11, 1976, 72, 481.

69. Abkowitz, M.; Monahan, A.R. J. Chem. Phys. 1973, 58, 2281.

70. Monahan, A.E.; Brado, J.A.; De Luca, A.F. J. Phys. Chem. 1972, 76, 446.

71. Lever, A.B.P. Adv. Inorg. and Radiochem. 1965, 7, 27.

72. Hughes, A. Proc. Roy. Soc. 1936, B155, 710.

73. Davison, A.T. J. Chem. Phys. 1982, 77, 168.

74. Kuhn, H. J. Chem. Phys. 1949, 17, 1198.

75. Kunh, H. Angew, Chem. 1959, 71, 93.

76. Basu, S. Indian J. Phys. 1954, 28, 511.

77. Schaffer, A.M.; Gouterman, M.; Davison, E.R. Theor. Chim. Acta 1973, 30, 9.

78. Edwards, L.; Gouterman, M. J. Mol. Spectrosc. 1970, 33, 292.

79. Almof, J. Int. J. Quantum Chem. 1974, 3, 915.

80. Case, D.A.; Karplus, M. J. Am. Chem. Soc. 1977, 99, 6182.

81. Zerner, M.; Gouterman, M. Theor. Chim. Acta 1966, 4, 44.

82. Ross, B.; Sundbom, N. J. Mol. Spect. 1970, 36, 8.

83. Weiss, C.; Kobayashi, H.; Gouterman, M. J. Mol. Spect. 1965, 16, 415.

84. Mc Hugh, A.; Gouterman, M.; Weiss, C. Theor. Chim. Acta, 1972, 24, 346.

85. Lever, A.B.P.; Pickens, S.R.; Minor, P.C.; Licoccia, S.; Ramaswamy, B.S.; Magnell, K. J. Am. Chem. Soc. 1981, 103, 6800.

86. Day, P.; Williams, R.J.P. J. Chem. Phys. 1962, 37, 567.

87. Chadderton, L.T. J. Phys. Chem. Solids 1963, 24, 751.

88. Davydov, A.S. Theory of Molecular Excitors (Eng. Transl) Kasha, M. Oppen Leimer Jr. M. (Ed.) New York, McGraw Hill 1962.

89. Hollebone, B.R.; Stillman, M.J. J. Chem. Soc. Faraday Trans. 11. 1978, 74, 2107.

90. Lucia, E.A.; Verderame, F.D. J. Chem. Phys. 1968, 48, 2674.

91. Dmietrierskii, D.; Ermolaev, V.L.; Teremin, A.N. Dokl. Akad. Nauk. SSSR. 1957, 114, 751.

92. Evstigneev, V.B.; Krasnoskii, A.A.; Gavrilova, V.A. Dokl. Akad. Nauk. SSSR, 1950, 70, 261.

93. Gachkovskii, V.T. Dokl. Akad. Nauk. SSSR. 1953, 82, 739.

94. Litvin, F.F.; Personov, R.I. Fiz. Prob. Spektroskopii 1963, 1, 229.

95. Lyalin, G.N.; Kobyshev, G.I. Opt. i. Spectroskopiya 1963, 15, 253.

96. Huang, T.H.; Rieckhoff, K.E.; Voigt, E.M. Chem. Phys. 1977, 19, 25.

97. Menzel, E.R.; Rieckhoff, K.E.; Voigt, E.M. J. Chem. Phys. 1973, 58, 5726.

98. Vincett, P.S.; Voigt, E.M.; Rieckhoff, K.E. J. Chem. Phys. 1971, 55, 4131.

99. Seybold, P.G.; Gouterman, M. J. Mol. Spectrosc. 1969, 31, 1.

100. Klemm, L.; Klemm, W. J. Prakt. Chem. 1935, 143, 82.

101. Senff, H.; Klemm, W. J. Prakt. Chem. 1939, 154, 73.

102. Havemann, R.; Haberditzl, W.; Mader, K.H. Z. Physik. Chem. 1961, 218, 71.

103. Martinsen, J.; Stanton, J.I. J. Am. Chem. Soc. 1985, 107, 6915.

104. Eley, D.D.; Parfit, G.D. Trans. Faraday Soc. 1955, 51, 1529.

105. Eley, D.D. Nature 1948, 162, 819.

106. Fielding, P.E.; Gutmann, F.J. J. Chem. Phys. 1957, 26, 411.

107. Vartanyan, A.T.; Karpovich, I.A. Zh. Fiz. Khim. 1958, 32, 178 and 274.

108. Eley, D.D.; Hazeldine, D.J.; Palmer, T.F. J.C.S. Faraday Trans. 11. 1973, 12, 1808.

109. Lever, A.B.P.; Minor, P.C. Adv. Mol. Rel. Inter. Process 1980, 18, 115.

110. Wolberg, A.; Manassen, J. J. Am. Chem. Soc. 1970, 92, 2982.

111. Rollman, L.D.; Iwamoto, R.I. J. Am. Chem. Soc. 1968, 90, 1455.

112. Taube, R. Pure Appl. Chem. 1974, 38, 427.

113. Boudier, L.J. Coordination Chemistry of Macrocyclic Compounds; Melson, G.A. (Ed.) New York, Plenum Press, 1979.

114. Felton, R.H.; Linschitz, H. J. Am. Chem. Soc. 1966, 88, 1113.

115. Clack, D.W.; Yandle, J.R. Inorg. Chem. 1972, 11, 1738.

116. Dodd, J.W.; Hush, N.S. J. Chem. Soc. 1964, 4607.

117. Day, P.; Hill, H.A.O.; Price, M.G. J. Chem. Soc. 1968, A19.

118. Myers, J.F.; Canham, G.W.R.; Lever, A. Inorg. Chem. 1975, 14, 461.

119. Taube, R. Z. Chem. 1966, 6, 8.

120. Clack, D.W.; Hush, N.S.; Yandle, J.R. Chem. Phys. Lett. 1975, 1, 157.

121. Linder, R.E.; Rowlands, J.R.; Hush, N.S. Mol. Phys. 1971, 21, 417.

122. Guzy, C.M.; Raynor, J.B.; Stodulski, L.P.; Symons, M.C.R. J. Chem. Soc. 1969, A 997.

123. Gauham, G.W.R.; Myers, J.; Lever, A.B.P. J.C.S. Chem. Commun. 1973, 483.

124. Ercolani, C.; Neli, C. J. Chem. Soc. 1967, A 1715.

125. Sawyer, D.T.; Gibian, M.J.; Morrison, M.M.; Seo, E. J. Am. Chem. Soc. 1978, 100, 627.

126. Wilshire, J.; Sawyer, D.T. Acc. Chem. Res. 1979, 12, 105.

127. Rosengerg, B.; Camiscoli, J.F. J. Chem. Phys. 1961, 35, 982.

128. Briegkh, G. Angew. Chem. Int. Ed. 1964, 3, 617.

129. Milazzo, G., Caroli, S. Tables of Standard Electrode Potentials, J. Wiley and Sons, New York, 1978.

130. Curry, J.; Cassidy, E.P. J. Chem. Phys. 1962, 57, 2154.

131. Kearus, D.; Calvin, M. J. Am. Chem. Soc. 1961, 83, 2110.

132. Petersen, J.L.; Schramm, C.S.; Stojakovic, D.R.; Hoffman, B.M.; Marks, T.J. J. Am. Chem. Soc. 1977, 99, 286.

133. Orr, W.A.; Dahlberg, S.C. J. Am. Chem. Soc. 1981, 101, 2875.

134. Kuznesof, P.M.; Nohr, R.S.; Wynne, K.J.; Kenney, M.E. J. Macromol. Sci. Chem. 1981, A16, 275.

135. Kuznesof, P.M.; Nohr, R.S.; Wynne, K.J.; Kenney, M.E. J.C.S. Chem. Comm. 1980, 121.

136. Nohr, R.S.; Kuznesof, P.M.; Wynne, K.J.; Kenney, M.E.; Siebenman, P.G. J. Am. Chem. Soc. 1981, 103, 487.

137. Nohr, R.S.; Wynne, K.J. J.C.S. Chem. Comm. 1981, 1210.

138. Bourdon, J., Schnuriger, B., Physics and Chemistry of the Organic Solid State, Vol.3, Fox, D., Labes, M., Weissberger, A. (Ed.), Interscience Pub. New York, 1967.

139. Loutfy, R.O.; Cheng, Y.C. J. Chem. Phys. 1980, 73, 2902.

140. Cheng, Y.C.; Loutfy, R.O. J. Chem. Phys. 1980, 73, 291.

141. Hamann, C.; Starke, M.; Wagner, H. Phys. Status Solidi. 1973, A16, 463.

142. Miller, C.Q.; Ranson, W.W. U.S. Patent. 1960, 2, 950, 285.

143. Kropf, H.; Gebert, W.; Franke, K. Tetrahedron Lett. 1968, 5527.

144. Schutheis, W.; Schimmelschnidt, K.; Hoffmann, H.; Baier, E. FH, DAS. 1, 163, 473.

145. Tanner, H.G. U.S. Patent. 1939, 2, 163, 768.

146. Ciba Ltd. British Patent 1953, 685, 582.

147. Taul, H.; Indest, H. U.S. Patent.

148. Gopala Rao; Sastri, T.P. Z. Anal. Chem. 160, 109.

149. Paquot, C. Bull Soc. Chim. 1941, 8, 695.

150. Paquot, C. Compt. rend, 1942, 214, 173.

151. Paquot, C. Bull Soc. Chim. 1945, 12, 450.

152. Uri. N. Nature, 1956, 177, 1177.

153. Tamamushi, B.I. Bull. Chem. Soc. Jpn. 1942, 17, 417.

154. Helberger, J.H. Naturwissenschaften, 1938, 26, 316.

155. Helberger, J.H.; Hever, D.B. Ber. Dent. Chem. Ges 1939, 1372, 11.

156. Weber, K.; Schulz, K.F.Arkivkemi, 1954, 26, 173.

157. Brouwer, W.M.; Traa, D.A.M.; De, W.; Pief, W. Angew Makromol. Chem. 1984, 128, 133.

158. Boston, D.R.; Bailas, Jr., J.C. Inorg. Chem. 11, 1972, 1578.

159. Rongzhong J.; Shaojum, D. J. Electroanal. Chem. 1988, 246, 101.

160. Yamagudie, H.; Fugiwara, R.; Kusuda, K. Macromol. Sci. Chem. A 24(344), 307.

161. Sautos, L.M.; Baldwin, R.P. Anal. Chem. 1986, 58, 848.

162. Halbert, M.K.; Baldwin, R.P. Anal. Chem. 1985, 57, 591.

163. Krofhage, K.M.; Ravichandran, K.; Baldwin, R.P. Anal. Chem. 1984, 57, 1514.

164. Guillon, D.; Skoulios, A.; Piecliocki, C.; Weber, P. Mol. Cryst. Liq. Cryst. 1983, 100, 275.

165. La Mar, G.N.; Jefferey, S.R.; Smith, K.M.; Langry, K.C. J. Am. Chem. Soc. 1980, 102, A835.

166. Grammatica, S.; Mort. J. Appl. Phys. Lett. 1981, 38, 445.

167. Sobezynski, A.; White, J.M. J. Mol. Catal. 1985, 29, 379.

168. Molaire, M.F. Appl. Opt. 1988, 27, 743.

169. Buck, T.; Woelirle, O., Schulz-Ekloff, G.; Andrew, A. J. Mol. Catal. 1991, 70(3) 259-68; CA 1992, 116, 1054395.

170. Miazik, J.J.; Hooper, A.; Tofield, B.C. J. Chem. Soc. Faraday Trans. 1986, 82, 1117.

171. Sawa Seikosha Co., Ltd. Jpn. Kokai, Tokkyo Koho JP 57, 108, 652, 1982; CA 1983, 46165 j.

CHAPTER - II

SYNTHESIS AND CHARACTERIZATION OF METAL PHTHALOCYANINES

2.1 SYNTHESIS OF METAL PHTHALOCYANINES

2.1.1 Synthesis of nickel, cobalt and copper phthalocyanines

A mixture of phthalic anhydride (0.5 mmol), urea (2 mmol), and a stoichiometric amount of metal chloride and catalytic amount of ammonium molybdate was heated in nitrobenzene at refluxing temperature (180°C) for 2 h. Nitrobenzene was recovered by distillation at reduced pressure. The crude product obtained as the residue was washed several times with ethanol till it was free of nitrobenzene. This was warmed with 10% NaOH to remove any unreacted acid and then with 2 M HCl. The powdered mass was washed with distilled water till the washings were neutral. It was slurried with conc. H_2SO_4 and dropped on ice. The precipitate formed was filtered washed with water and dried.

The metal phthalocyanines obtained were further purified by soxhlet extraction with benzene and acetone to remove impurities and then the metal phthalocyanine was extracted into DMF.

2.1.2 Synthesis of (nickel, cobalt, copper) 4,4',4",4'"-tetranitrophthalocyanine

Nickel 4,4',4",4'"-tetranitrophthalocyanine (NiTNPc), cobalt 4,4',4",4'"-tetranitrophthalocyanine (CoTNPc) and

copper 4,4',4",4'"-tetranitrophthalocyanine (CuTNPc) were synthesized by modified Wyler's method.[1] Metal chloride (10 mmol), nitrophthalimide (30 mmol), urea (48 mmol) and catalytic amount of ammonium molybdate tetrahydrate were ground together to a fine powder. Nitrobenzene (140 ml) was heated to 180°C in a 500 ml three necked flask fitted with a thermometer and condenser. The solid mixture was slowly added into refluxing nitrobenzene with stirring, keeping the temperature between 160-180°C, and refluxed for 3 h. Nitrobenzene was removed by distillation under reduced pressure. The phthalocyanine obtained was further purified by the procedure described in section 2.1.1.

2.1.3 Synthesis of (nickel, cobalt, copper) 4,4',4",4'"-tetraaminophthalocyanine

Nickel 4,4',4",4'"-tetraaminophthalocyanine (NiTAPc), cobalt 4,4',4",4'"-tetraaminophthalocyanine (CoTAPc) and copper 4,4',4",4'"-tetraaminophthalocyanine (CuTAPc) were obtained by the reduction of the corresponding nitrophthalocyanine with $SnCl_2$ and HCl.

MTNPc (M = Ni, Co, Cu) (1 g) was added to cold 16 ml 5 M HCl. This suspension was cooled to 5°C, and 3.6 g $SnCl_2$ in 20 ml of 5 M HCl was added dropwise with

stirring, the temperature being kept at 5°C during the addition. After dilution with water the bright green precipitate was filtered, washed free of acid and dried.

2.1.4 Synthesis of (nickel, cobalt, copper) 4,4',4",4'"-tetra(n-dodecanoylamino)Pc

Nickel 4,4',4",4'"-tetrakis(n-dodecanoylamino)-phthalocyanine (NiDAPc) was synthesized as follows: NiTAPc (0.9 mmol) was added to dry pyridine (30 ml), stirred for 4 h at room temperature and then at 100°C for 8 h. The solution was allowed to cool, n-dodecanoyl chloride (12.6 mmol) was added to the solution, stirred at room temperature for 1 h, and then at 100°C for 30 h. The hot reaction mixture was filtered and the solvent was removed by distillation under reduced pressure. The resulting solid was dissolved in $CHCl_3$, washed with 4% sodium carbonate followed by water. After drying over molecular sieve 4Å for 1 day the solvent was removed by distillation under reduced pressure. The final product was purified by column chromatography over silica gel using EtOH/$CHCl_3$ (2% v/v) as mobile phase.

Cobalt 4,4',4",4'"-tetrakis(n-dodecanoylamino)Pc (CoDAPc) and copper 4,4',4",4'"-tetrakis(n-dodecanoylamino)Pc

(CuDAPc) were synthesized and purified according to the procedure given in section 2.1.4.

2.1.5 Synthesis of (nickel, cobalt, copper) 4,4',4",4"'-tetrakis(n-octadecanoylamino)Pc

Nickel 4,4',4",4"'-tetrakis(n-octadecanoylamino)Pc (NiOAPc), cobalt 4,4',4",4"'-tetrakis(n-octadecanoylamino)Pc (CoOAPc) and copper 4,4',4",4"'-tetrakis(n-octadecanoylamino)Pc (CuOAPc) were synthesized and purified by the procedure given in 2.1.4 using n-octadecanoylchloride.

All these acylated derivatives of metal phthalocyanines have good solubility in chloroform, dichloromethane, DMSO and DMF.

2.1.6 Synthesis of tetrakissodium salt of (nickel, cobalt, copper) 4,4',4",4"'-tetrasulfophthalocyanine dihydrate

The mono sodium salt of 4-sulfophthalic acid (0.09 mmol), urea (0.97 mmol) ammonium molybdate (0.6 mmol) and stoichiometric amount of metal sulfate were ground together to a fine powder. Nitrobenzene (140 ml) was heated to 180°C in a 250 ml three-necked flask fitted with a thermometer, condenser and a stopper. The solid mixture was added slowly and then refluxed for 8 h. The crude

product was ground and washed with ethanol. The washed solid was added to one litre of 1 M HCl saturated with sodium chloride. This was heated to boiling, cooled and filtered. The resulting solid was dissolved in 500 ml 0.1 M sodium hydroxide. The solution was heated to 90°C and the insolubles were separated by filtration. Sodium chloride (270 g) was added to the solution, the precipitate was centrifuged and washed with 80% aqueous ethanol. The product was refluxed in ethanol filtered and dried.

2.1.7 Synthesis of 4,4',4",4"'-tetra(1-aminoethyl-sulfonamido)phthalocyanine

4,4',4",4"'-tetra(1-aminoethylsulfonamido)phthalocyaninecobalt(II) (CoTESPc) was synthesized as follows. Cobalt 4,4',4",4"'-tetrasulfonic acid was heated with PCl_3 in nitrobenzene for 4 h at 120°C. The cooled reaction mixture was poured into ice, the CoPc tetrasulfonyl chloride precipitated was filtered, washed and dried.

Freshly prepared CoPc tetrasulfonyl chloride (9.69 g) was mixed with crushed ice (300 g) and treated rapidly by stirring with ethylene diamine and NaOH (10%). The mixture on stirring came to solution at 5-10°C. The solution was acidified with dil. HCl. The precipitate

obtained was centrifuged and redissolved in water. Water was removed by distillation under vacuum.

4,4',4",4'"-Tetra(1-aminoethylsulfonamido)-phthalocyaninenickel(II) (NiTESPc) and 4,4',4",4'"-tetra(1-aminoethylsulfonamido)phthalocyaninecopper(II) (CuTESPc) were also synthesized and purified by the same procedure.

2.1.8 Synthesis of 4,4',4",4'"-tetra(sulfonamidobenzene-4-sulfonic acid)phthalocyaninecobalt(II) (CoTSSPc)

CoTSSPc was synthesized by a procedure similar to that described in section 2.1.7 using sulphanilic acid and CoPc tetrasulfonyl chloride.

2.1.9 Synthesis of 4,4',4",4'"-tetraaminophthalocyanine-cobalt(II) 3,3',3",3'"-tetrasulfonic acid (CoTASPc)

CoTASPc was synthesized as follows. CoTAPc was heated with chlorosulfonic acid at 120°C for 3 h. The crude product was added to 500 ml 1 M HCl saturated with sodium chloride. This was heated to boiling, cooled and filtered. The resulting solid was dissolved in 500 ml 0.1 M NaOH. The insolubles were separated by filtration, NaCl was added to the solution and the precipitated CoTASPc was centrifuged and dried.

2.2 CHARACTERIZATION OF METAL PHTHALOCYANINES

2.2.1 Elemental analysis

The metal phthalocyanines synthesized were characterized by the following physical and chemical methods. Nitrogen was determined with CHN Analyzer. Sulfur content of the compounds was determined by Schoniger oxygen flask method.[2] The metal content was determined by AAS after digestion with con. HNO_3 and appropriate manipulations recommended.[3] Elemental analysis of metal phthalocyanines and their derivatives are presented in Table 2.1.

2.2.2 Absorption spectra

The electronic absorption spectra of metal phthalocyanines were taken in 18 M sulphuric acid and the infrared spectra were recorded in Nujol/KBr. Table 2.2 shows the electronic absorption spectral data of metal phthalocyanine in 18 M sulphuric acid.

The visible spectra of acylated metal phthalocyanines and sulfonato and sulfamido metal phthalocyanines depend on the solvent used. In chloroform, acylated phthalocyanines show different spectra compared to those in DMF/EtOH probably due to molecular association. Tables 2.3 and 2.4 shows the visible absorption spectral

Table 2.1: Elemental analysis of metal phthalocyanines and their derivatives

sample	% nitrogen		% sulfur		% metal	
	found	calcd.	found	calcd.	found	calcd.
NiPc	20.7	19.6			9.9	10.3
CoPc	20.1	19.6			10.2	10.3
CuPc	20.9	19.5			10.8	11.0
NiTNPc	23.8	22.4			7.3	7.3
CoTNPc	23.0	22.4			7.8	7.9
CuTNPc	22.7	22.2			8.4	8.4
NiTAPc	26.0	26.6			9.2	9.3
CoTAPc	26.9	26.6			9.0	8.3
CuTAPc	25.9	26.4			9.9	10.0
NiDAPc	12.1	12.4			4.0	4.3
CoDAPc	12.0	12.4			4.2	4.3
CuDAPc	12.8	12.3			4.3	4.7
NiOAPc	9.8	9.9			3.5	3.5
CoOAPc	9.4	9.9			3.5	3.5
CuOAPc	9.4	9.9			3.0	3.7
NiTSPc	11.7	11.4	12.90	13.5	4.9	5.8
CoTSPc	11.9	11.0	11.5	12.6	5.1	5.7
CuTSPc	11.8	11.0	11.7	12.6	5.9	6.2
CoTESPc	21.1	21.6	11.8	12.1	5.4	5.5
CoTSSPc	10.7	11.1	16.2	16.9	3.3	3.9
CoTASPc	17.1	12.7	12.9	13.5	5.7	6.2

Table 2.2: Electronic absorption spectral data of MPcs in 18 M sulphuric acid

sample	λ_{max}	logϵ	λ_{max}	log ϵ	λ_{max}	log ϵ
NiPc	774	4.57	694	4.18	302	4.61
CoPc	782	5.09	700	4.48	291	4.72
CuPc	794	5.36	704	4.56	306	4.76

data of acylated and sulfonamides of MPcs respectively. In the case of sulfonated and sulfamido phthalocyanines the spectra in water are different from those in ethanol/water. This may be due to the formation of aggregates as evidenced by the concentration dependence of their absorption spectra.

Table 2.3: Visible absorption spectral data of acylated phthalocyanines in chloroform/DMF

sample	λ_{max}, (nm)	
	monomer	dimer
NiDAPc	678.0	610.0
CoDAPc	683.5	621.4
CuDAPc	690.5	614.0
NiOAPc	703.5	610.5
CoOAPc	679.5	619.5
CuOAPc	706.2	619.5

Table 2.4: Visible absorption spectral data of sulfonamides of cobalt phthalocyanines in 20% v/v ethanol/water

sample	λ_{max}, (nm)	
	monomer	dimer
CoTESPc	668	630
CoTSSPc	659	659
CoTASPc	688	639

2.2.3 Infrared spectra

Infrared spectral studies have been used as the main tool for the investigation of the metal phthalocyanines because of the characteristic "finger print" of the substituent and the phthalocyanine ring. Proof of the formation of substituted metal phthalocyanines has been based mainly on correlation of the infrared spectrum. The characteristic absorptions in the infrared spectra of metal phthalocyanines are presented in Table 2.5.

The infrared spectra of sulfonamides and aminosulfonic acids of cobalt phthalocyanine show strong

Table 2.5 Characteristic absorptions (cm^{-1}) in the ir spectra of metal phthalocyanenes*

Correlations	NiPc	CoPc	CuPc	CoTNPc	CoTAPc	CoDAPc	CoCAPc	Ni(Pc)I	Co(Pc)I	Cu(Pc)I
ø (C-C)	428w, 485w 530w, 575w 630w	435w, 490w 525w, 575w 625w	434w, 490w 530w, 570w 625m	554m, 622w 640s	490s, 530s 560s, 630w	465w, 535w 675m	540m, 610w 680m	530w, 570w 630w	525w, 540w 578w, 630m	495w, 540w 580w
δ(N-H)	725s	730s	728s	755s	740s	715s, 745sh	745sh	730s	728s	724s
ν(C-H)	730s, 740s 750s, 780m	735m, 745s 750s, 774m	740s, 750s 782sh	780sh	760sh, 830sh	772w, 810sh	770w, 810sh	755s, 780m	758s, 780s	750s, 770m
γ(C-H)	870m	868m	880m	854s, 872m	850s			870w	880s	880w
Pyrrole ring β(C-H)	1090m, 1095m 1100m, 1120m	1092s, 1088s 1170m	1080s, 1115s 1164s	1165s, 1180w	1130m, 1180s	1072s, 1080s	1090w, 1110sh	1090s, 1120s 1160w	1070s, 1092m 1120s, 1160w	1085w, 1120s 1160w
(C-C)	1290s, 1330s 1422s, 1465w 1610w	1290s, 1332s 1420s, 1468m 1590w, 1610m	1288s, 1330s 1420s, 1464w 1610m	1258s, 1296s 1344w, 1450s 1600s	1250s, 1320w 1340w, 1390s 1450s, 1610m	1240s, 1270sh 1290s, 1320w 1440w	1180w, 1195w 1290s 1370s 1400sh, 1450s	1290s, 1330s, 1425w, 1463w 1525w, 1600w	1290s, 1330s 1420s, 1460w 1520s, 1600m	1290w, 1330w 1415w, 1480w 1600m
-(NO_2)				1575s						
χ(C=O)						1530br m (amide II) 1680s (amide I)	1530br.m (amide II) 1690s (amide I)			
ν(N-H)	3200 br	3220 br	3230 br		3220 s	3200 br	3200 br	3200w	3230w	3220w

Intensity: w weak; m medium; strong: br broad; sh shoulder

* The infrared spectral absorption of the $-NO_2$, $-NH_2$, amido and sulfonamido derivatives of CoPc alone are presented in the table. The spectral bands of CuPc and NiPc derivatives are not listed in the table. The spectra of these derivatives were recorded and the characteristic absorption bands are more or less at the same positions as those of CoPc derivatives.

absorption at 1330-1360 cm^{-1}, 1160-1180 cm^{-1} indicative of the presence of sulfonamide functional group. These phthalocyanine derivatives also show peaks at 750-780, 870-890 and 1080-1180 cm^{-1} which are characteristic of metal phthalocyanines.

REFERENCES

1. Venkataraman, K.; The Chemistry of Synthetic Dyes, Academic Press, New York, 171, 271.

2. Schoniger, W. Mikrochim. Acta 1956, 869.

3. Louis Meites, Handbook of Analytical Chemistry; McGraw Hill, 1963.

CHAPTER - III

SELF - ASSEMBLING FEATURES OF ACYLATED PHTHALOCYANINES

3.1 INTRODUCTION

The optical and electrical properties of phthalocyanines (Pcs) have been studied extensively. Metal-free and metal-ligated Pcs tend to assemble into aggregates of varying sizes by weak van der Waals forces.[1,2] The aggregation of dye molecules in concentrated aqueous solutions was first suggested to explain their deviation from Beer's law. Aggregation of dye molecules has fundamental consequences in applications as diverse as photography,[3] tunable dye lasers,[4] micro-electronic devices based on organic substances,[5] liquid crystals,[6] and phototherapy.[7] The formation of aggregates modifies the absorption spectrum, and physical and photophysical properties.

Absorption and fluorescence spectroscopy are the techniques most widely used in the study of aggregates. Valuable information on the aggregation of complex organic molecules in solution could be derived from spectral shifts, nonconformity with Beer's law and fluorescence quenching at higher concentrations arising from second order spectroscopic interference of dye chromophores. An analysis of the changes occurring in the absorption

spectrum due to the change in the concentration of the dye allows the evaluation of the equilibrium constant for association. Several mathematical treatments have been developed for this purpose.[8]

The association between two or more dye molecules depends on the structure of the dye, the solvent, the temperature and the presence of electrolytes. The dimers and other aggregates of phthalocyanines, chlorophylls etc., are found to be important both in solid matrices and in solutions. Many investigations have focused on the mechanistic details of inter-molecular interactions in phthalocyanine type molecules. It has been found that spectroscopic investigations in solutions are more amenable to give unambiguous information, since interferences from polymorphs can be eliminated.

Metal phthalocyanines (MPcs) exhibit high chemical and thermal stabilities among organic compounds. Unsubstituted Pc molecules have some limitations in organizing in a desired array due to insolubility in common organic solvents, and polymorphism in the solid phase.

One of our objectives in this study is to control the lattice architecture and electron delocalisation in

films of molecular semiconductors which find applications as components in molecular electronic devices. For this purpose, the Pcs should be soluble in a suitable solvent. Another requirement is that the Pc molecules are capable of arranging in a one-dimensional (1-D) linear stack with van der Waals thickness.

Metal phthalocyanines with four amino groups converted to the amide of long chain aliphatic acid have been synthesized. Ni, Co and CuPc derivatives were prepared. If the four secondary amide units were symmetrically introduced on the Pc ring, the most favourable structure expected is a 1-D stacking array due to hydrogen bonding. The hydrophilic amides can impart ordered film-forming ability to the Pc molecules. In biological systems, the secondary amides are well known to play an important role in fixing the functional moieties into a specific conformation through directional hydrogen bonding.[9]

Aggregation of Pc in solution to form dimers and higher aggregates has been studied for tetrasulfonated CuPc in aqueous and alcoholic solution[10] and for tetrakis[((cobalt(II) 9,6,23-trineopentoxyphthalocyanin-2-yl)-oxy)-methyl]methane in o-dichlorobenzene.[11,12] Ni, Co and

Cu phthalocyanines with four long chain amide groups are soluble in a variety of solvents and can be conveniently incorporated into polymer matrices.

3.1.1 Diffusion of dyes into polymers

Polymers are used as matrices for dye lasers and optical recording films,and in certain cases to improve the photostability of organic dyes. Introduction of dyes into polymers can be realised either by the polymerisation of the monomer in a solution of the dye or by the diffusion of the dye into swollen polymer in a concentration gradient. Dye lasers have been successful in lase tuning at any wavelength between near infrared and ultraviolet, in pulsed as well as cw operation. The advances in dye lasers and in other optical devices like optical recording films in which organic dyes play a major role, require a study on the fundamental properties of the dyes. Further developments in the application of organic dyes for various optical devices, have been hindered by their inadequate photo-chemical stability. Photodegradation of the dye imposes greater restrictions on devices in which dye molecules are incorporated into a solid matrix, or when the active element is cast with a binder. Phthalocyanines, because of their thermal and photochemical stability deserve special attention.

The diffusion of a dye from a solution into polymeric or gel media and the characteristics imparted to the host matrices depend on the extent of aggregation and the nature of the aggregate formed.

3.2 EXPERIMENTAL

Nickel, cobalt and copper derivatives of 4,4',4",4"'-tetrakis(n-dodecanoylamino)Pc and 4,4',4",4"'-tetrakis(n-octadecanoylamino)Pc were synthesized and purified according the procedure described in sections 2.1.4 and 2.1.5. The self assembling features of these substituted phthalocyanines and their aggregation equilibria in DMF, $CHCl_3$ and in DMF-$CHCl_3$ mixtures were studied by spectrophotometry.

Solutions for aggregation studies were prepared by diluting a freshly prepared solution of the phthalocyanine. Spectra were recorded immediately after each dilution.

3.3 RESULTS AND DISCUSSION

The acylated phthalocyanines (APcs) of nickel, cobalt and copper were characterized by elemental analysis, UV-vis and IR spectra. The X-ray diffraction experiments

and observation under a polarizing microscope were performed for CoOAPc. The studies suggest that the phthalocyanine derivatives do not exhibit any liquid crystalline behaviour. CoOAPc becomes isotropic at 57°C and the crystalline structure is lamellar with a layer spacing of about 38.5 Å. No texture characteristics of liquid crystals was detected for CoOAPc.

Phthalocyanines possess degenerate Q bands originating from π-π^* transitions. These bands are comprised of both metal and ligand transitions with the same energies and oscillator strength along the Pc ring. Fig.3.1 shows the molecules structure of acylated metal phthalocyanine (MAPc).

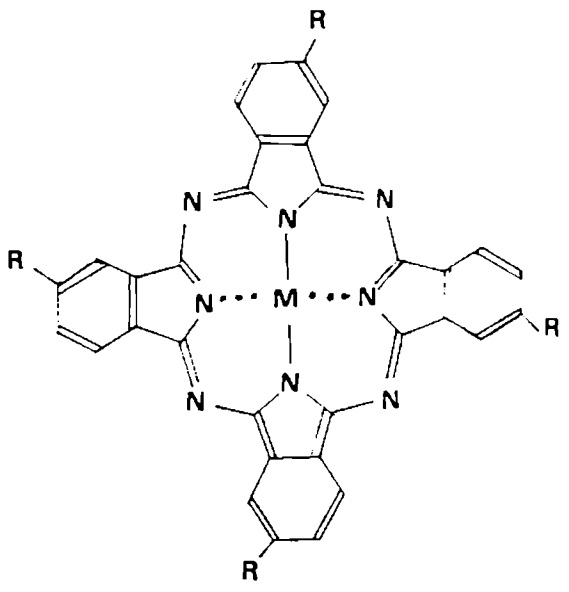

M = Ni, Co, Cu

R = $-NH-\overset{\overset{O}{\|}}{C}-C_{12}H_{25}$

R = $-NH-\overset{\overset{O}{\|}}{C}-C_{18}H_{37}$

Fig.3.1: Molecular structure of acylated metal phthalocyanine (MAPc).

The Q band of the electronic spectrum is considered as a sensitive probe in characterising the self assembling features of acylated Pc (APc) in solution and in polymer matrices. Fig.3.2 shows the absorption spectra of NiDAPc, NiOAPc, CoDAPc, CoOAPc, CuDAPc and CuOAPc in chloroform. The spectra of MAPcs in $CHCl_3$ solution are comprised of intense Q bands located in the 605-625 nm range and a weak satellite Q band located in the range 675-705 nm. The λ_{max} for the main Q bands of these acylated Pcs are strongly blue-shifted by about 70 nm from the λ_{max} of the satellite band.

Figs.3.3a, 3.3b, 3.4a and 3.4b show the effect of concentration on the absorption spectra of NiDAPc, CoDAPc, CuDAPc and CoOAPc respectively in $DMF/CHCl_3$,(4% v/v). The Q band region of NiDAPc consists of two bands, one with λ_{max} at 610 nm and a shoulder at 678 nm. The 610 nm band intensity increases relative to that at 678 nm with increasing phthalocyanine concentration. The 610 nm and 678 nm bands are the dimer and monomer bands respectively. The λ_{max} values of monomer and dimer forms of APc are tabulated in Table 3.1. The dimer λ_{max} values of Cu and Ni derivatives are more blue-shifted than those of the corresponding Co compound.

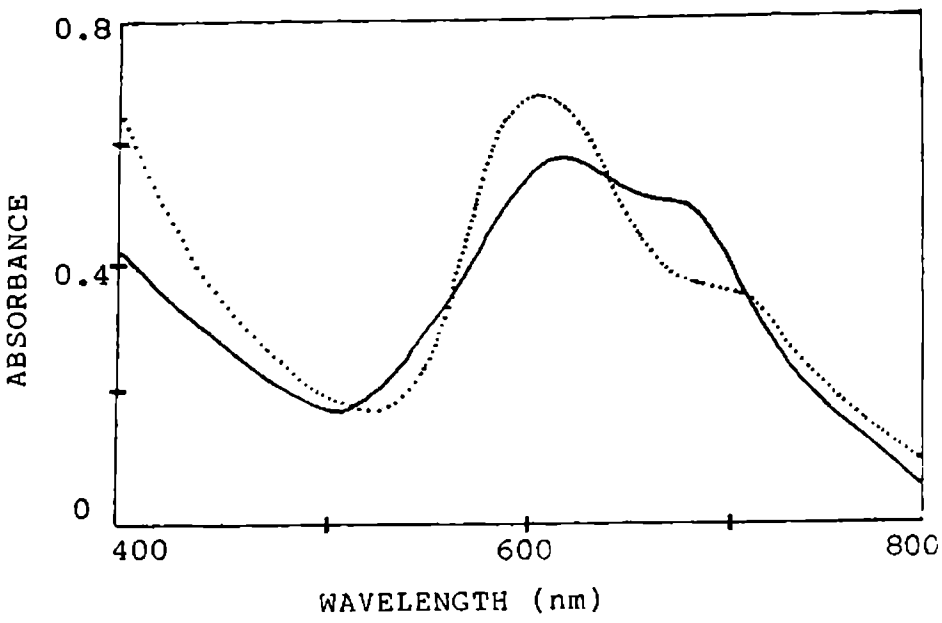

Fig.3.2a: Absorption spectrum of NiDAPc and NiOAPc in $CHCl_3$; Concentration: 3×10^{-4} M

—— NiDAPc NiOAPc

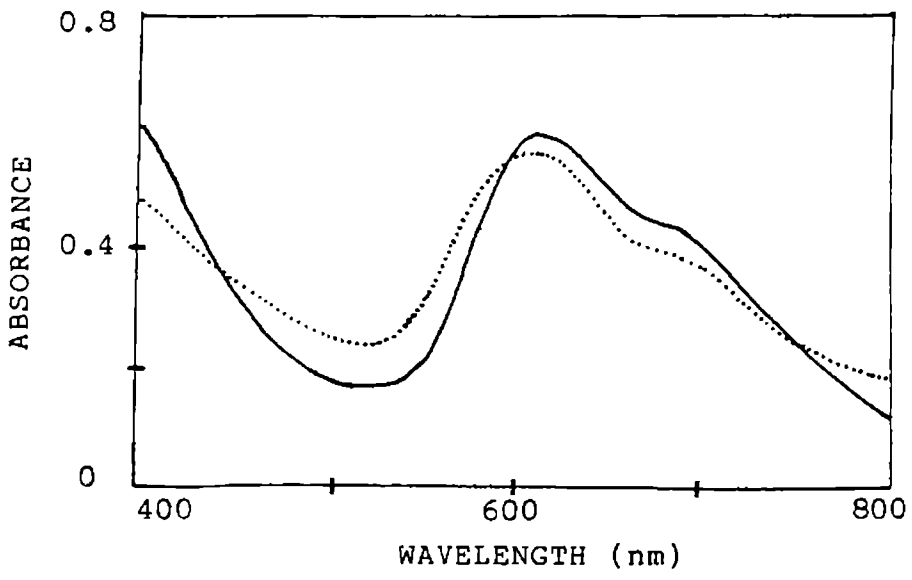

Fig.3.2b: Absorption spectrum of CoDAPc and CoOAPc in chloroform; Concentration: 6×10^{-5} M

—— CoDAPc CoOAPc

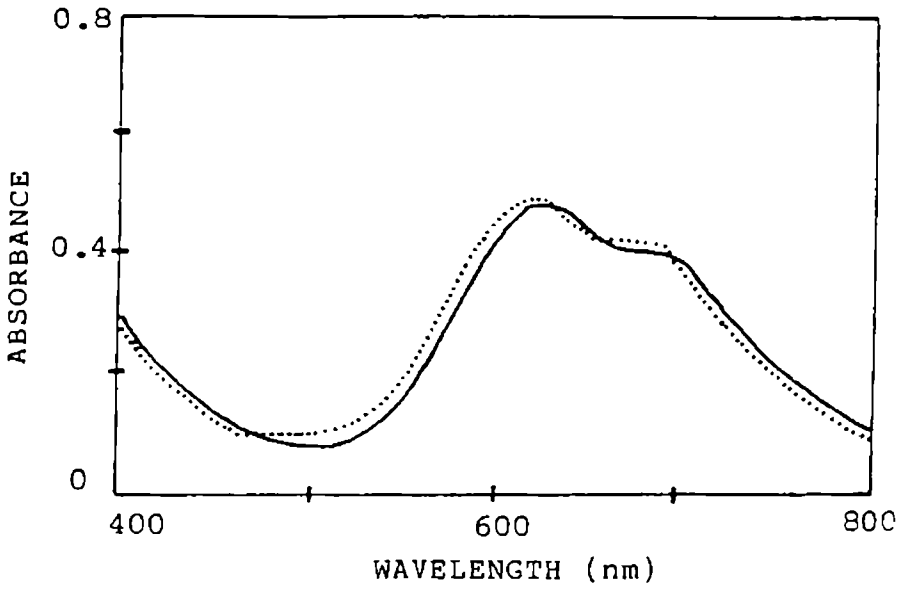

Fig.3.2c: Absorption spectrum of CuDAPc and CuOAPc in $CHCl_3$; Concentration: 3×10^{-4} M

——— CuDAPc CuOAPc

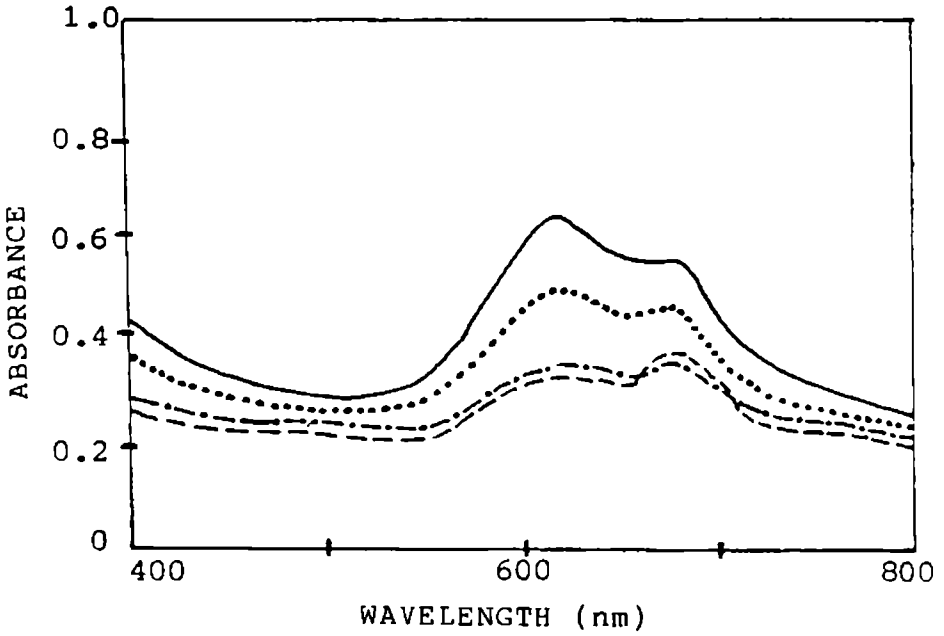

Fig.3.3a: The effect of concentration on the absorption spectra of NiDAPc in $DMF/CHCl_3$ (4% v/v)

——— 3.56×10^{-4} 2.24×10^{-4}

—·—·— 1.16×10^{-4} – – – – 1.032×10^{-4}

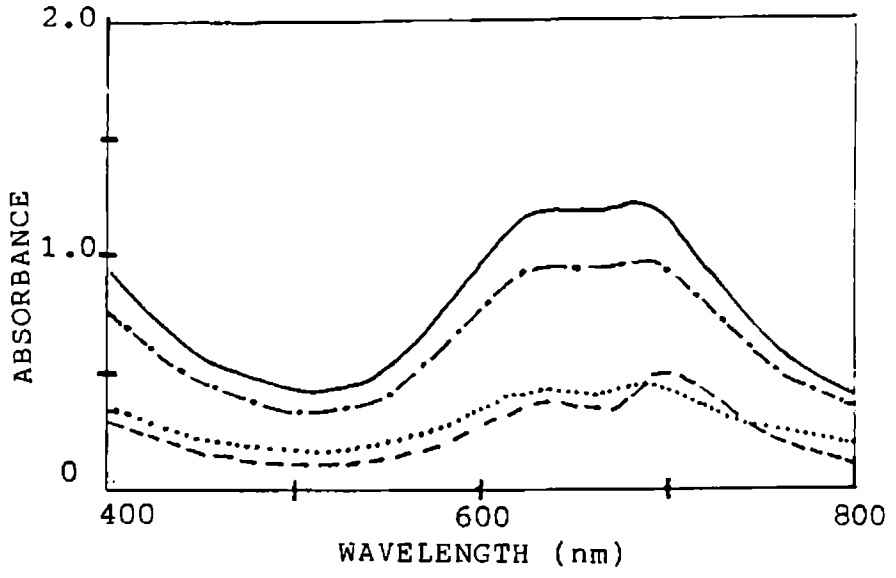

Fig.3.3b: The effect of concentration on the absorption spectra of CoDAPc in $DMF/CHCl_3$ (4% v/v)

——— 8.43×10^{-5} M —·—·— 6.32×10^{-5} M

3.50×10^{-5} M – – – – 2.21×10^{-5} M

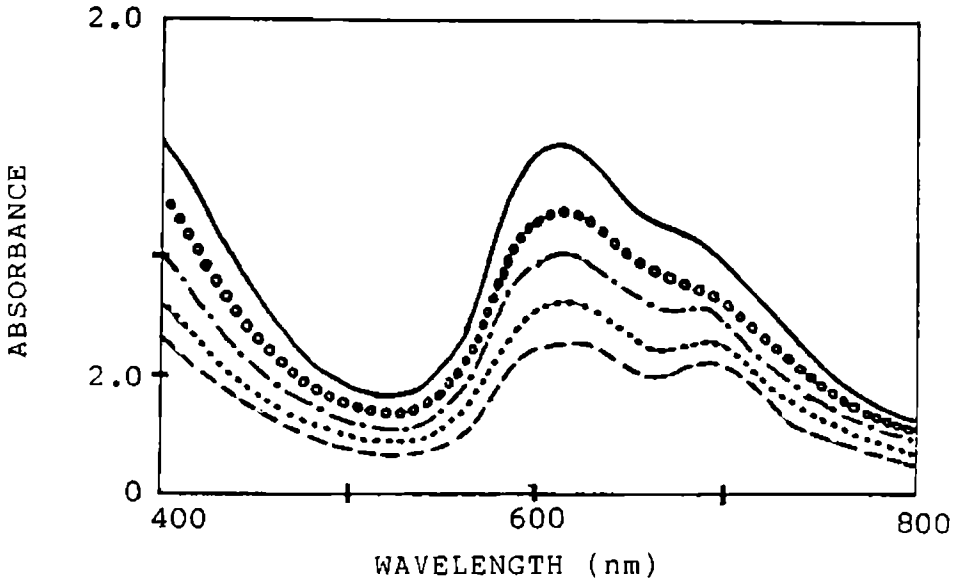

Fig.3.4a: The effect of concentration on the absorption spectra of CuDAPc in $DMF/CHCl_3$ (4% v/v)

—— 9.96×10^{-4} M
3.296×10^{-4} M
- - - - 1.96×10^{-4} M
°°°°° 8.30×10^{-4} M
-·-·- 6.23×10^{-4} M

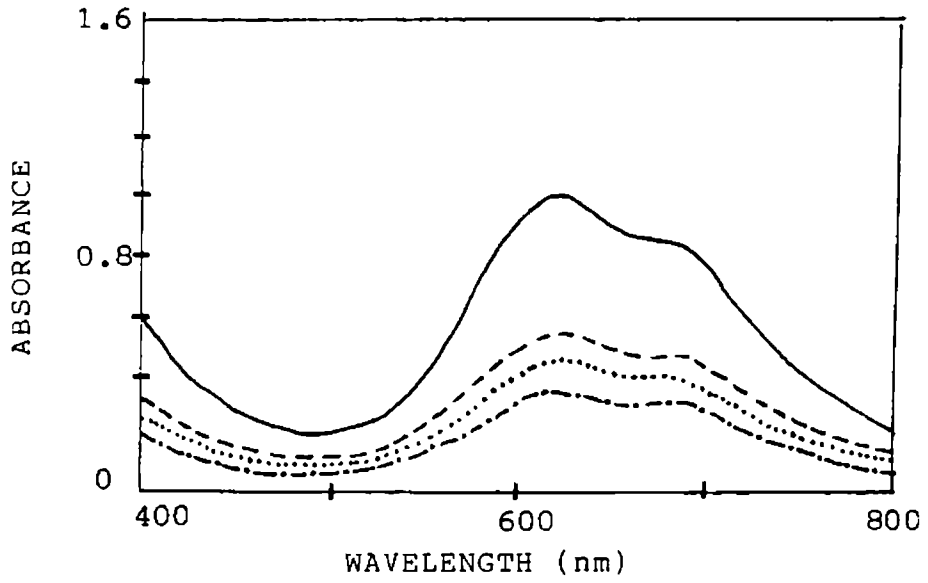

Fig.3.4b: The effect of concentration on the absorption spectra of CoOAPc in $DMF/CHCl_3$ (4% v/v)

—— 7.45×10^{-4} M
5.54×10^{-4} M
- - - - $5.591\ 10^{-4}$ M
-·-·- 2.802×10^{-4} M

Table 3.1: Visible spectra of acylated phthalocyanines in chloroform

materials	Observed λ_{max} (nm)	
	monomer	dimer
NiDAPc	678.0	610.0
CoDAPc	683.5	621.4
CuDAPc	690.5	614.0
NiOAPc	703.5	610.5
CoOAPc	679.5	619.5
CuOAPc	689.4	612.0

Such broadening and blue-shifting of the Q band for acylated phthalocyanines is found to be characteristic of the Q band spectra of 1-D linearally stacked Pc polymers with van der Waals thickness, as in O-linked metal tetra(tert-butyl) phthalocyanine polymer, $(TBPcMO)_n$[13] and O-linked PcM polymer $(PcMO)_n$.[14]

An equilibrium between the monomer (M) and the dimer (D) forms of MPc exists in solution,

$$M + M \rightleftharpoons D$$

where K_d is the dimerization constant, given by $K_d = C_D/C^2_M$ C_M and C_D are the concentrations of monomer and dimer respectively at a total concentration C_T. If a simple monomer-dimer equilibrium alone exists a plot of log C_M vs. log C_D would give a straight line of slope equal to '2' as seen for several mononuclear cobalt phthalocyanines in o-dichlorobenzene.[15] Calculation of the values of C_M and C_D at any given total concentration is normally carried out using the relative intensities at the λ_{max} of the monomeric and dimeric species using the equation given below:

$$C_M = \frac{A - C_T(\epsilon_D)/2}{\epsilon_M - (\epsilon_D)/2}$$

$$C_D = \frac{C_T - C_M}{2}$$

where A - absorbance of monomer at λ_{max}

C_T - total concentration of MPc

ϵ_D and ϵ_M - molar absorptivities of dimer and monomer respectively

C_D and C_M - molar concentration of dimer and monomer respectively.

The equilibrium constant for the dimerization of MAPc in DMF/$CHCl_3$ (4% v/v) was evaluated. Tables 3.2, 3.3, 3,4 and 3.5 show the monomer-dimer equilibrium for NiDAPc, CoDAPc, CuDAPc and CoOAPc in DMF/$CHCl_3$.

Table 3.2: Monomer-dimer equilibrium of NiDAPc in $DMF/CHCl_3$ (4% v/v) at 28 ± 2°C

total conc. of NiDAPc mol l^{-1} ($\times 10^4$)	monomer conc. mol l^{-1} ($\times 10^4$)	dimer conc. mol^{-1} ($\times 10^4$)	equilibrium constant l mol^{-1} ($\times 10^{-4}$)
3.560	0.957	1.302	1.42
3.255	0.937	1.159	1.32
2.240	0.768	0.730	1.24
1.160	0.528	0.317	1.13
1.032	0.478	0.277	1.21

Average value of $K_d = 1.26 \times 10^4$ l mol^{-1}

Table 3.3: Monomer-dimer equilibrium of CoDAPc in $DMF/CHCl_3$ (4% v/v) at 28 ± 2°C

total conc. of CoDAPc mol l^{-1} ($\times 10^4$)	monomer conc. mol l^{-1} ($\times 10^4$)	dimer conc. mol^{-1} ($\times 10^4$)	equilibrium constant l mol^{-1} ($\times 10^{-4}$)
0.843	0.316	0.263	2.63
0.632	0.284	0.174	2.16
0.350	0.180	0.085	2.62
0.221	0.127	0.047	2.91

Average value of $K_d = 2.58 \times 10^4$ l mol^{-1}

Table 3.4: Monomer-dimer equilibrium of CuDAPc in $DMF/CHCl_3$ (4% v/v)at 28 ± 2°C

total conc. of CuDAPc mol l^{-1} ($\times 10^4$)	monomer conc. mol l^{-1} ($\times 10^4$)	dimer conc. mol l^{-1} ($\times 10^4$)	equilibrium constant $l\ mol^{-1}$ ($\times 10^{-4}$)
9.960	1.350	4.305	2.36
8.301	1.201	3.550	2.40
6.230	1.100	2.565	2.12
3.296	0.760	1.268	2.20
2.420	0.640	0.890	2.17
1.960	0.550	0.705	2.33

Average value of $K_d = 2.27 \times 10^4\ l\ mol^{-1}$

Table 3.5: Monomer-dimer equilibrium of CoDAPc in $DMF/CHCl_3$ (4% v/v)at 28 ± 2°C

total conc. of CoDAPc mol l^{-1} ($\times 10^4$)	monomer conc. mol l^{-1} ($\times 10^4$)	dimer conc. mol l^{-1} ($\times 10^4$)	equilibrium constant $l\ mol^{-1}$ ($\times 10^{-5}$)
7.450	0.448	3.501	1.81
6.745	0.385	3.180	2.15
5.591	0.337	2.627	2.31
5.544	0.380	2.582	1.79
2.802	0.240	1.281	2.22

Average value of $K_d = 2.05 \times 10^5\ l\ mol^{-1}$

Figs.3.5a, 3.5b, 3.6a and 3.6b show the plots of log C_M vs. log C_D for NiDAPc, CoDAPc, CuDAPc and CoOAPc respectively. Slope values of 2.08, 1.89, 2.20 and 1.97 were obtained for NiDAPc, CoDAPc, CuDAPc and CoOAPc respectively. This indicates the existence of dominant monomer-dimer equilibria in these systems in the concentration range studied.

3.3.1 Effect of DMF addition on the absorption spectra of acylated phthalocyanines

The effect of the addition of DMF on the absorption spectra of dodecyl and octadecyl amides of Ni, Co and CuPc was studied. Figs.3.7a, 3.7b, 3.8a and 3.8b show the effect of DMF addition on their absorption spectra. DMF addition results in the dedimerization of NiDAPc, CoDAPc, CuDAPc and CoDAPc. In the case of octadecylamides of NiPc and CuPc the monomer is not generated by DMF addition, indicating the formation of stable dimer in solution. Figs.3.9a, 3.9b, 3.10a and 3.10b shows the monomer and dimer forms of MAPcs.

3.3.2 Conclusion

Ni, Co and Cu phthalocyanines substituted with four dodecyl amide groups have very good solubility in organic solvents. The octadecyl amides of Ni, Co and Cu

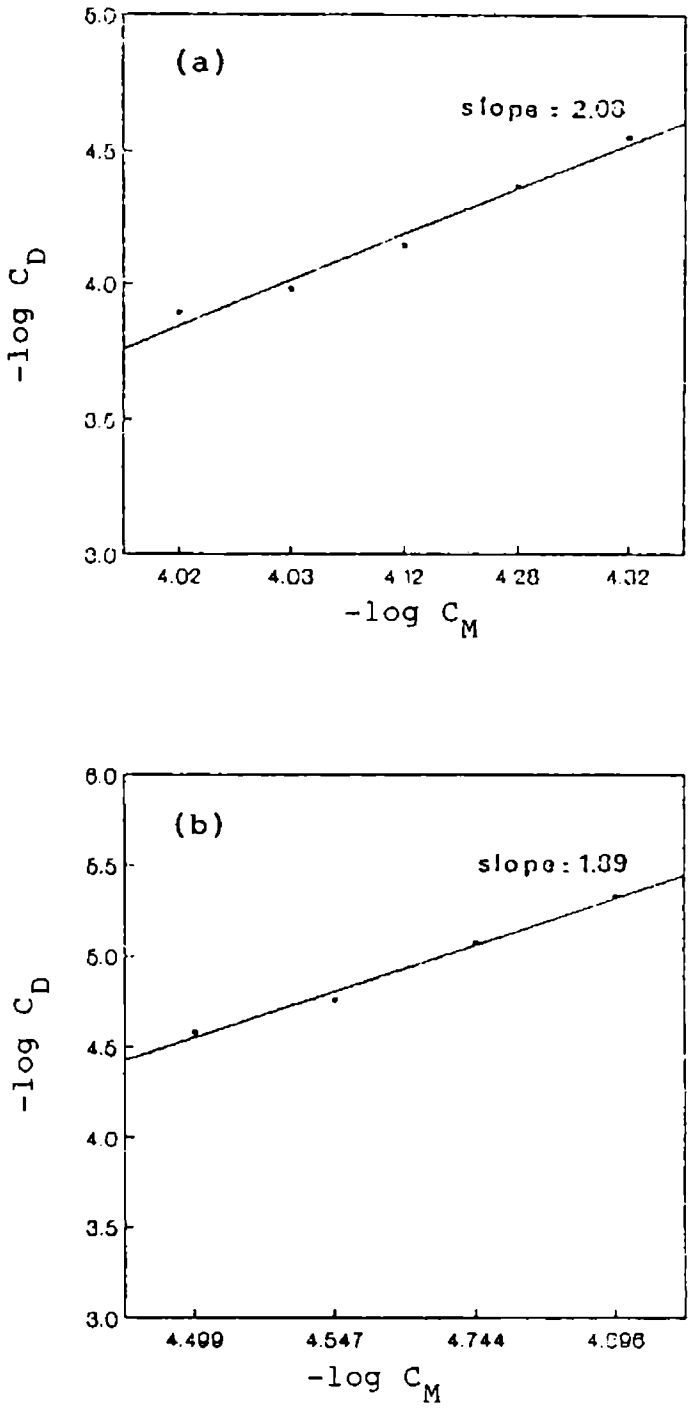

Fig.3.5: Plot of log C_M versus log C_D for (a) NiDAPc; (b) CoDAPc in DMF/$CHCl_3$ (4% v/v) at 28 ± 2°C

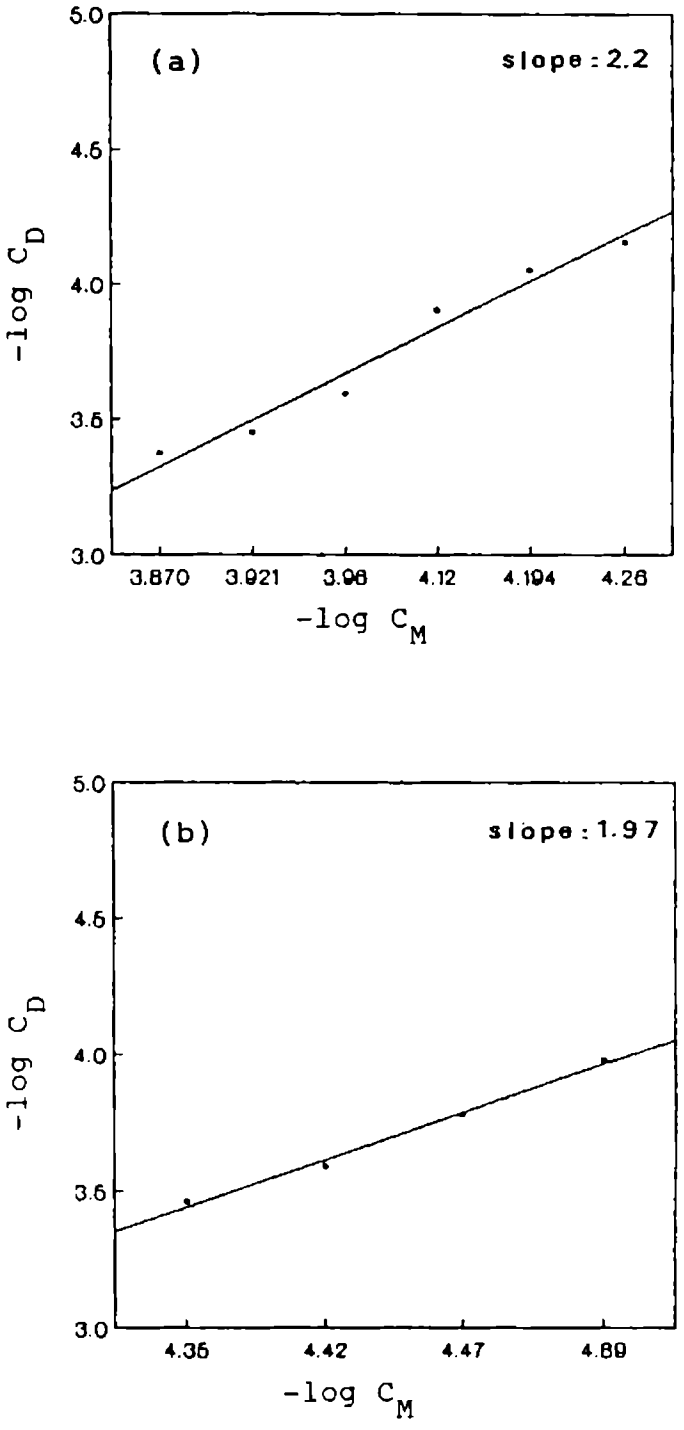

Fig.3.6: Plot of log C_M versus log C_D for (a) CuDAPc; (b) CoOAPc in DMF/$CHCl_3$ (4% v/v) at 28 ± 2°C

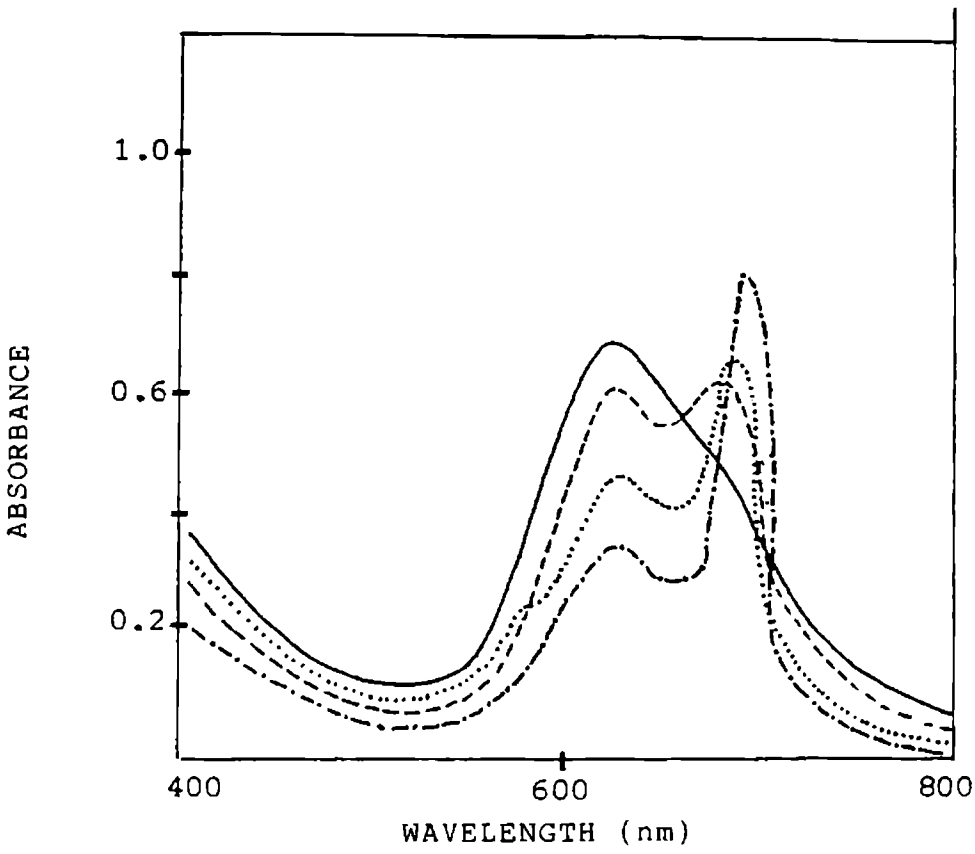

Fig.3.7a: The effect of the addition of DMF on the absorption spectra of NiDAPc in $CHCl_3$; concentration: 3.56×10^{-4} M

—— 0% DMF; - - - 5% DMF; ····· 10% DMF; -·-·- 20% DMF

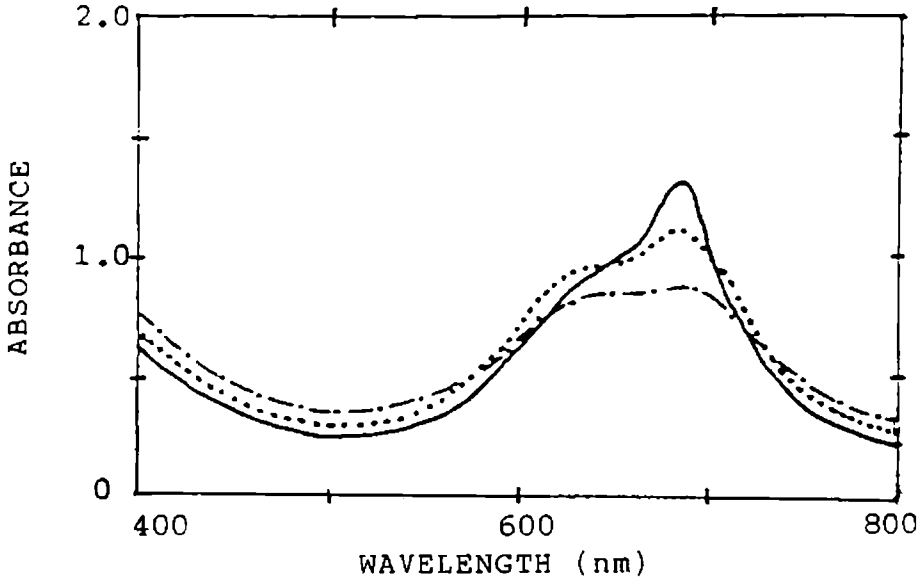

Fig.3.7b: The effect of the addition of DMF on the absorption spectra of CoDAPc in $CHCl_3$; Concentration: 6.02×10^{-5} M

-·-·- 0% DMF; ····· 10% DMF; —— 20% DMF

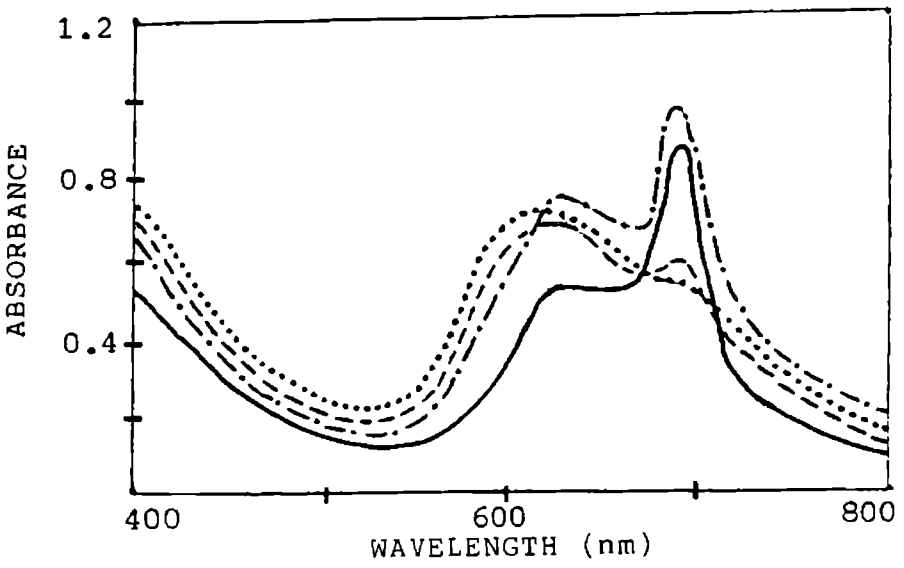

Fig.3.8a: Shows the effect of DMF addition on the absorption spectra of CuDAPc in $CHCl_3$; Concentration: 1.32×10^{-4} M

0% DMF — — — 5% DMF

—— 10% DMF ·—·—· 20% DMF

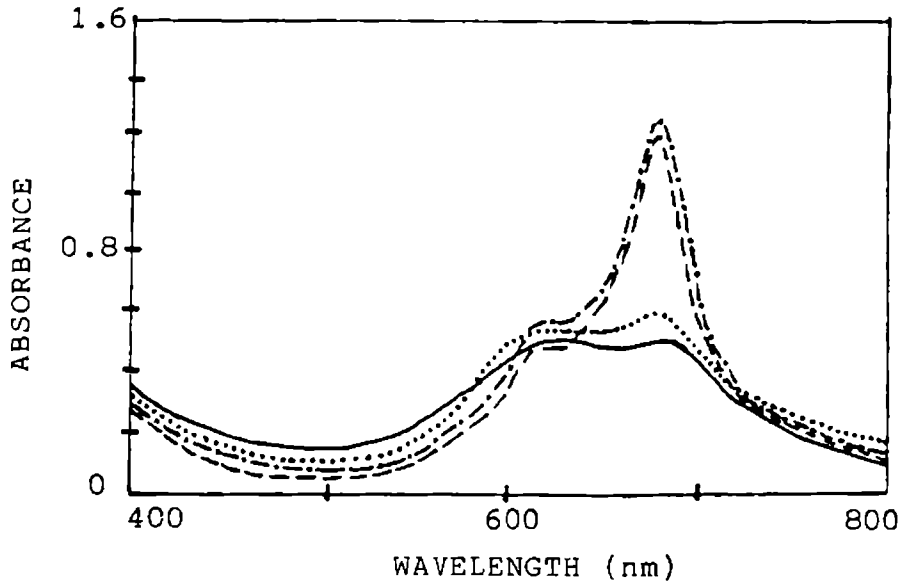

Fig.3.8b: Shows the effect of DMF addition on the absorption spectra of CoOAPc in $CHCl_3$; Concentration: 5.50×10^{-4} M

—— 0% DMF 5% DMF

— — — 10% DMF ·—·—· 20% DMF

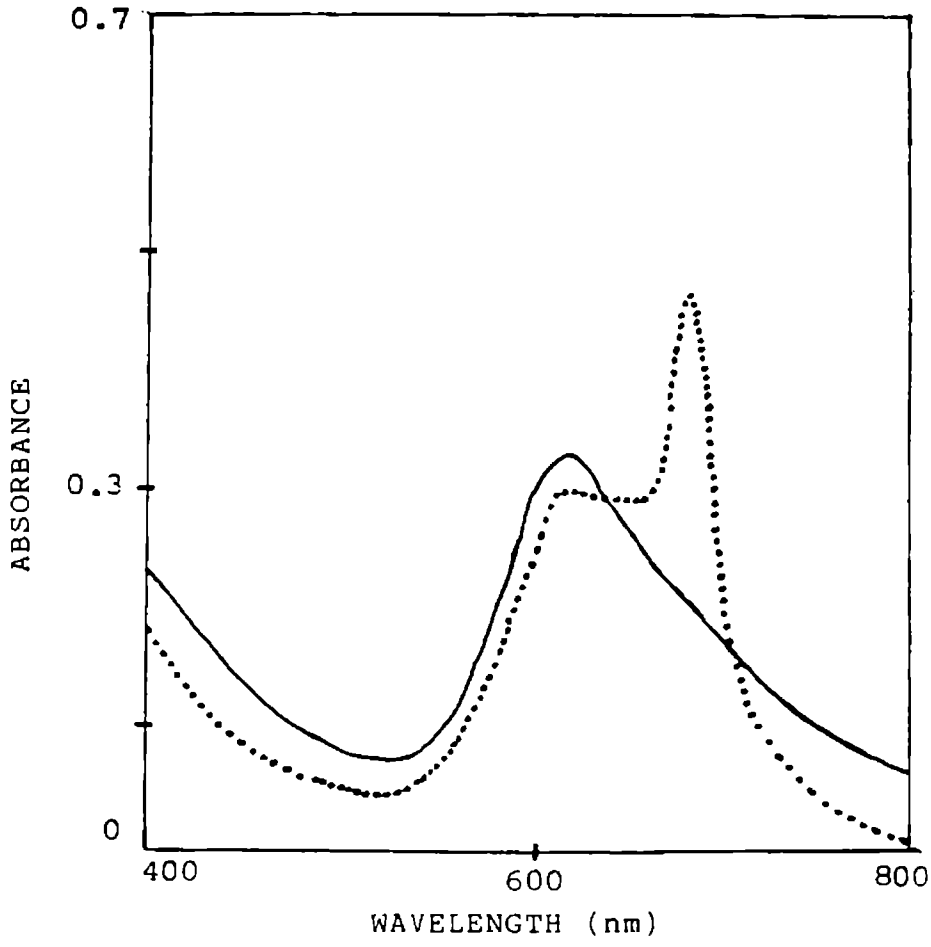

Fig.3.9a: Absorption spectra of the monomer and dimer forms of NiDAPc

—— dimer ($CHCl_3$) monomer (DMF)

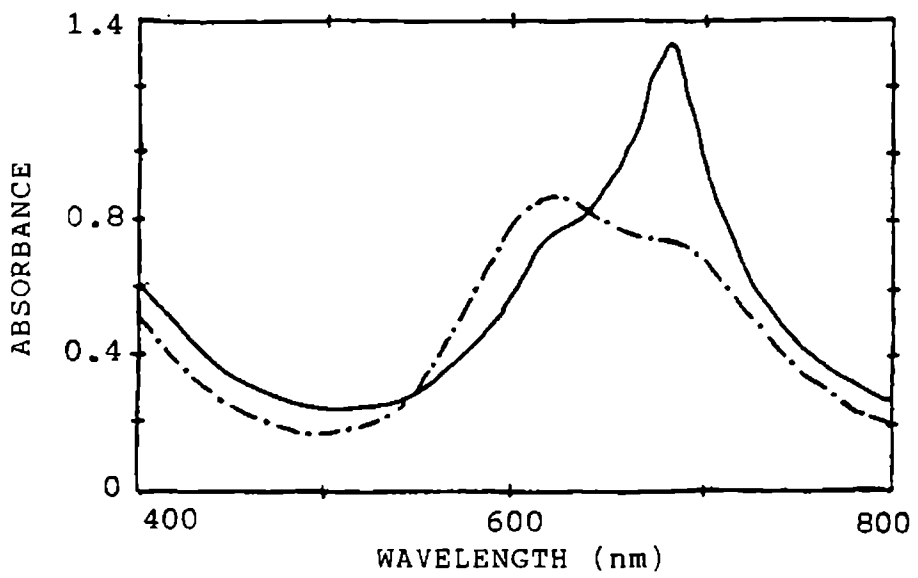

Fig.3.9b: Absorption spectra of the monomer and dimer forms of CoDAPc

·—·— dimer ($CHCl_3$) —— monomer (DMF)

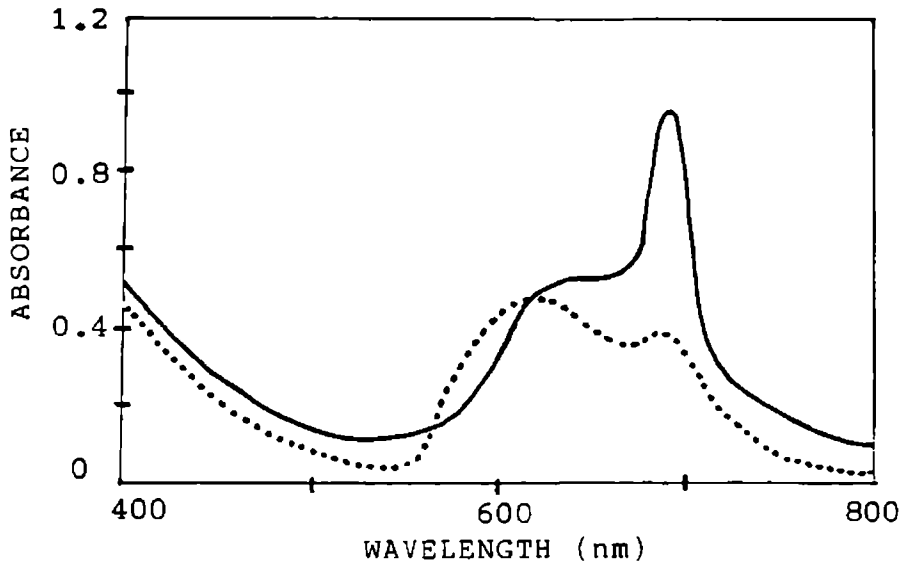

Fig.3.10a: Absorption spectra of the monomer and dimer forms of CuDAPc

dimer ($CHCl_3$) —— monomer (DMF)

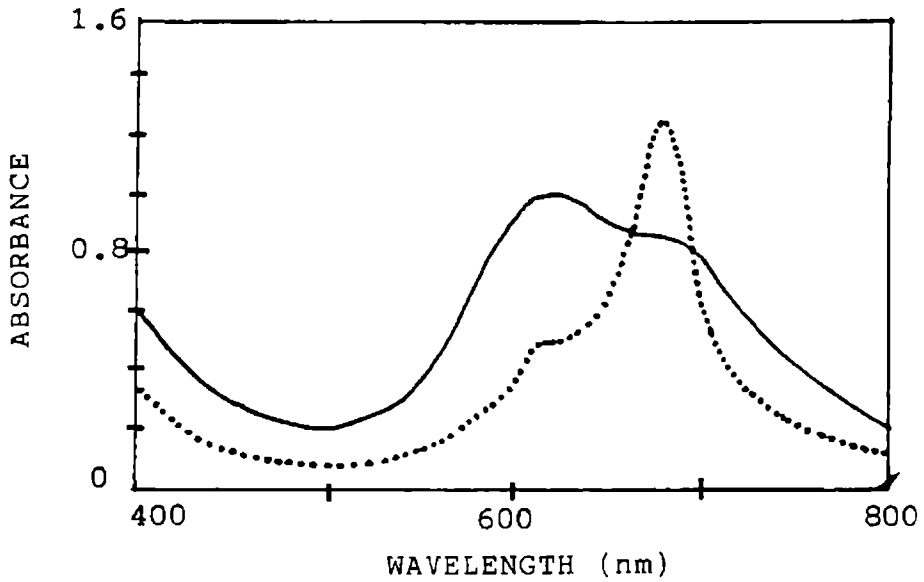

Fig.3.10b: Absorption spectra of the monomer and dimer forms of CoOAPc

—— dimer ($CHCl_3$) monomer (DMF)

phthalocyanines were also synthesized and the effect of aliphatic group on the self assembling features of these phthalocyanines were studied. These substituted phthalocyanines are shown to have one-dimensional self assembled structures with van der Waals thickness. This arises from the directional hydrogen bonding of the secondary amide in the solid state and in solution, which is evident from the electronic spectra. The Ni and Cu compounds are found to form more stable dimers than the cobalt analogue. As the length of the aliphatic chain on the amide group increases solubility of the phthalocyanines also increases. Addition of dimethyl formamide results in the generation of monomer in the case of dodecyl amide of Ni, Co, Cu and octadecylamide of CoPc. NiOAPc and CuDAPc do not form monomer even in pure DMF, indicating strong aggregation. In the case of CoDAPc the axial coordination of solvent may sterically hinder dimerization. These results are in good agreement with those obtained by Lever et al.[17] The electronic spectra of these substituted phthalocyanines in solution and in cast film are similar. This indicates that these molecules cofacially assemble with van der Waals thickness in the solid matrices also.

The metal phthalocyanines which sublime at $\sim$400°C, melt at 60-80°C on substituting with long chain aliphatic group. The low melting phthalocyanines can be used in photorecording by melt-flow technique. The acylated phthalocyanines can be spin coated over substrates for application as electron beam negative resists.

REFERENCES

1. Nohr, R.S.; Kuznesof, P.M.; Kenney, M.E.; Siebenmann, P.G. J. Am. Chem. Soc. 1981, 103, 4371.

2. Froster, Th.; Konig, E.Z. Elektrochem. 1957, 61, 344.

3. Norland, K.; Ames, A.; Taylor, T. Photogr. Sci. Eng. 1970, 14, 295.

4. Yuzhakov, V.I. Russ. Chem. Rev. (Engl. Transl.) 1979, 48, 1076.

5. Baker, S.; Petty, M.C.; Roberts, G.G.; Twigg, M.V. Thin Solid Films 1983, 99, 53.

6. Guillon, D.; Skoulis, A.; Piechoki, C.; Simon, J.; Weber, P. Mol. Cryst. Liq. Cryst. 1983, 100, 275.

7. Mac Robert, A.J.; Philips, D. Chemistry & Industry 1992, 17.

8. Monahan, A.R.; Blossey, D.F. J. Phys. Chem. 1970, 74, 4014.

9. Boucher, L.J.; Co-ordination Chemistry of Macrocyclic Compounds; Melson, G.A.; Ed. Plenum Press: New York, 1979, Chapter 7.

10. Warren, L.; Jeffrrey, J.; Kolstad, J. Inorg. Nucl. Chem. 1976, 38, 1835.

11. Monalian, A.R.; Brado, J.A.; Deluca, A.F. J. Phys. Chem. 1972, 76, 446.

12. Nevin, W.A.; Hempstead, M.R.; Liu, W.; Leznoff, C.C.; Lever, A.B.P. J. Inorg. Chem. 1987, 26, 570.

13. Muto, R.J.; Kobayashi, K. Phy. Status Solids (a) 1984, 84, K29.

14. Higuchi, F.; Muto, J. Phys. Lett. 1981, 86, 51.

15. Metz, J.; Pawlowski, G.; Hanack, M.Z.; Naturforsch, 1983, 38B, 378.

16. Disk, C.W.; Inabe, T.; Schoch, K.F. Jr.; Marks, T.J. J. Am. Chem. Soc. 1983, 105, 1539.

17. Nevin, W.A.; Melnik, M.; Lenoff, C.C.; Lever, A.B.P. J. Inorg. Chem. 1987, 26, 891.

CHAPTER - IV

AGGREGATION OF SULFONAMIDES OF COBALT PHTHALOCYANINES

4.1 INTRODUCTION

The optical properties of heterocyclic compounds with extended π system like phthalocyanines and porphyrins, have been the focus of attention for many investigations. These compounds have structural similarity with biologically important compounds like haemoglobin and chlorophyll. It is established that chlorophyll performs its functions through photoassisted electron transfer in its aggregated state. Also these systems are semiconductors and photoconductors. Phthalocyanines find applications as cyans in reprographic systems, and in transducers. The aggregation characteristics of soluble phthalocyanines and the mechanism of photoassisted electron transfer in these compounds are less understood.

Most of the studies on charge transport and photoassisted charge transport in MPcs have been in the solid phase. Except for a report on the optical properties of 4,4',4",4"'-tetraoctadecylsulfonamidophthalocyanine-copper(II) in carbon tetrachloride and in benzene,[1] this aspect remains largely unexplored.

The spectral characteristics of dyes in solution depend on the extent of aggregation, the nature of the association centres, and the nature of the solvent. In most of the macromolecules, the influence of solvent on the aggregation characteristics is more pronounced than that of the neighbouring molecules in the solid phase. The dye molecules are more polarized in the field of the solvent than in the field of adjacent molecules in the crystal lattice. This leads to a hypsochromic shift of the major absorption bands during the aggregation of the dye. Aggregation of water soluble MPcs is also accompanied by a hypsochromic shift from 670 nm to 630 nm as in $CuPc(SO_2O^-)_4$

The field of dye aggregation has received considerable attention, especially regarding dyes used in laser technology. Formation of aggregates reduces the output of the dye laser by a combination of absorption of radiation by non-fluorescent aggregates and quenching of the monomer excited state.

No single mechanism for dye association can be advanced, and in most cases the association is controlled by a combination of forces. Various mechanisms have been suggested to explain the forces holding dye monomers

together in solution. These included additive forces of the van der Waals type,[2] intermolecular hydrogen bonding,[3] hydrogen bonding with the solvent,[4] and coordination with metal ions.[5]

From the physicochemical stand point two cases of interaction between molecules in a dimeric associate, composed of planar molecules of the porphyrin type, can occur. In the first case the chromophores are stacked like a deck of cards. As a result of broadening of the region accommodating the π electrons of the chromophore this interaction involves a bathochromic shift of band. A single long wave band appears in the spectrum of dimeric associate. As more molecules are accumulated in the aggregate, another bathochromic shift follows, and the number of bands increases with their concomitent broadening.

The second case is a 'plane-edge' association, in which the centre of the chromophore of the porphyrin molecule contacts the edge of planar chromophore. In such a dimer the first molecule is acted upon by the chromophore centre and loses most of its solvation sheath. The second molecule is acted upon by the first one at the planar

chromophore and loses only an insignificant portion of the solvation sheath. The action of the centre of the phthalocyanine molecule involves hydrogen bonding and leads to a slight shift of the band, normally towards the short wave length region.

4.2 AGGREGATION OF 4,4',4",4"'-TETRA(1-AMINOETHYL-SULFONAMIDO)PHTHALOCYANINECOBALT(II), (CoTESPc)

4.2.1 Introduction

When two or more phthalocyanine molecules in solution are separated by a short enough intermolecular distance, the ring can interact electrostatically to form aggregates such as dimers, trimers etc. The formation of these aggregates depends on many factors such as the molecular structure of the dye, its concentration, pH of the medium, nature of the solvent and temperature.

Owing to the molecular interactions, the visible absorption spectrum of phthalocyanines in the monomeric form is different from that of the aggregates. This interaction can be treated by the exciton theory[6,7] which involves a quantum mechanical approach. Exciton theory predicts that the excited-state levels of the monomer split into two upon dimerization. One level is of lower and the

other of higher energy than the monomer excited state. This splitting is a consequence of the two possible arrangements (in-phase and out-of-phase oscillation) of the transition dipoles of the chromophores in the dimer. The interaction energy between the chromophores is a function of the transition moment of the monomer, and the angle and distance between the transition dipoles.

A transition from the ground state to either of the excited states is possible. The number of bands observed depends on the geometry of the dimer.

(a) For parallel dimers (H-type), the transition to the lower energy excited state is forbidden and the spectrum consists of a single band blue-shifted with respect to the monomer.

(b) For head-to-tail dimers (J-type), the transition to the higher energy excited state is forbidden and the spectrum shows a single band red-shifted with respect to the monomer.

(c) In dimers having intermediate geometries, both transitions are partially allowed and band splitting is observed. The absorption spectrum shows two bands of similar bandwidth.

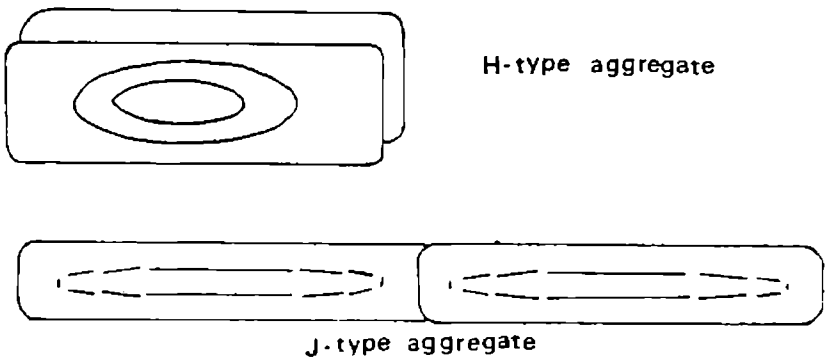

Fig.4.1: Representation of H-type and J-type aggregates

The corresponding energy diagram for the dimer excited states, shown in Fig.4.2 is based on the molecular orbital theory. So two absorption bands one at a lower and the another at a higher energy than the monomer, are expected for the dimer absorption spectrum. Since the monomer and the dimer forms of phthalocyanines present different absorption properties, the visible absorption spectrum can be used to probe the dimerization process.

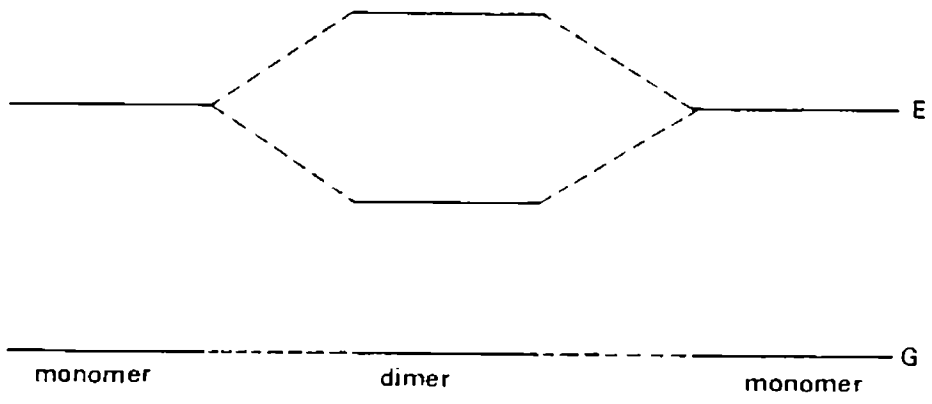

Fig.4.2: Energy diagram of the ground (G) and excited (E) state of the monomer and dimer

4.2.2 Experimental

The 4,4',4",4"'-tetra(1-aminoethyl-sulfonamido)-phthalocyaninecobalt(II) (CoTESPc) was synthesized and purified according to the procedure described in section 2.1.7. For each experiment, fresh solutions were prepared by diluting aliquots from a stock solution. The absorption spectra were recorded using Shimadzu UV-2001 or UV-240,

UV-visible Spectrophotometer. CoTESPc was incorporated into polyvinyl alcohol matrix by casting thin films of PVA using a solution of CoTESPc in 1% PVA. A 0.01% solution of glutaraldehyde was used as crosslinking agent.

4.2.3 Results and Discussion

Fig.4.3 shows the visible absorption spectrum of CoTESPc in ethanol/water (20% v/v). An analysis of the spectra evidences the existence of a monomer-dimer equilibrium in the concentration range 8.0×10^{-6} to 2.4×10^{-4} M. The molar absorptivity at the monomer absorption maximum (668 nm) decreases upon increasing the CoTESPc concentration and simultaneously the molar absorptivity at 630 nm increases. This is attributed to the formation of a new species in concentrated solution. The presence of an isobestic point in the absorption spectrum indicates that the new species is in equilibrium with the monomer, as in xanthene dyes.[8] It is attributed to the dimer form of CoTESPc. The dimer is formed at the loss of monomer and the absorption spectrum of CoTESPc in ethanol/water tends towards that of dimer form upon increasing the concentration. The molar absorptivity of the dimer is lower at its λ_{max} (630 nm) than that of the monomer at its λ_{max} (668 nm).

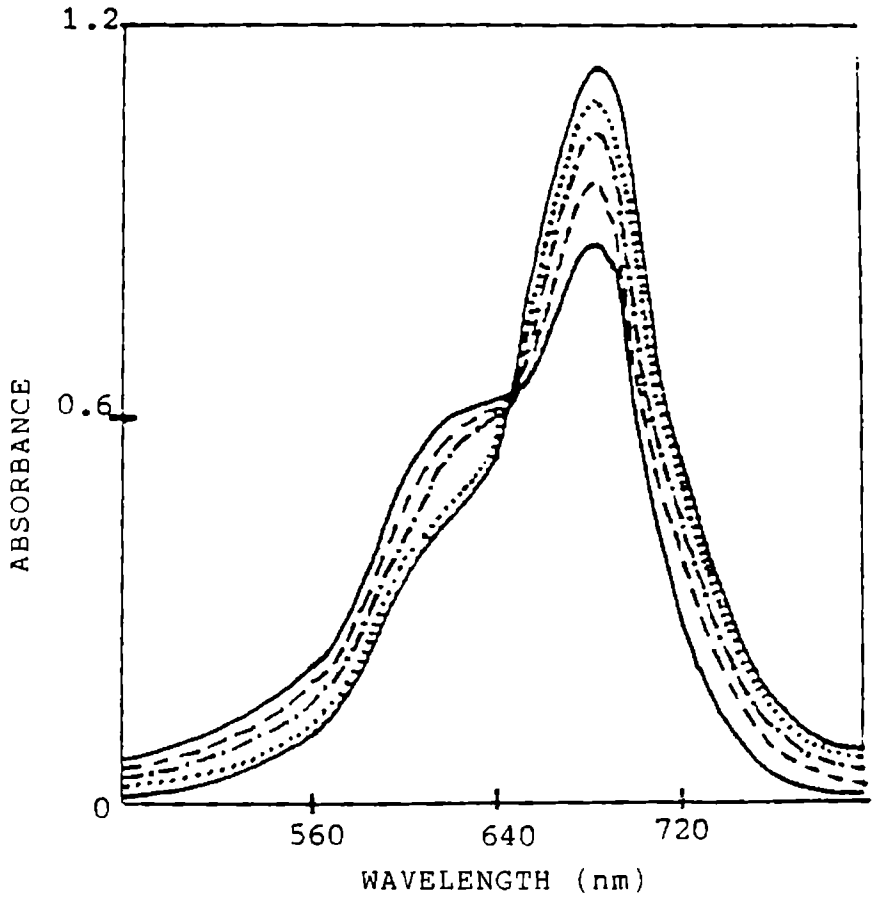

Fig.4.3: visible absorption spectra of CoTESPc in ethanol/water (20% v/v) at different concentrations at room temperature

—— 2.4×10^{-4} M
-·-·- 5.6×10^{-5} M
—— 8×10^{-6} M
--- 8×10^{-5} M
2.4×10^{-5} M

The absorption spectra of CoTESPc in 50% v/v ethanol/water and in pure ethanol are independent of concentration in the same concentration range. This indicates that dimer does not exist in solutions of high ethanolic content. The absorption spectrum of CoTESPc in water indicates the presence of a dimer alone. All these conclusively prove that aggregation of CoTESPc in solution strongly depends on the solvent.

The dimerization process in CoTESPc can be visualised as,

$$2M \rightleftharpoons D$$

where M and D represent the monomer and dimer respectively.

The equilibrium constant, K_d is given by,

$$K_d = \frac{[D]}{[M]^2} = \frac{1 - x}{2C_T x^2} \qquad (4.1)$$

where x is the monomer mole fraction at concentration C_T. Applying Beer-Lambert law, the total absorbance and the molar absorptivity are given by equations (4.2) and (4.3) respectively.

$$A = \epsilon_m(M)b + 2\,\epsilon_d(D)b$$

$$= \epsilon_m C_T\, x\, b + \epsilon_d\, c(1-x)b \qquad (4.2)$$

$$\epsilon = A/cb = \epsilon_m\, x + \epsilon_d\,(1-x) \qquad (4.3)$$

where ϵ_d is the molar absorptivity of the monomer in the dimer and b is the optical path length. The absorption spectrum at a concentration of about 8×10^{-6} M is essentially the monomer spectrum and $\epsilon = \epsilon_m$ at this concentration.

A knowledge of the monomer mole fraction is necessary for calculating the equilibrium constant. The monomer mole fraction can be estimated from the absorption spectrum by considering the ratio of the peak heights at the λmax of the dimer (A_D), and that at the λmax of the monomer (A_M).

$$R = \frac{A_D}{A_M} = \frac{\epsilon_{m_1} x + \epsilon_{d_1}(1-x)}{\epsilon_{m_2} x + \epsilon_{d_2}(1-x)}$$

$$R_o = \epsilon_{m_1}/\epsilon_{m_2} \quad \text{and}$$

$$x = R_o/R$$

where $\epsilon_{m_1} \approx \epsilon_{d_1}$ and $\epsilon_{d_2}(1-x) \ll \epsilon_{m_2} x$

The results of the application of this relationship for the estimation of monomer-dimer ratio at room temperature are summarised in Table 4.1. The value of the dimerization constant varies slightly in the concentration range studied probably due to deviations from the assumptions involved in the approximations. An average value of 2.1×10^3 l mol^{-1} is obtained for the dimerization constant for CoTESPc in 20% v/v ethanol/water.

Table 4.1: Dimerization constant, K_d, for CoTESPc in 20% v/v ethanol/water; temperature 28 ± 2°C

total dye concentration C_T(M)	ABSORBANCE 630 nm (D)	ABSORBANCE 668 nm (M)	$R = \frac{A_D}{A_M}$	$x = \frac{R_o}{R}$	K_d l mol^{-1} x 10^3
8.0×10^{-6}	0.494	1.137	0.435(R_o)	--	--
2.4×10^{-5}	0.512	1.089	0.470	0.926	1.8
5.6×10^{-5}	0.535	1.051	0.509	0.855	1.5
8.0×10^{-5}	0.579	0.992	0.584	0.745	2.9
2.4×10^{-4}	0.624	0.891	0.701	0.621	2.1

Average value of $K_d = 2.06 \times 10^3$ l mol^{-1}

4.2.3.1 Effect of ethanol content on the absorption spectrum of CoTESPc in ethanol/water

The absorption spectra of 7.3×10^{-5} M CoTESPc in solutions with different ratio of ethanol and water are given in Fig.4.4. The spectra of CoTESPc in water show a peak at 630 nm and a shoulder of 668 nm, due to the dimer. As the proportion of ethanol increases to 20%, the intensity of the peak at 668 nm increases. This is due to the dissociation of the dimer. The spectrum in 80% v/v ethanol water shows only one peak at 668 nm and this corresponds to pure monomer of CoTESPc. Fig.4.5 shows the absorption spectra of monomer and dimer of CoTESPc.

4.2.3.2 Tetramer formation

When NaCl is added to a solution of CoTESPc in water, the spectrum is modified as illustrated in Fig.4.6. At concentrations exceeding 0.02 M the maximum in the spectrum shifts to shorter wavelengths and also the absorbance at λmax decreases. As concentration of NaCl in the solution increases to about 0.8 M the shift in λmax approaches a limit of 610 nm.

The molar absorptivity is calculated from the relationship ϵ_{obs} = absorbance/C_T, where C_T is given by

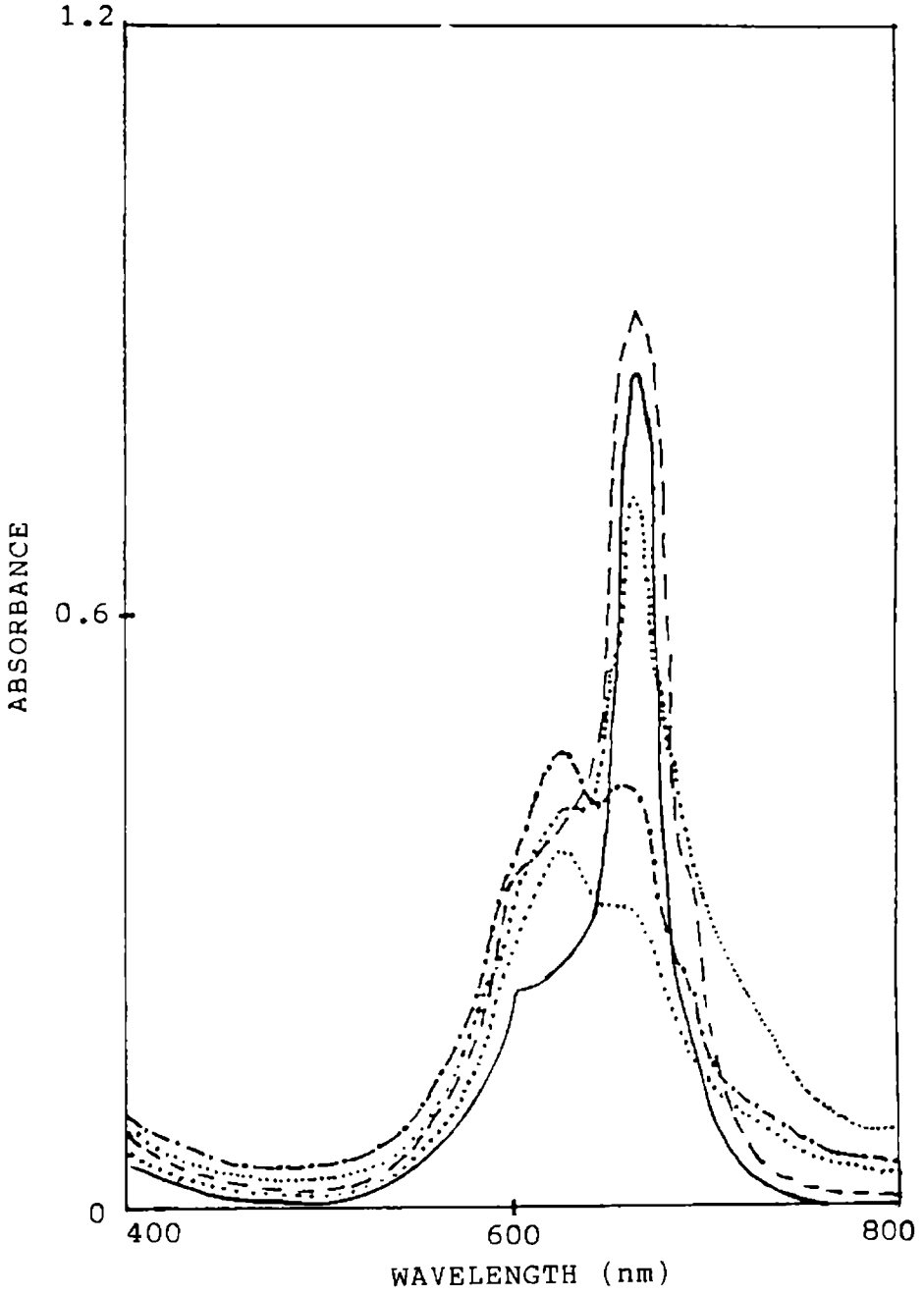

Fig.4.4: Visible absorption spectra of 7.3×10^{-5} M CoTESPc in aqueous ethanol solutions at room temperature

water; -·-·- 20% ethanol; 40% ethanol
—— 60% ethanol; - - - 80% ethanol

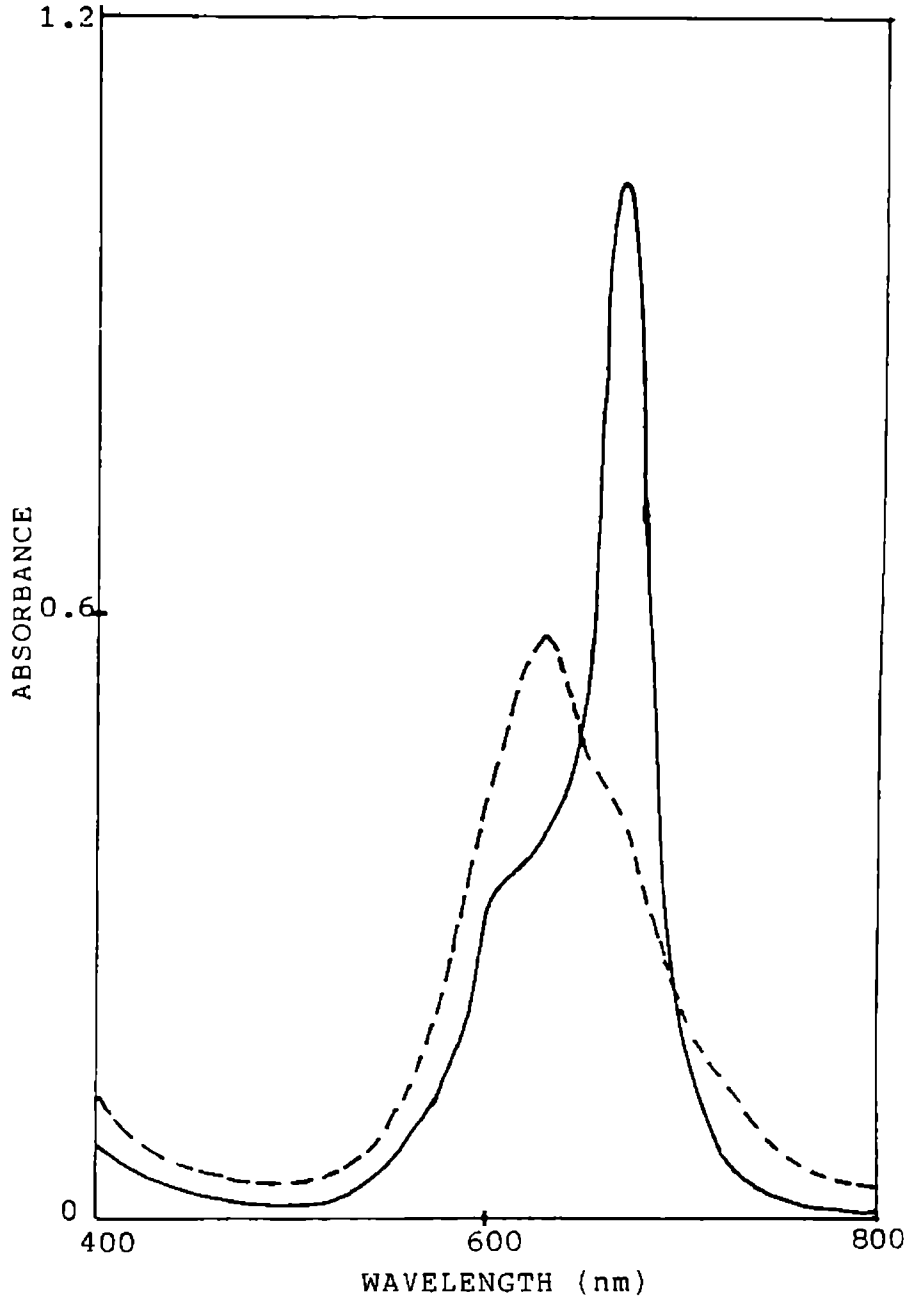

Fig.4.5: Visible absorption spectra of monomer and dimer forms of CoTESPc; Concentration: 4 x 10^{-4} M

—— monomer (ethanol); ---- dimer (water)

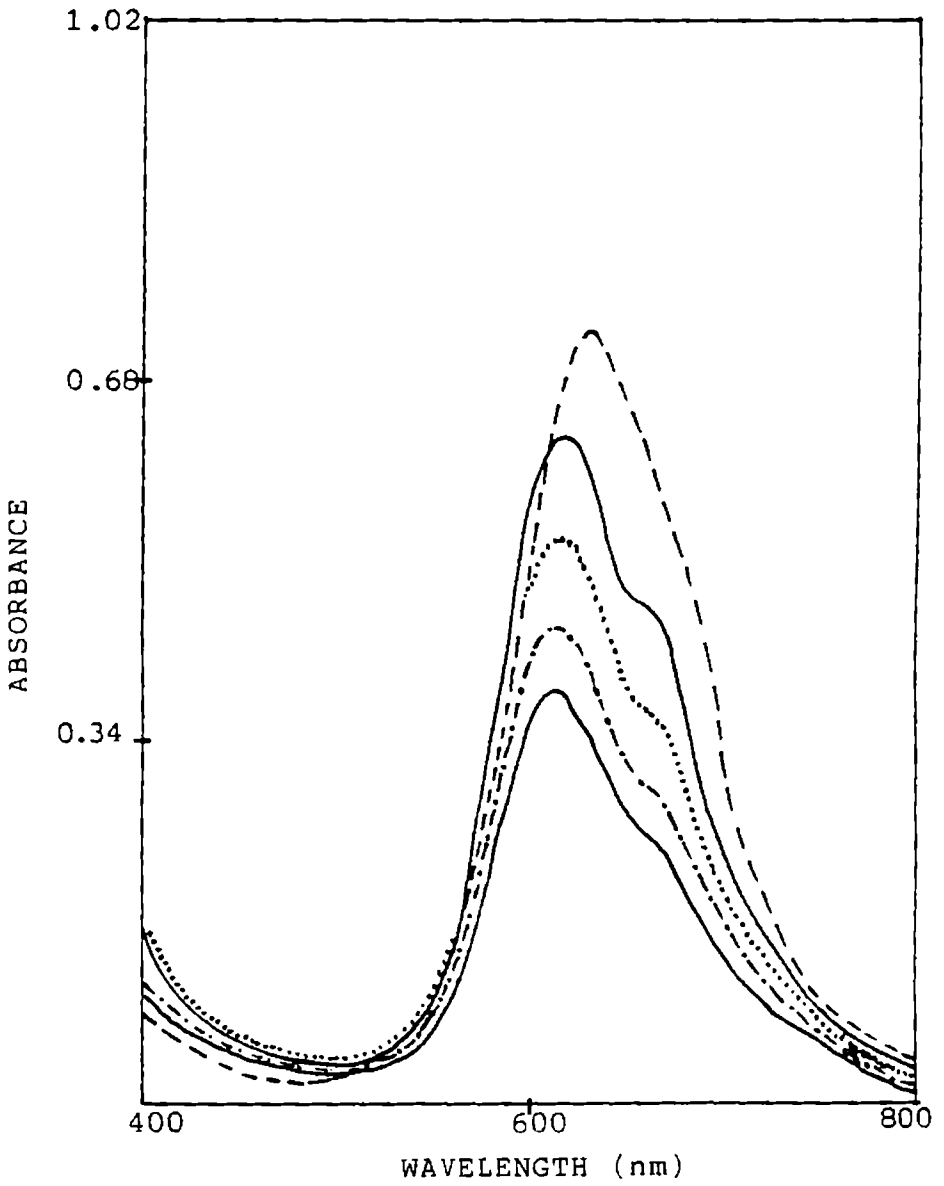

Fig.4.6: Spectral shifts for aqueous solution of 1.45×10^{-5} M CoTESPc with varying NaCl concentration

---- no NaCl added; —— 0.02 M NaCl
0.06 M NaCl —·—·— 0.6 M NaCl
——— 0.8 M NaCl

$C_T[M] + 2[D]$. The dimer concentration is one-half of monomer concentration at constant C_T, the molar absorptivity of the monomer and dimer are approximately equal at their respective absorption maxima. The ϵ_{obs} at 610 nm (2.8×10^4 l $mol^{-1}cm^{-1}$) is about one-quarter of the value (1.02×10^5 l $mol^{-1}cm^{-1}$) for the monomer at its λ_{max} 668 nm. This suggests that a tetramer is formed on the addition of NaCl.

The solubility of sulfonated phthalocyanine is due to the presence of sulfonic acid groups. The aggregation characteristics of sulfonamide of cobalt phthalocyanine with a free amino group, viz. CoTESPc, and free sulfonic acid group, viz. 4,4',4",4'"-tetra(sulfonamidobenzene-4-sulfonic acid)phthalocyaninecobalt(II) (CoTSSPc) were studied. The association of CoTASPc in solution was compared with that of CoTESPc and CoTSSPc.

The aggregation characteristics of CoTESPc, which has separate λ_{max} values for the monomer and dimer, were studied. The blue shifted ($\Delta\lambda_{max}$ = 38 nm) dimer absorption band indicates H-type aggregation in CoTESPc. In the case of CoTESPc the bands overlap and the monomer has nearly twice the absorbance of the dimer. Fig.4.7 shows the

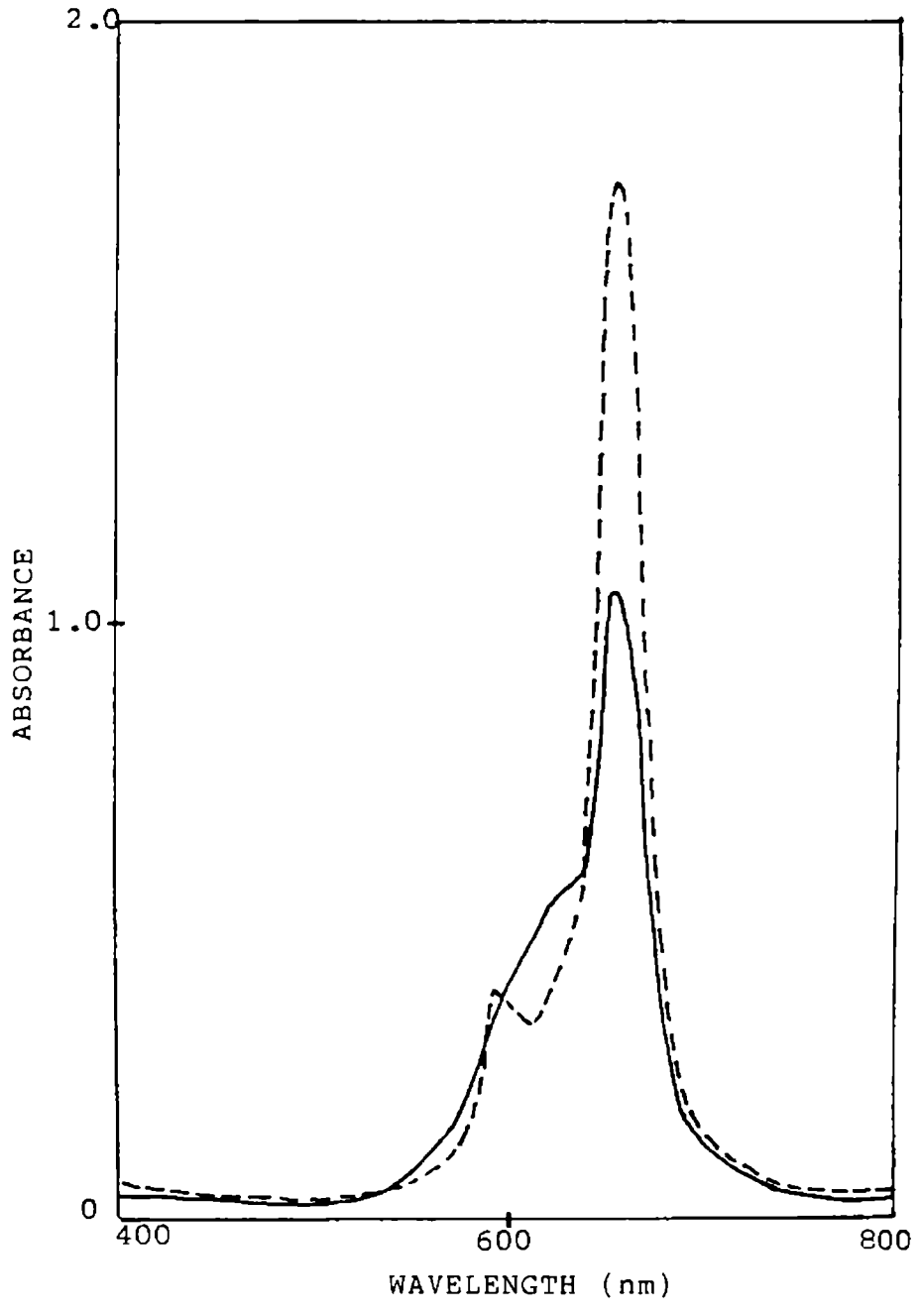

Fig.4.7: Visible absorption spectrum of monomer and dimer forms of CoTSSPc; Concentration: 4 x 10^{-4} M

---- monomer (ethanol); ——— dimer (water)

absorption spectrum of the monomer and dimer forms of CoTSSPc. This is analogous the observations reported by Monahan et al.[9] for copper 4,4',4",4"'-tetraalkylphthalocyanine. Fig.4.8 shows the visible absorption spectrum of CoTASPc in water. The spectrum has a broad band with λ_{max} at 688 nm and shoulder at 639 nm. Addition of ethanol affects the absorbance at both λ_{max} by the same ratio. Hence the existence of a monomer-dimer equilibrium could not be ascertained. The zwitter ion formation between the sulfonic acid group and the amino group at the adjuscent positions of the phthalocyanine ring may suppress dimerization.

4.2.4 Incorporation of sulfonamide and amino sulfonic acid derivatives of MPc into poly(vinyl alcohol) matrix

For optical recording media metallic or semi-metallic materials such as tellurium alloys are best used.[10] In addition to them, organic dyes such as cyanines and phthalocyanines which have many advantages, are also being increasingly considered. The reasons are: (i) possibility of high data storage density due to low heat conductivity of these media (ii) low manufacturing cost due to the spin coatability of organic dyes (iii) possibility

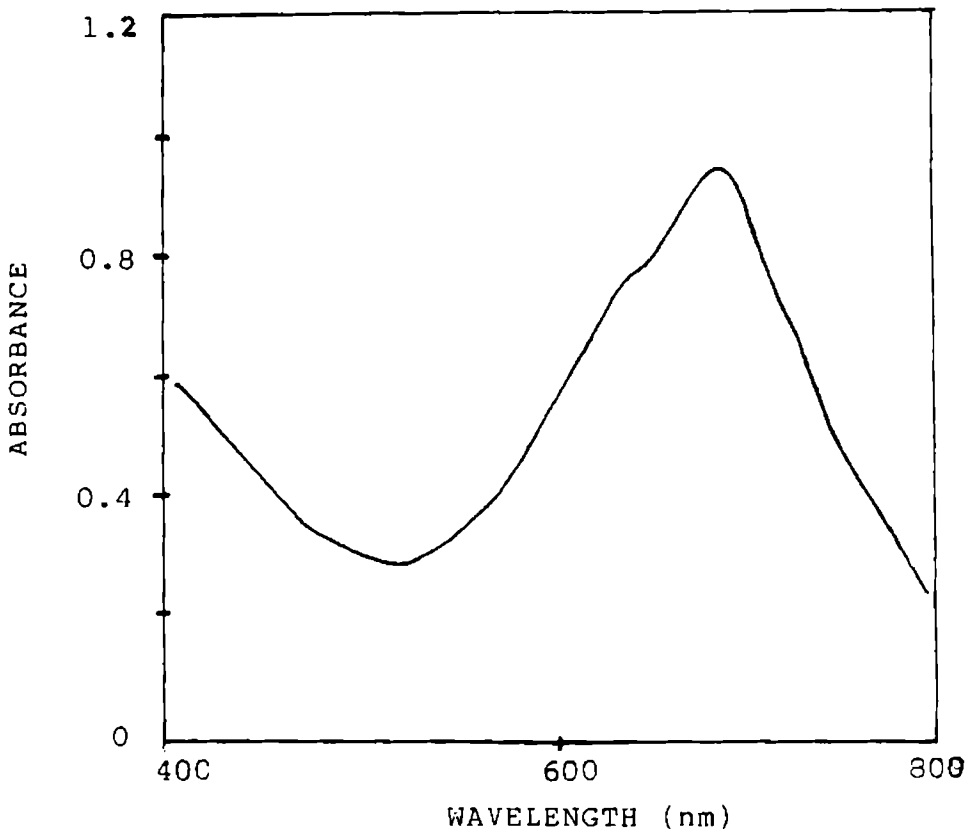

Fig.4.8: Visible absorption spectrum of CoTASPc in water (5×10^{-5} M)

of high recording sensitivity (iv) stability to moisture and (v) lack of toxicity. The effect of the physical properties of the dye or dye-polymer layer on the recording characteristics have been least studied.

The solubility of phthalocyanine sulfonamides and aminosulfonic acid in water and alcohol helps their easy incorporation into PVA matrix. PVA crosslinked with glutaraldehyde is highly resistant to moisture. Phthalocyanine sulfonamides and aminosulfonic acid can be easily incorporated into PVA matrix along with glutaradehyde as crosslinking agent, and can be cast into films for optical recording.

An aqueous solution of CoTSSPc or CoTASPc (2.0×10^{-4} M, 50 ml) was mixed with 50 ml of a 1% solution of PVA in water. Glutaraldehyde (0.01%) was used as crosslinking agent. The solution was allowed to evaporate at 50°C on a stainless steel substrate to get good films of the dye-polymer.

Fig.4.9 shows the absorption spectrum of CoTSSPc in PVA matrix. The spectrum shows a strong peak at 672.5 nm with a shoulder at 605 nm on going from solution

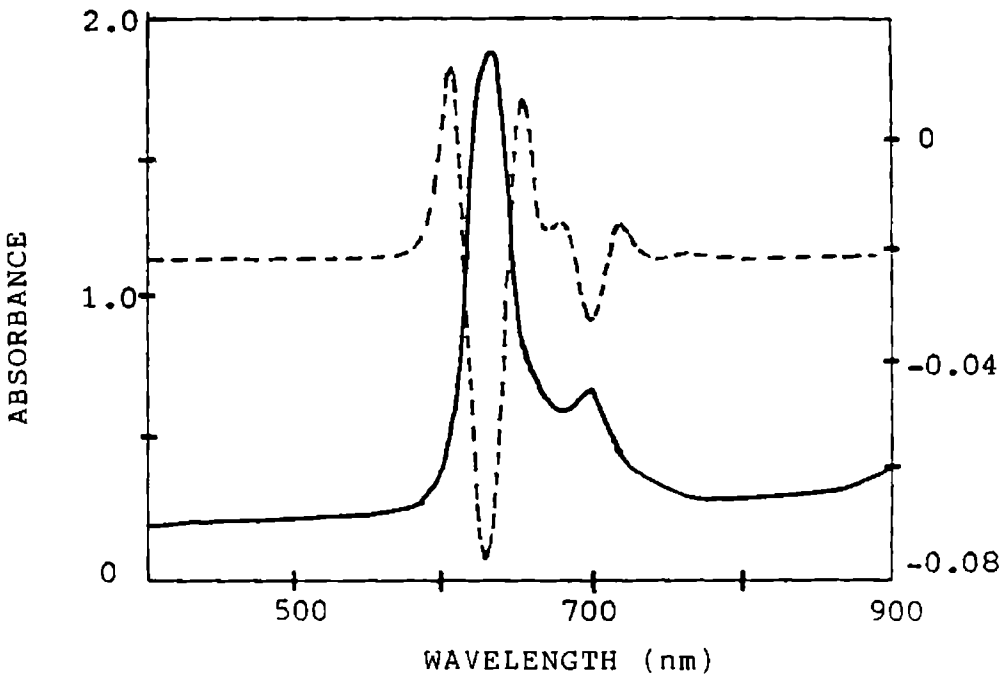

Fig.4.9: Visible absorption spectrum of CoTSSPc in poly(vinyl alcohol) matrix; Concentration 10 mg/0.5 g

derivative spectrum

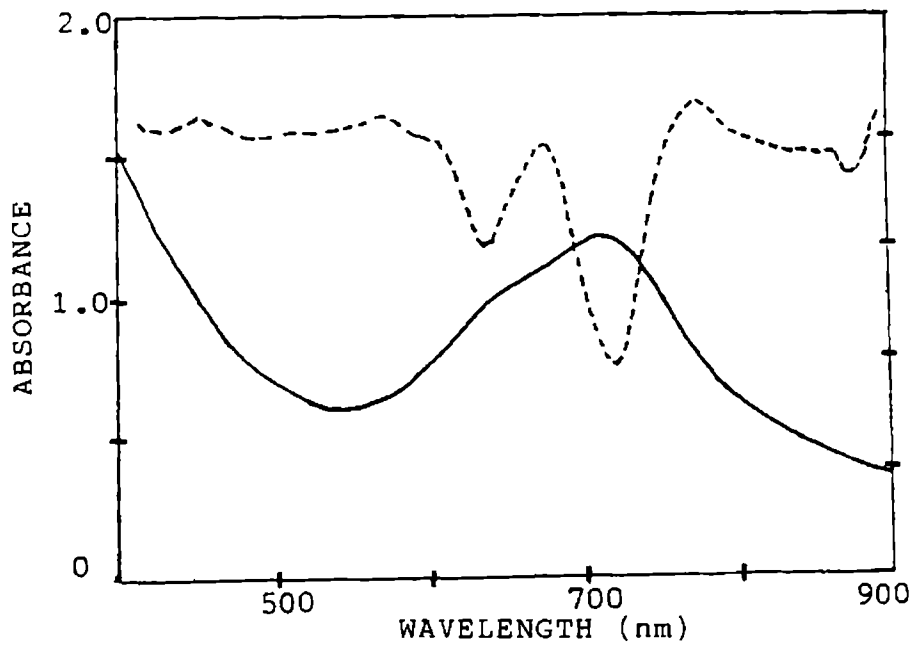

Fig.4.10: Visible absorption spectrum of CoTASPc in poly(vinyl alcohol) matrix; Concentration 10 mg/0.5 g

derivative spectrum

to PVA matrix. The shoulder at 590 nm in water is also red-shifted to 605 nm when CoTSSPc was incorporated in PVA. The films are transparent and blue in color.

A similar behaviour is also found with CoTASPc. Fig.4.10 shows the spectrum of CoTASPc in PVA matrix. The peak at 688 nm in solution is red-shifted to 717 nm in PVA matrix.

4.2.5 Conclusion

The sulfonamide and aminosulfonic acid of CoPc show good solubility both in ethanol and in water. The studies show that the sulfonamide exists as monomer in ethanol and in ethanol/water (1:1). The dye exists as a dimer in water. A dimerization constant of $2.0 \times 10^{+3}$ l mol^{-1} was observed for CoTESPc in 20% v/v ethanol/water.

The dyes can be easily incorporated into polyvinyl alcohol matrix and can be cast into thin films. The processability of phthalocyanine can thus be improved by polymer incorporation. The phthalocyanine-incorporated polymer is a candidate material for optical recording.

REFERENCES

1. Monahan, A.R.; Brado, J.A.; DeLuca, A.F. J. Phys. Chem. 1972, 76, 446.

2. Rabinowitch, E.; Epstein, L.F. J. Am. Chem. Soc. 1941, 63, 69.

3. Levschin, V.L.; Krotova, L.V. Opt. Spectrosc. (Engl. Transl.) 1962, 13, 457.

4. Sheppard, S.E.; Gedder, A.L. J. Am. Chem. Soc. 1944, 66, 2003.

5. Valdes-Aguilesa, O.; Neekers, D.C. J. Phys. Chem. 1988, 92, 4286.

6. Kasha, M. Radiat. Res. 1963, 20, 55.

7. McRae, E.G.; Kasha, M. In Physical Processes in Radiation Biology; Augenstein, L.; Rosenberg, B.; Mason, S.F., Eds. Academic Press: New York, 1963.

8. Lopez Arbeloa, I. J. Chem. Soc., Faraday Trans. 2, 1981, 77, 1725.

9. Monahan, A.R.; Brado, J.A.; DeLuca, A.F. J. Phys. Chem. 1972, 76, 1994.

10. Burgers, A.N.; Evans, K.E.; Mackay, M.; Abbott, S.J. J. Appl. Phys. 1987, 61, 74.

CHAPTER - V

SOLID - STATE ELECTROCHEMICAL STUDIES ON METAL PHTHALOCYANINE - IODINE SYSTEMS

5.1 INTRODUCTION

There has been renewed interest in solid electrolyte galvanic cells during recent years because such cells offer solutions to several problems encountered with aqueous systems. One conspicuous short-coming of aqueous cells is their limited shelf-life. This usually results from the corrosion of the electrode materials in highly conducting electrolytes. A second problem is electrolyte leakage, which necessitates special sealing techniques. A third limitation is the rather short temperature range over which such cells can efficiently operate. Finally, in many applications, it is difficult to achieve appreciable miniaturization with aqueous systems. Solid electrolyte galvanic cells overcome such disadvantages of the aqueous electrolyte systems.

Solid electrolyte batteries can be used for high energy density and high current applications such as traction of vehicles, or for energy storage (eg., sodium-sulfur battery). Other cells are useful only for low current applications. Such applications demand a long shelf life (eg., silver oxide batteries).

A galvanic cell can be represented as given in Fig.5.1. In most cases the anode is a pure metal, which is compatible with the electrolyte used.

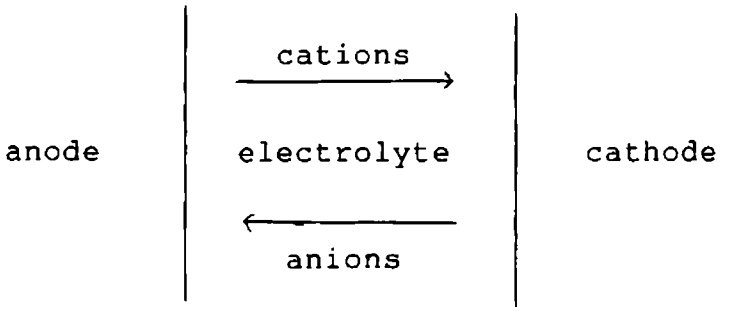

Fig.5.1: Schematic representation of a galvanic cell

The electrode materials must also be good electronic conductors. The electrolyte separating the electrode phases may be a cationic or anionic conductor. The most promising electrolytes for solid battery applications are cationic conductors. A solid electrolyte galvanic cell can be represented:

Electrode(s)/Electrolyte(s)/Electrode(s)

An example is,

$Ag(s)/Ag_4RbI_5(s)/RbI_3(s)$

Most silver ion conductors suitable for galvanic cell applications are based on α-AgI stabilized with additives. In this group Ag_3SI is one of the first materials to be developed with acceptable conductivity ($\sim 0.01\ \Omega^{-1}\ cm^{-1}$) at ambient temperature. Takahashi and Yamamoto[1] reported the cell $Ag(s)/Ag_3SI(s)/C(I_2)(s)$. Ag_3SI has only silver ion conduction and the cell fabricated from it showed very favourable properties, such as lack of polarization upto 100 $\mu A/cm^2$. The cell showed only limited shelf-life.

Most of the AgI based cells use iodine cathodes. The important factor which limits the shelf-life is the migration of iodine through the electrolyte. A possible solution to overcome this is to use triiodide cathodes in which iodine is fixed as a complex ion.

Another promising cathode material is the charge transfer-complex (CTC) of iodine. Although they lower the open circuit voltage of a galvanic cell, their electronic conductivity is moderately high ($\sim 0.1\ \Omega^{-1}\ cm^{-1}$), and no additive is needed to maintain conductivity during discharge. A cell with perylene-iodine complex (mole ratio

2:3) was made by Louzos et al.[2] The discharge characteristics were not very promising.

Recently Pampallona et al.[3] investigated silver based cells using other iodine-charge-transfer complexes. The results are very promising, especially with phenothiazine, and N-methyl phenothiazine-iodine complex (mole ratio 2:3). This cell gives an open circuit voltage of 0.64 V. A discharge efficiency of 80% could be reached. Due to their superior stability and electrical conductivity the conductive molecular compounds of iodine and metal phthalocyanines are worth investigating for their usefulness as cathode materials for solid state batteries.

Crystals composed of molecular ions and exhibiting strongly anisotropic metallic behaviour are of current experimental and theoretical interest.[4] These materials invariably consist of stacks of strongly interacting planar inorganic (eg. $Pt(CN)_4^{-2}$) or organic (eg. $TCNQ^{-2}$) ions. Weak interaction between the stacks leads to anisotropic transport properties. High conductivity requires a non-integral formal oxidation state for the ions in the stack. In most instances, sub-stoichiometric oxidation of planar organic molecules, or transition metal complexes of

integral oxidation state do not consistently produce the desired mixed valencies. Iodine is an advantageous oxidant, because of the high stability of I_3^- ions, and because of the ability of the planar I_3^- to accommodate itself into the channels of one-dimensional lattices.[5,6]

The oxidation of a divalent metal complex would yield a trivalent metal ion if I^- were produced. A non-integral oxidation state would result if all metal sites in the material were crystallographically similar and if only I_3^- were formed; eg., $(LM)(I_3^-)_{1/3}$, where M has a formal oxidation state of 2.33.[7]

The oxidation of Fe, Co, Ni, Cu, Zn, Pt phthalocyanines and metal-free phthalocyanine by iodine in the vapour phase, or in solution (chlorobenzene, CCl_4), results in darkly coloured solids with a range of stoichiometries. The exact composition depends upon the reaction condition.

Treatment of (phthalocyaninato) nickel(II), (NiPc) with elemental iodine affords (phthalocyaninato) nickel iodide, Ni(Pc)I. CoPc and CuPc also undergo oxidation with iodine resulting in the formation of molecular metals Co(Pc)I and Cu(Pc)I.[8] These compounds consist of metal-

over-metal columnar stacks of partially (1/3) oxidized M(Pc) units that are surrounded by chains of I_3^- ions.[9] The change in the oxidation state of central metal atom introduces qualitative modification in the electronic structure of the M-(L) based molecular conductors without associated changes in the crystal structure.

NiPc incorporates a d^8-Ni^{2+} ion. Oxidation of NiPc occurs at the ring, and the charge carriers of Ni(Pc)I are associated with the highest occupied delocalised molecular orbital of Pc.[9] Co(Pc)I is a metal-spine conductor. CoPc incorporates a d^7-Co^{2+} ion. The iodination proceeds by oxidation of the metal from $Co^{"2+"}$ to $Co^{"2.33+"}$ Thus the charge-transport in Co(Pc)I proceeds along a one-dimensional chain of metal centres, as in Krogmann salts.[7] The Co(dz^2) bands of Co(Pc)I is 1/3 filled, whereas the orbital band of Ni(Pc)I is 5/6 filled. Cu(Pc)I is also a ring oxidised conductor and shows metallic conductivity like Ni(Pc)I. Co(Pc)I does not show metallic conductivity.

In this chapter the synthesis and the results of the solid-state electrochemical studies carried out on Ni(Pc)I, Co(Pc)I and Cu(Pc)I are described. A solid-state

electrochemical cell that employs a silver anode, a solid silver ion conductor and M(Pc)I cathode was used in these studies.

5.2 EXPERIMENTAL

5.2.1 Preparation of materials

NiPc, CoPc and CuPc were synthesized and purified according to the procedure described in section 2.1. Iodine (resublimed), silver powder (-60 mesh) and silver iodide (98.8%) were obtained from BDH. Ni(Pc)I, Co(Pc)I and Cu(Pc)I were synthesized by solution doping. A known weight of finely powdered MPc was stirred with an appropriate weight of iodine in the form of CCl_4 solution for 48 h. M(Pc)I samples with varying I_2/MPc ratio were synthesized. Excess iodine was removed by washing repeatedly with CCl_4, drying at 80°C for 2 h and then weighing.

Powdered samples of the materials (Ag, AgI and M(Pc)I) to be cast into disc were separately introduced into the cavity of the pelletizer. The cylindrical ram was inserted and the powder was compacted by applying hand pressure. The compacted pellet was taken out and pellets

of the three materials were placed in the cavity of the pelletizer to get a cell configuration Ag/AgI/M(Pc)I The pellets were compressed together in the hydraulic press at a pressure of 2 tons/cm^2. The compacted cell was taken out and the round edge of the compact was ground with fine emery paper until three clear-cut layers appeared. The cylindrical surface was repeatedly wiped with tissue paper to remove any adhering powder.

5.2.2 EMF measurements

Emf measurements were made using a high impedance ($\sim 10^{12}\,\Omega$) electrometer. This ensured that current drain from the cell during measurement and concomitant mass transfer polarization problems are minimized. The solid electro-chemical cell mounted in the measuring assembly is shown in Fig.5.2. Gold plated cylindrical copper electrodes held in position by metal springs were used to establish electrical contact. The discharge characteristics of the cells were measured using 100 KΩ, 1 MΩ and 2 MΩ loads.

5.3 RESULTS AND DISCUSSION

5.3.1 EMF of Ag/AgI/M(Pc)I cells

The cell Ag/AgI/M(Pc)I can be used to measure the formation properties of M(Pc)I. This cell, Ag/AgI/M(Pc)I,

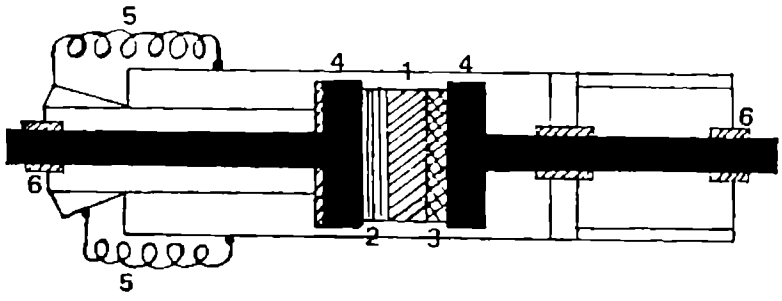

1 - AgI 2 - Ag 3 - M(Pc)I
4 - Gold plated copper electrode
5 - Springs 6 - Teflon spacers

Fig.5.2: Cell used for emf measurements

gives an emf of 0.6 V at 290 K. The emf of the cell depends on the presence of free iodine or I_3^- in M(Pc)I.

EMF data obtained with samples of different (I_2/MPc) ratios for NiPc, CoPc and CuPc are presented in Tables 5.1, 5.2, 5.3 respectively. Small changes in emf were observed with time after compaction. In the case of M(Pc)I with lower dopant concentrations, higher emf variations with time were observed compared with those of higher I_2/MPc ratio. This may be due to an interaction of iodine with the MPc units, which is controlled by the diffusion of I_2 into the solid matrix. The emf became steady after about 30 h and final values of emf were measured after 48 h.

At low concentrations of I_2 it is reasonable to assume that the iodine atom losses its electron to MPc. As the iodine ratio increases the electron transfer comes to a saturation as indicated by the attainment of a steady emf. Further addition of I_2 has little effect since the electrode is in effect an iodine electrode. This is evident from Fig.5.3 which shows the plots of emf of the cells vs. I_2/MPc ratio for Ni(Pc)I, Co(Pc)I and Cu(Pc)I.

Table 5.1: Variation of cell emf with I_2/NiPc ratio for $Ag_{(s)}/AgI_{(s)}/Ni(Pc)I_{(s)}$ cell

I_2/NiPc mole ratio	emf of the cell (mV)		
	5 min	1 h	48 h
0.063	184	198	192
0.126	282	284	288
0.254	570	573	575
0.380	601	607	609
0.507	612	612	616
0.634	609	614	617
0.867	612	620	620
1.14	618	624	622

Table 5.2: Variation of cell emf with I_2/CoPc ratio for $Ag_{(s)}/AgI_{(s)}/Co(Pc)I_{(s)}$ cell

I_2/CoPc mole ratio	emf of the cell (mV)		
	5 min.	1 h	48 h
0.063	194	210	212
0.126	440	442	440
0.254	490	491	490
0.380	539	541	540
0.507	558	562	560
0.634	560	565	565
0.887	562	567	570
1.14	575	582	580

Table 5.3: Variation of cell emf with I_2/CuPc ratio for $Ag_{(s)}/AgI_{(s)}/Cu(Pc)I_{(s)}$ cell

I_2/CoPc mole ratio	emf of the cell (mV)		
	5 min.	1 h	48 h
0.063	180	186	192
0.126	452	454	457
0.254	550	550	556
0.380	610	612	613
0.507	615	618	620
0.634	619	621	622
0.887	620	622	624
1.14	620	624	628

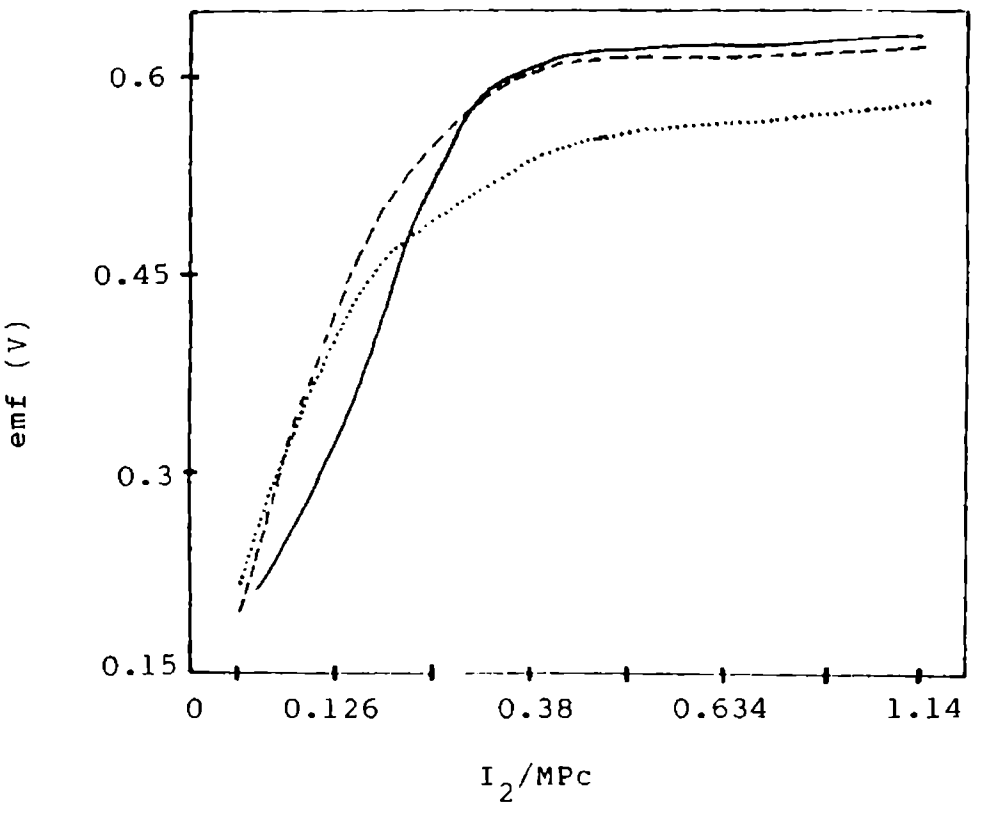

Fig.5.3: Plot of emf of the cell Ag /AgI/M(Pc)I versus I_2/MPc ratio.

—— Ni(Pc)I Co(Pc)I

– – – Cu(Pc)I

NiPc, CoPc and CuPc show steady increase in emf with increasing concentration of I_2. When the molar ratio of iodine exceeds 0.5, the emf of the cell reaches a saturation.

The incorporation of 0.5 mole of I_2 per mole of MPc indicates that the iodine species exists as I_3^-. The corresponding increase in oxidation state is 0.33 which may rest on the central metal as in the case of CoPc or on the Pc ring as in the case of CuPc and NiPc. The data obtained in these studies support the spectroscopic and magnetic susceptibility studies reported on these compounds.

5.3.2 Discharge characteristics of Ag/AgI/M(Pc)I cells

The active electrodes employed in these cells have a surface area of 0.8 cm^2 and contained 22.3 mg (0.088 m M) of iodine and 99.9 mg (0.175 m M) of MPc. The discharge characteristics of the cells at different current densities of the cell are presented in Figs.5.4, 5.5 and 5.6. At low discharge density the cell gives a steady closed circuit voltage except for an initial fall. At higher current densities the fall in voltage is very sharp. The initial sharp fall may be due to the concentration polarization

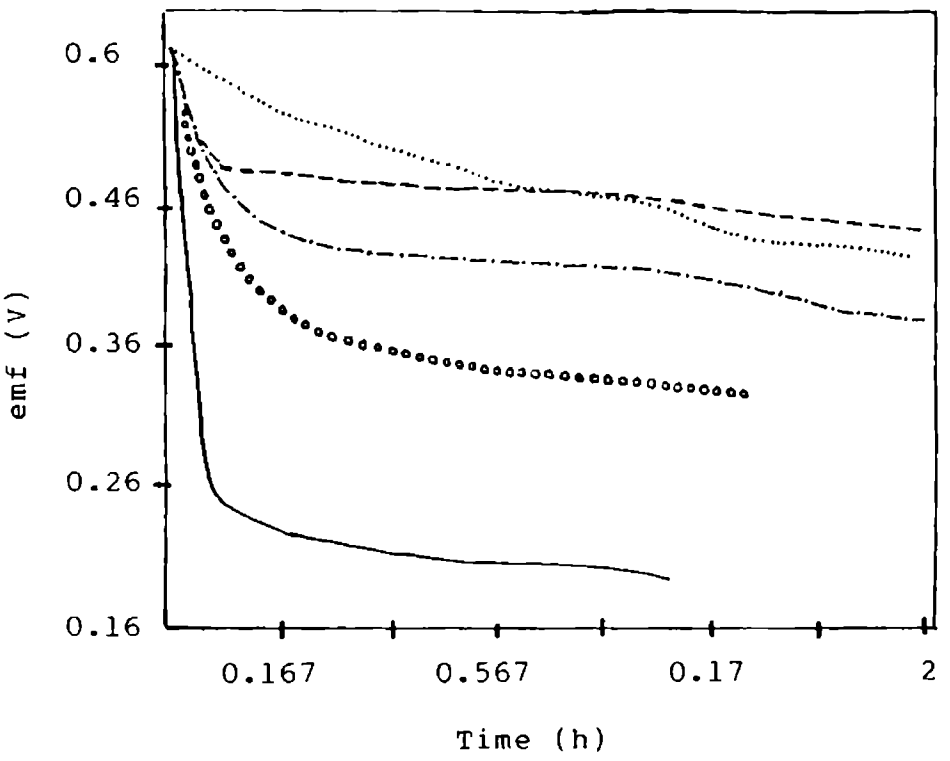

Fig.5.4: Discharge characteristics of Ag/AgI/Ni(Pc)I at different current densities.

0.3μA --- 0.6 μA ·-·-· 1.2 μA

ooooo 3.0 μA —— 6 μA.

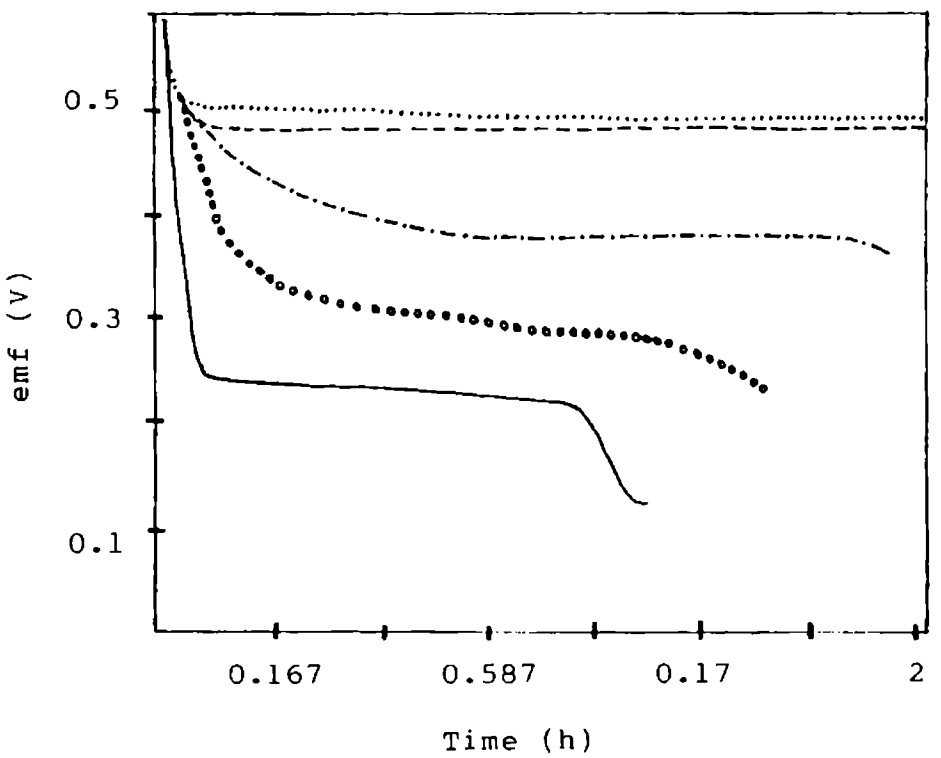

Fig.5.5: Discharge characteristics of Ag/AgI/Co(Pc)I at different current densities.

– – – 0.3 μA 0.6 μA 1.2 μA

ooooo 3 μA —— 6 μA

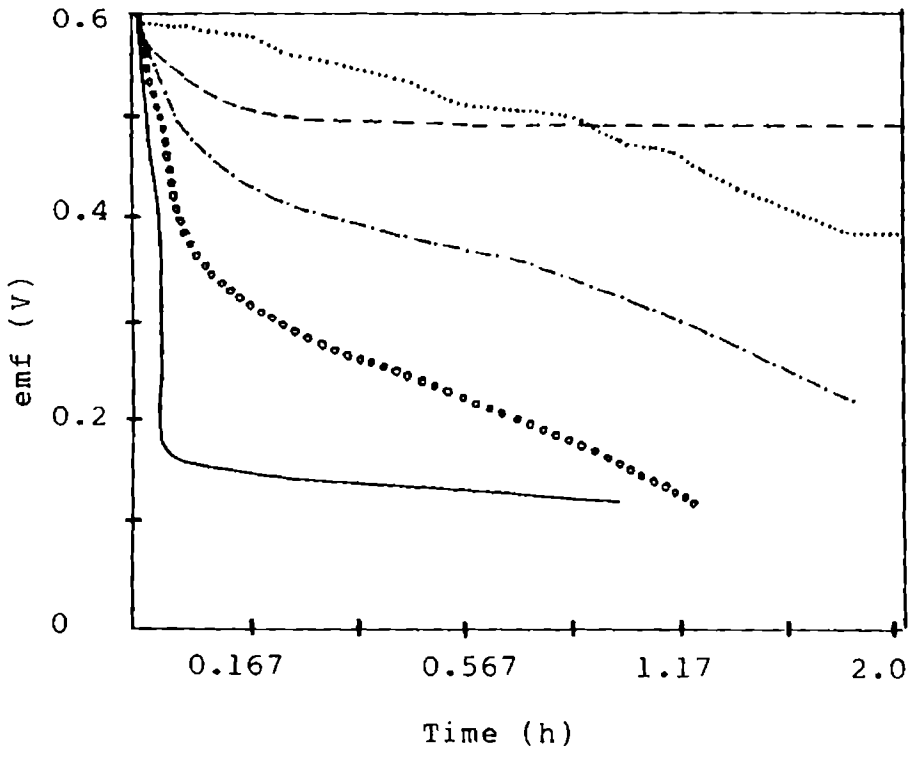

Fig.5.6 Discharge characteristics of Ag/AgI/Cu(Pc)I at different current densities.

---- 0.3 μA 0.6 μA -·-· 1.2 μA

ooocccc 3.0 μA —— 6.0 μA

resulting from the internal resistance associated with the solid electrolyte.

In the case of Co(Pc)I cell the discharge characteristics are more regular than with Ni(Pc)I or Cu(Pc)I. Within a time lapse of 2 h it gives a discharge yield of 80 coulombs. The power output corresponds to 295 watts/kg of $MPc^{2.33}I$. Such cells are likely to give steady low current for a reasonable duration in a thin layer configuration where the polarization characteristics associated with active electrode are less critical.

5.3.3 Proof of central metal atom oxidation in FePc and CoPc by iodine

During the iodination studies of MPc it was observed that the iodinated MPcs show unusual solubility in acetone in the case of CoPc and FePc. Metal phthalocyanines of transition metals as a whole are insoluble in acetone. However, Fe(Pc)I and Co(Pc)I showed limited extractability into acetone. The UV-vis absorption spectra presented in Figs.5.7 and 5.8 showed the existence of a central metal atom at higher oxidation state. The Q band in the absorption spectrum of FePc is split into a doublet

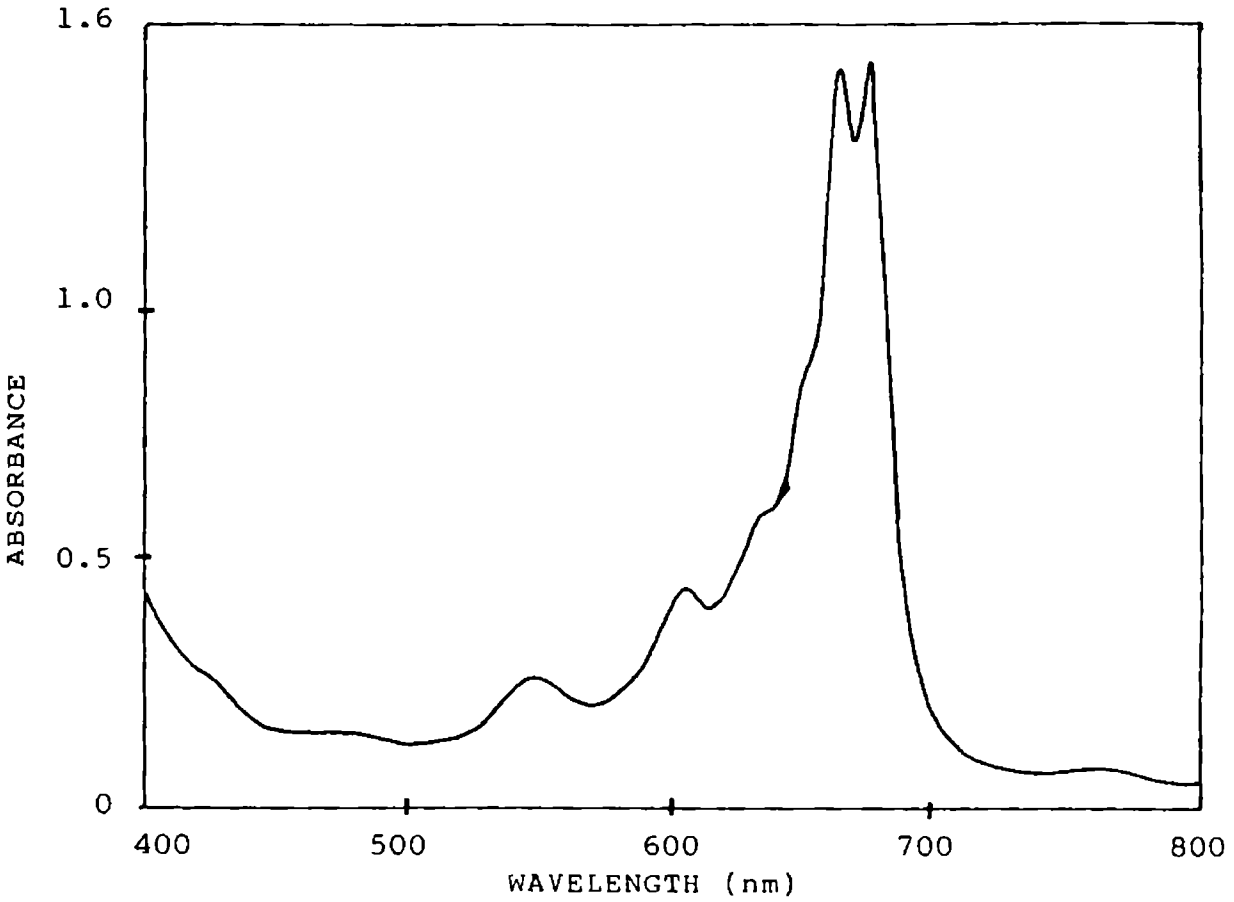

Fig.5.7: Absorption spectrum of the acetone soluble fraction of Fe(Pc)I.

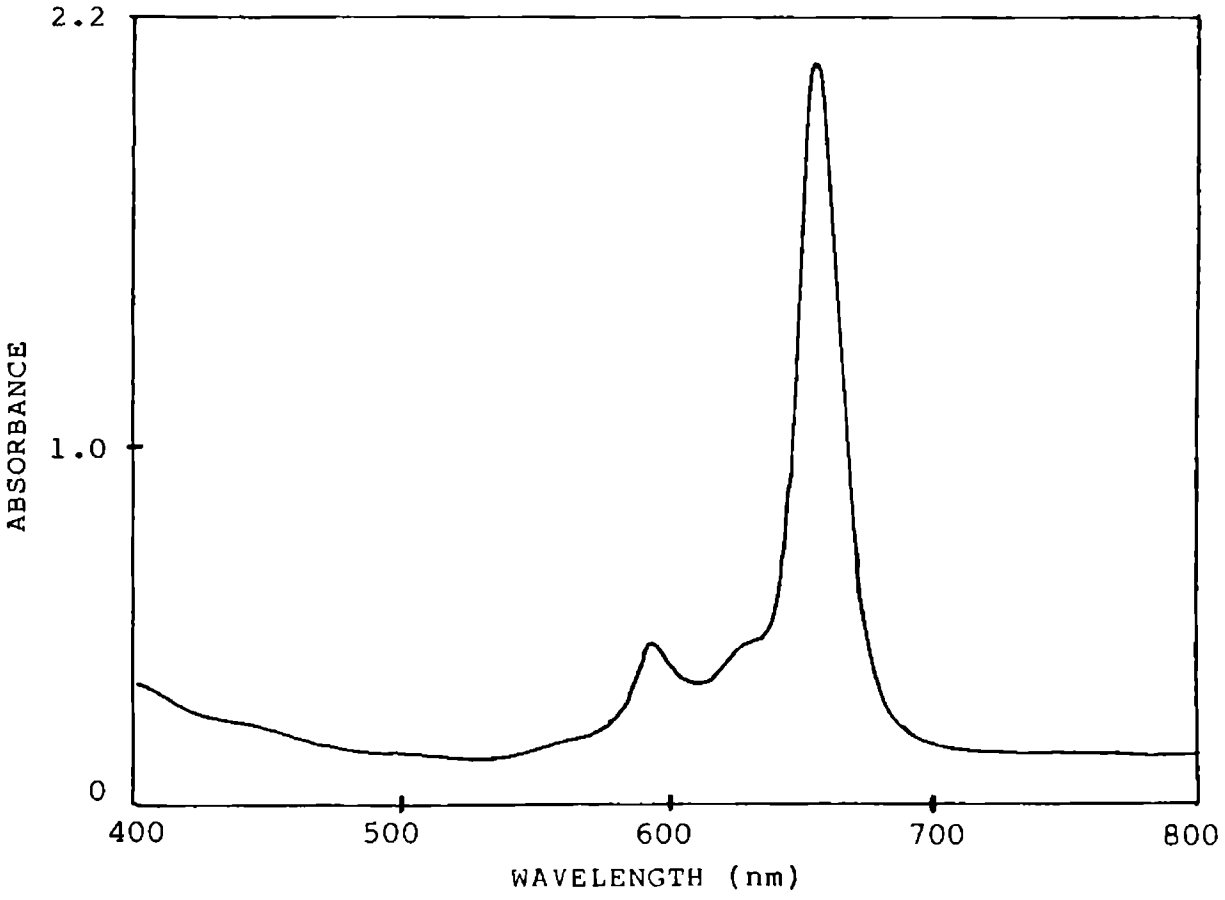

Fig.5.8: Absorption spectra of the acetone soluble fraction of Co(Pc)I.

of equal height. Similar observation was made by Lever et al.[10] on the oxidation of ferrous phthalocyanine to ferric phthalocyanine by dioxygen. In the case of CoPc, in the acetone soluble species the λ_{max} of the Q band shifts to shorter wavelength. In both cases elemental iodine or I_3^- do not evidence their presence in the spectra.

5.4 CONCLUSION

Iodine-doped phthalocyanines are stabler materials than phenothiazine and pyrene-iodine adducts. M(Pc)I has the added advantage that the MPc matrix is inert to common reagents, non-toxic and more conductive. An all-solid galvanic cell fabricated from M(Pc)I with solid AgI as electrolyte has an open circuit voltage of 0.6 V. When discharged at 100 nA/cm^{-2} it maintains a steady closed circuit voltage at 0.5 V. At a discharge current density greater than 0.3 μA polarization becomes very critical. The cell is promising for applications where a rugged, compact source with very low discharge current density is desired.

REFERENCES

1. Takahashi, T.; Yamamoto, O. Electrochem. Acta. **1966**, 11, 779.

2. Louzos, D.V.; Darland, W.G.; Mellors, G.W. J. Electrochem. Soc. **1976**, 120, 1151.

3. Pampallona, M.; Ricci, A.; Scrosati, B.; Vincent, C.A. J. Electrochem. Soc. **1976**, 123, 1063.

4. Thomas, T.W.; Underhill, A.E. Chem. Soc. Rev. **1972**, 1, 99.

5. Gleizes, A.; Marks, T.J.; Ibers, J.A. J. Am. Chem. Soc. **1975**, 97, 3545.

6. Endres, H.; Keller, H.J.; Megnamise, B.M.; Moroni, W.; Nothe, D. Inorg. Nucl. Chem. Lett. **1974**, 10, 467.

7. Zeller, H.R.; Beck, A.J. Chem. Phys. Solids, **1974**, 35, 77.

8. Ogwa, M.Y.; Martinsen, J.; Palmer, M.S.; Stantou, L.T.; Tanaka, J.; Greene, L.R.; Hoffmann, M.B.; Ibers, A.J. J. Am. Chem. Soc. **1987**, 109, 1115.

9. Ogwa, M.Y.; Martinsen, J.; Palmer, M.S.; Stantou, L.T.; Tanika, J.; Greene, L.R.; Hoffmann, M.B.; Ibers, A.J. J. Am. Chem. Soc. **1985**, 107, 6915.

10. Lever, A.B.P.; Wilshire, J.P. Inorg. Chem. **1978**, 17, 1145.

CHAPTER - VI

ELECTRICAL PROPERTIES OF METAL PHTHALOCYANINES

6.1 INTRODUCTION

The semiconducting properties of phthalocyanine and porphyrin complexes have enormous potentials for exploitation. Extensive research into the semiconductor properties of metal phthalocyanines, chlorophyll, and their analogues has been conducted by Vartanyan.[1-4] These compounds with a conjugated system of double bonds in their molecular structure exhibit pronounced intrinsic dark conductivity, which may be responsible for energy migration in biological systems.[5,6] This property can be put to wide use in semiconductor engineering.[7]

The electrical conductivity of a semiconductor increases exponentially with temperature,

$$\sigma = \sigma_o \exp(-E_a/2kT)$$

where σ - specific conductivity at temperature T in $\Omega^{-1}cm^{-1}$

σ_o - specific conductivity at infinite temperature

E_a - activation energy for conduction

k - Boltzmann constant.

The most important characteristic of an organic semiconductor is E_a. It determines the minimum amount of energy required to produce a charge carrier (electron or hole) in the solid matrix. The values of σ_o and E_a may be strongly dependent on the method of sample preparation. Values of E_a for H_2Pc reported by various investigators using samples prepared by different methods vary from 1.7 eV for single crystals and also for a vacuum deposited layer to 0.9 eV for a layer deposited by smearing on a quartz substrate. Such a spread in magnitude of the values of E_a is due to the different intermolecular and crystalline interactions. Therefore it is particularly important to prepare samples under identical conditions for the evaluation of conductivity parameters.

If the samples are prepared under strictly identical conditions, the electrical conductivity parameters can be used for assaying the purity of phthalocyanine complexes.[8,9] Dark conductivity method has made it possible to establish an interaction between the O_2 molecules and the central metal atom of the MPc. Any interaction of O_2 with the central metal atom increases the value of σ_o and reduces E_a. Except for a brief report[10] on

copper and platinum phthalocyanines no systematic report on the conductivity of MPcs and the effect of the central metal atom on their conductivity is found in the literature.

Studies on the dark conductivity of polymeric phthalocyanines based on pyromellitic acid have shown that the activation energy decreases down to about 0.8 eV in polymers. This tendency is ascribed to the growing length of the conjugated system in the polymer.[11]

Interesting information can be found in a work by Danzing et al.[12] The electrical conductivity of CuPc and two of its structural analogues, namely tetrapyridineporphyrazine and tetrapyrazine porphyrazine, were measured under comparable conditions. The activation energy values were found to be 1.3 and 0.81 eV respectively. The corresponding conductivities at 28°C were 3.0×10^{-11} and 3.0×10^{-8} $\Omega^{-1}cm^{-1}$. The values of σ_o were nearly the same.

Koifman et al.[13] used substituted osmium phthalocyanines, namely, X_2OsPc where X = Cl, Br, I and $\frac{1}{2}SO_4$, for demonstrating the influence of extra coordination on

semiconductor properties. A decrease in the value of E_a in the series I, Br, Cl may be due to the increasing electronegativity of these elements.

Phthalocyanines may be obtained in two crystallographic modifications (α and β) with a difference in conductivity of the two phases. The phthalocyanine molecules in the β-phase are arranged in stacks. The molecular planes are 3.38 Å apart. The α-phase which is a low temperature modification has a tetragonal structure.[14] Since the interactions of the molecules in organic crystals is of the van der Waals type, the rearrangement of molecules at the phase transition would alter the energy gap between the conduction and filled bands.[15] In organic crystals this interaction would affect the polarization energy contribution to the band gap.

Metal phthalocyanines are p-type semiconductors.[16] Their electrical conductivity can be enhanced by doping. The oxidation of MPc by iodine in the vapour or in solution results in darkly coloured solids with a range of stoichiometries.[17] These materials exhibit truly mixed valency. The high electrical conductivity associated with iodine-doped phthalocyanine is attributed to the partial oxidation

state induced on the phthalocyanine moiety, or on the central metal atom.[18]

In this chapter the work done on the electrical properties of MPcs are presented. The charge transport in pristine MPc and iodine-doped MPc has been probed by dc and ac conductivity, and dielectric constant. The effect of oxygen on the conductivity of CuPc and Cu(Pc)I were also studied.

6.2 EXPERIMENTAL

The metal phthalocyanines (NiPc, CoPc, CuPc) were synthesized and purified as described in section 2.1.1. The iodinated metal phthalocyanines were prepared according to the procedure given in section 5.2.

6.2.1 Infrared spectra

The infrared spectra were recorded using polytech FIR-30 Fourier Far IR Spectrometer or Shimadzu 8001 FTIR Spectrophotometer.

6.3 INFRARED SPECTRA OF M(Pc)I

The absorption peaks occurring in MPcs at 1090 cm^{-1}, 1290 cm^{-1} and 1330 cm^{-1} are retained in iodine-

doped MPcs. The low frequency infrared absorption of MPc are shifted to longer wavelength in the case of M(Pc)I. This indicate a change in the nature of metal-ligand bonding in doped phthalocyanines. The shift in the infrared absorption band to longer wavelength indicates the presence of charge-transfer interaction with dopant.[19]

6.4 ELECTRICAL CONDUCTIVITY MEASUREMENTS

An electromagnetically shielded cell described in section 6.5.1 is used for measuring conductivity. Powdered sample was pressed at 900 kg/cm^2 to form pellets of about 2 mm thickness and 10 mm diameter. The pellets were used for conductivity studies.

6.4.1 Fabrication of conductivity cell

Fig.6.1 shows the schematic diagram of the conductivity cell. The cell consists of a base plate on which six terminals are provided. The terminals are made of brass, sleeved with teflon and rendered vacuum tight with viton O-rings. The terminals are connected to the conductivity electrodes, thermocouple leads and dc supply powering the heater winding of the furnace. Pressed pellet or sheet of samples can be mounted between two gold plated

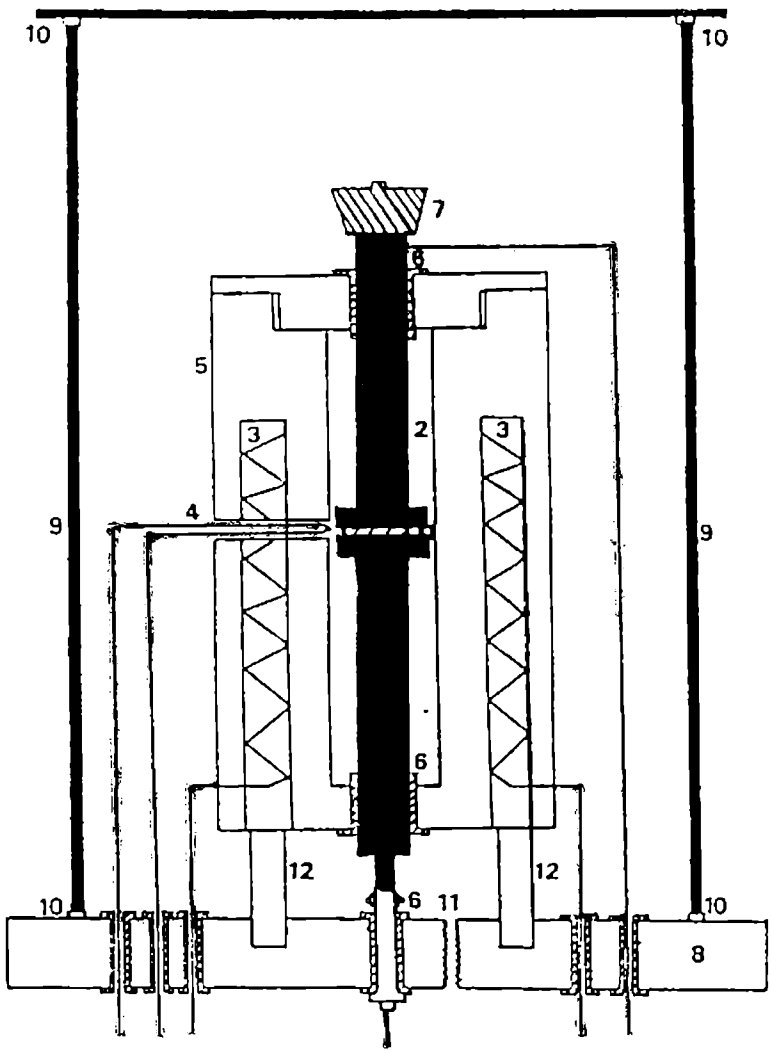

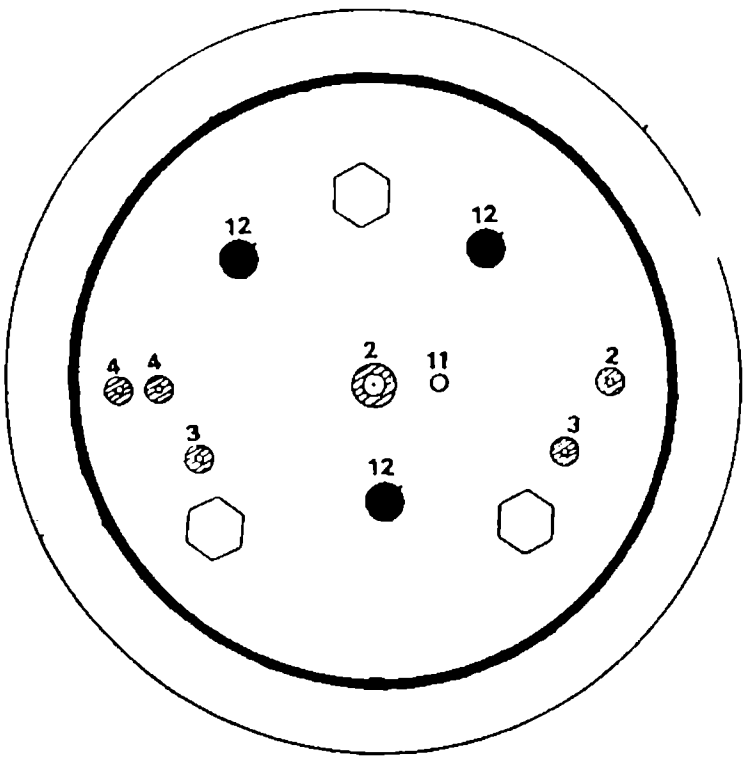

1. Sample pellet
2. Gold coated conductivit electrode
3. Heating element
4. Thermocouple
5. Aluminium block furnace
6. Teflon spacers (loose fittig)
7. Constant weight (200 g)
8. Base plate
9. Metal shield
10. O-ring
11. Vacuum line
12. Support

Fig. 6.1. Schematic diagram of the conductivity cell

brass cylinders which act as electrodes. The upper electrode (ram) is loaded with a constant weight (typically 200 g). The lower electrode is fixed and the upper electrode is movable inside an anodised aluminium block furnace. The electrodes are insulated from the furnace by teflon spacers. The aluminium block is heated by resistance wires inserted into radially spaced bore-holes in the aluminium block. The furnace is shielded by a metal cylinder resting on the base plate over an O-ring. The cylinder is closed with a MS disc rendered vacuum tight with O-ring. The lid is held in position by gravity and vacuum. The cell assembly is mounted on a frame. The electrical terminals communicate with a panel. Vacuum is applied through a metal tube mounted on the base plate and connected to a vacuum pump. The thermocouple head is placed very close to the sample to ensure the fidelity of temperature measurement.

Controlled atmosphere and vacuum studies were possible using this cell. The cell enables measurement with oxygen and moisture sensitive materials. The cylindrical electrodes of which the major surface area is inside the furnace block, ensures uniform and identical thermal communications with the furnace block. The furnace

block being of aluminium maintains uniform temperature throughout its body. DC heating minimises noise from the furnace. The outer metal cylinder which is earthed acts as a shield for electromagnetic waves.

6.4.2 Circuit

The circuit used in dc and ac conductivity measurements are given in Figs.6.2 and 6.3 respectively. The sample was mounted in the shielded cell. The sample was connected in series with a standard resistance of 1 MΩ and to the dc source. The voltage drop across the standard resistor was measured using high impedance DMM.

For ac conductivity and dielectric constant measurements the sample was mounted in the cell and the sample leads were connected to the LCZ meter and the built in source of the LCZ meter was used. It is assumed that the lead resistance is negligible in both cases. For capacitance measurements the leads and fringe capacitance was eliminated by the method suggested in the instruction manual. The measurements were repeated to ensure reproducability. All the measurements were done in N_2 atmosphere unless otherwise specified.

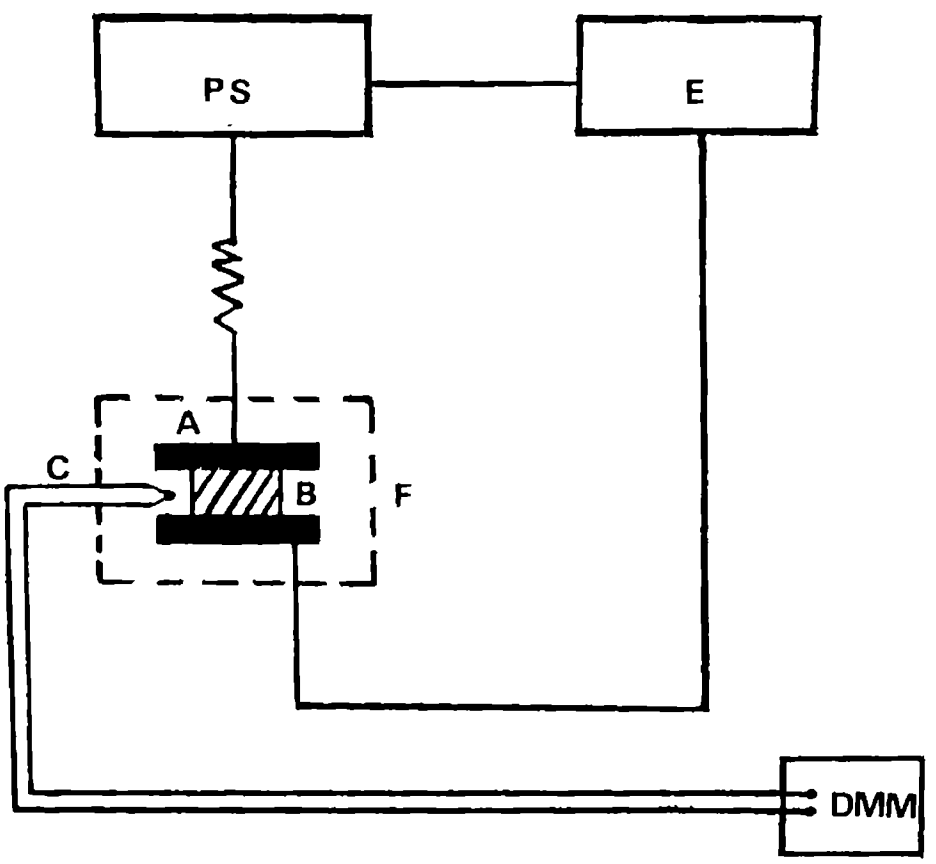

A - conductivity cell

B - sample

C - thermocouple

DMM - digital multimeter

E - Electrometer

F - furnace

PS - potentiostat

Fig.6.2: Circuit used in the measurement of dc conductivity

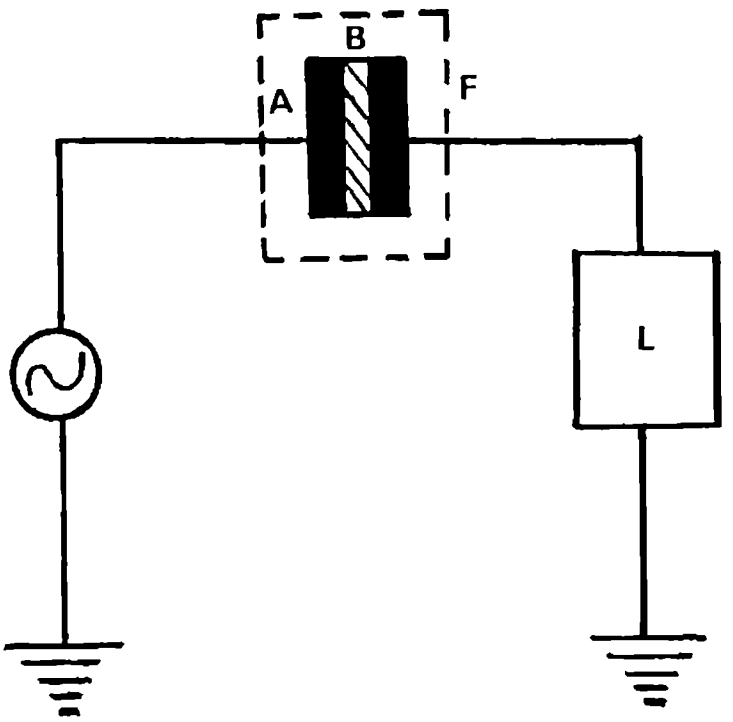

A - conductivity cell
B - sample
F - furnace
L - LCZ meter

Fig.6.3: Circuit used in the measurement of ac conductivity

6.5 DC CONDUCTIVITY STUDIES

Of the electrical properties of materials, dc conductivity is one of the parameters that can be easily evaluated. This parameter has the advantage that it can be measured in wide range $(10^{-15}\,\Omega^{-1}cm^{-1}$ to $10^{6}\,\Omega^{-1}cm^{-1})$ with an appropriate measuring device like high impedance electrometer and a shielded cell. However, it has only limited application since the transient properties like dipolar orientation cannot be measured by this technique.

DC conductivity represents the flow of carriers across the sample in an applied dc field. This in turn depends on the mobility of carriers and the density of states associated with conduction. The temperature dependence of dc conductivity is given by

$$\sigma_{dc}(T) = \sigma_{o} \exp(\frac{-E_a}{2kT})$$

This means that the Arrhenius plot of dc conductivity is linear with a slope given by $E_a/2k$ This linear dependence is expected in cases where the medium is homogeneous, eg., a crystalline phase. With disordered semiconductors the dependence of σ_{dc} on temperature assumes

a different format. A typical treatment is given by Austin and Mott.[20] When the charge carriers undergo variable hopping σ_{dc} is given by,

$$\sigma_{dc}(T) = \left\{ 0.39[N(E_F)\alpha K_B T]^{\frac{1}{2}} \nu_o e^2 \right\} \exp-(T_o/T)^{\frac{1}{4}}$$

where $T_o = 16\alpha^3/K_B N(E_F)$

α^{-1} - decaylength of the localised state

ν_o - hopping attempt frequency

$N(E_F)$ - the density of states at the Fermi energy E_p

e - electronic charge

k_B - Boltzmann constant

Thus the nature of dependence of σ_{dc} on temperature is a diagnostic criterion for the mechanism of conduction.

6.5.1 Results and discussion

The dc conductivity data for pristine and iodine-doped MPc were plotted in the log σ_{dc} vs. 1/T and log σ_{dc} vs. $T^{-\frac{1}{4}}$ formats. Figs.6.4-6.6 and 6.7-6.9 represent the plot of log σ_{dc} vs. 1/T and log σ_{dc} vs. $T^{-\frac{1}{4}}$ respectively.

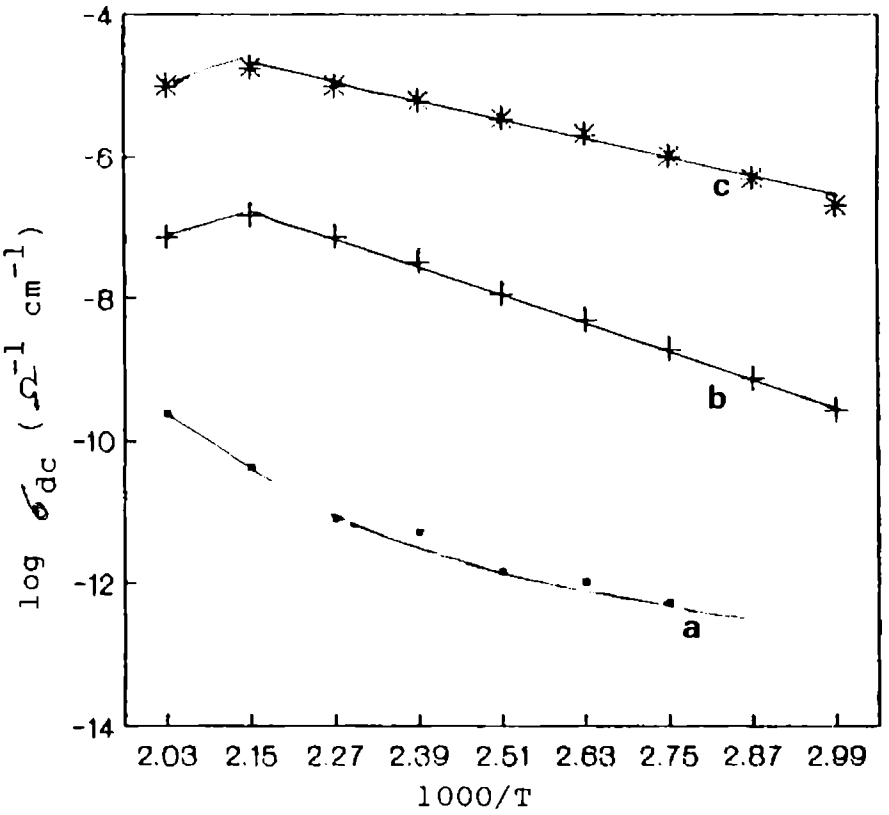

Fig.6.4: Plot of log σ_{dc} versus 1/T for NiPc and $Ni(Pc)I_x$

a - NiPc b - $Ni(Pc)I_{0.2}$ c - $Ni(Pc)I_{0.4}$

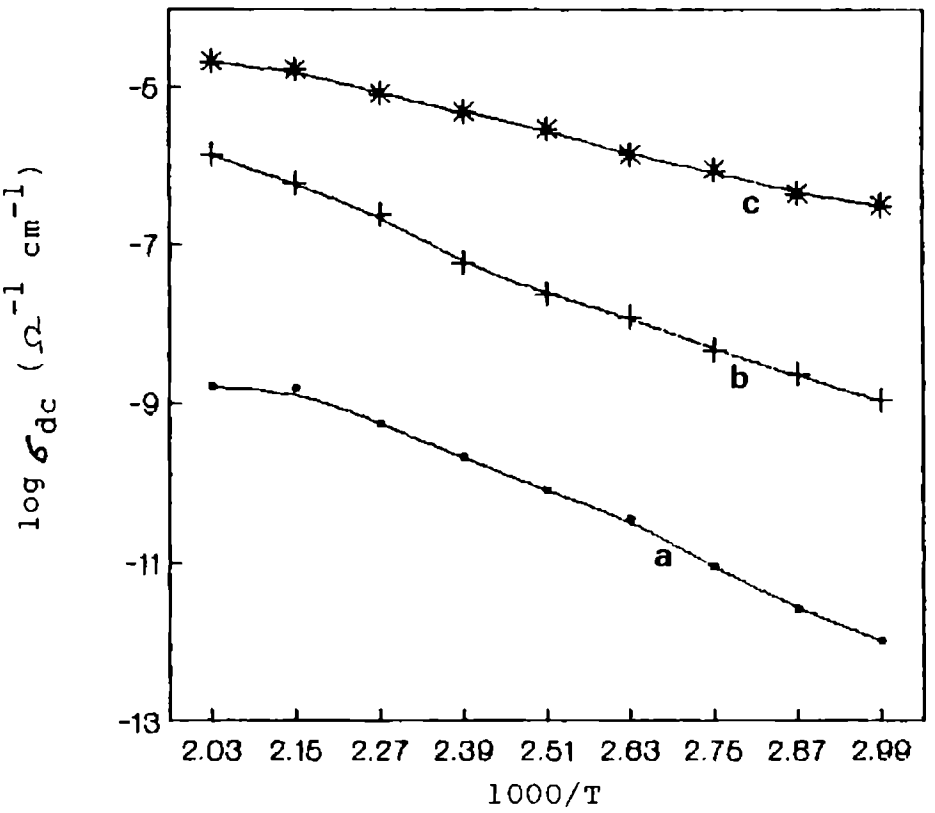

Fig.6.5: Plot of log σ_{dc} versus 1/T for CoPc and $Co(Pc)I_x$

a - CoPc b - $Co(Pc)I_{0.2}$ c - $Co(Pc)I_{0.4}$

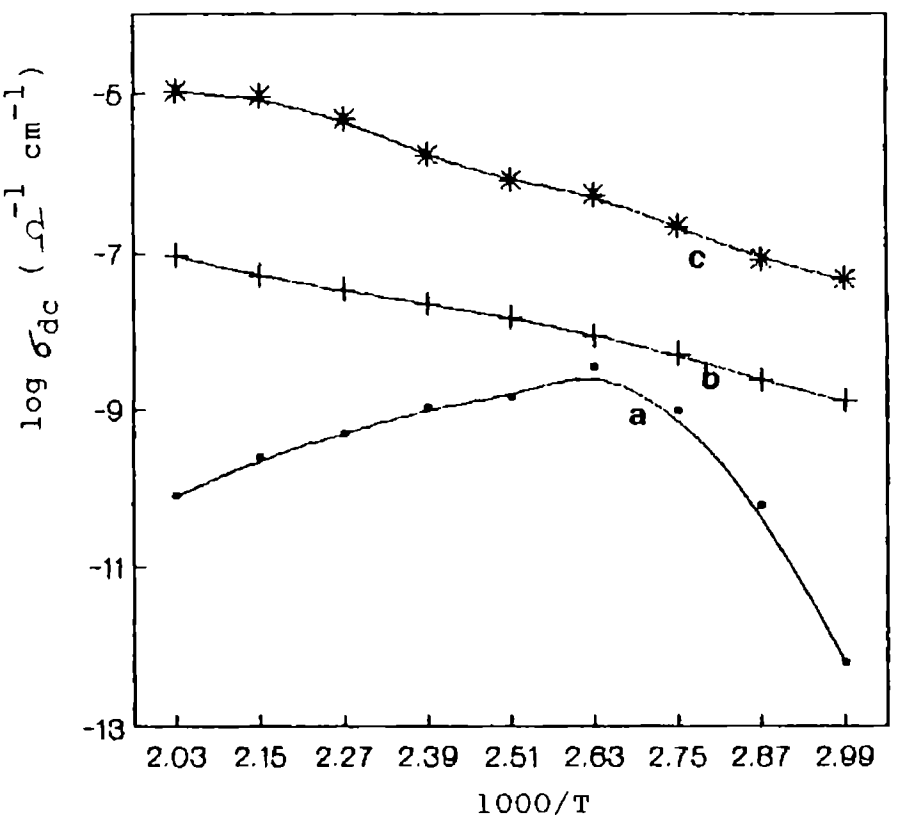

Fig.6.6: Plot of log σ_{dc} versus 1/T for CuPc and $Cu(Pc)I_x$

a - CuPc b - $Cu(Pc)I_{0.2}$ c - $Cu(Pc)I_{0.4}$

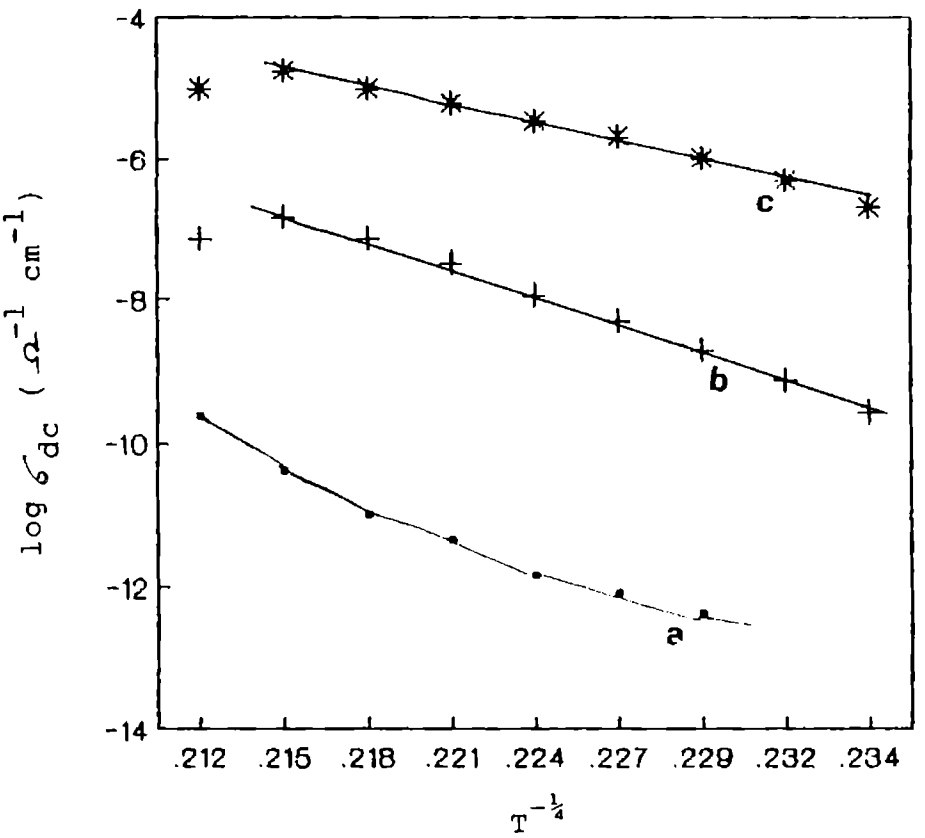

Fig.6.7: Plot of log σ_{dc} versus $T^{-\frac{1}{4}}$ for NiPc and $Ni(Pc)I_x$

a - NiPc b - $Ni(Pc)I_{0.2}$ c - $Ni(Pc)I_{0.4}$

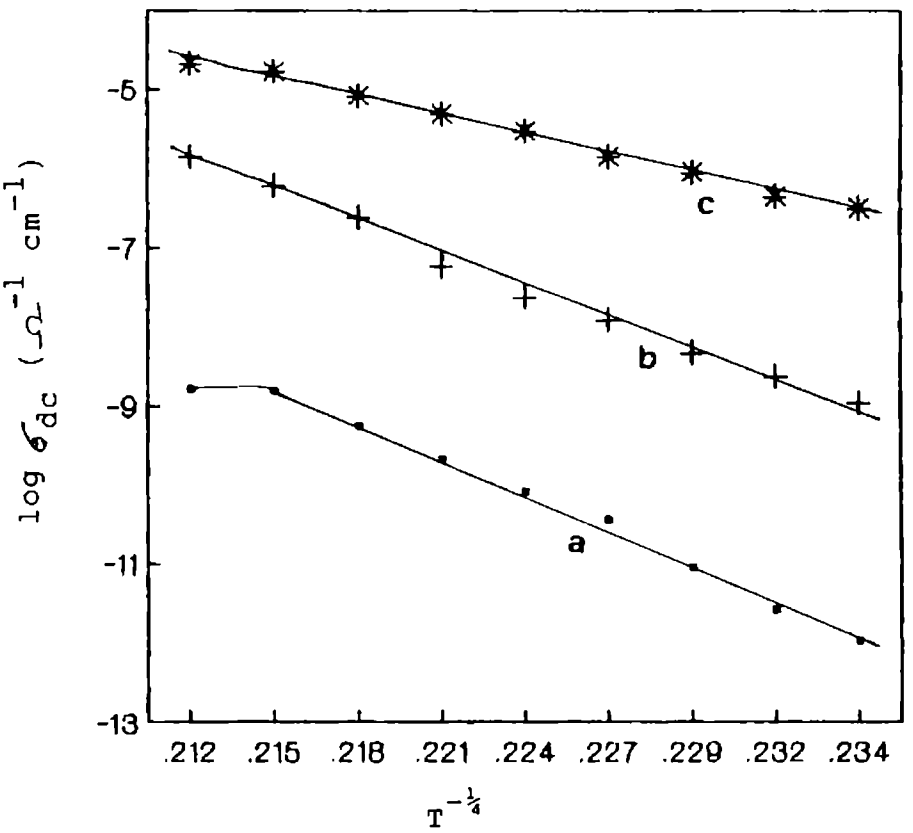

Fig.6.8: Plot of log σ_{dc} versus $T^{-\frac{1}{4}}$ for CoPc and $Co(Pc)I_x$

a - CoPc b - $Co(Pc)I_{0.2}$ c - $Co(Pc)I_{0.4}$

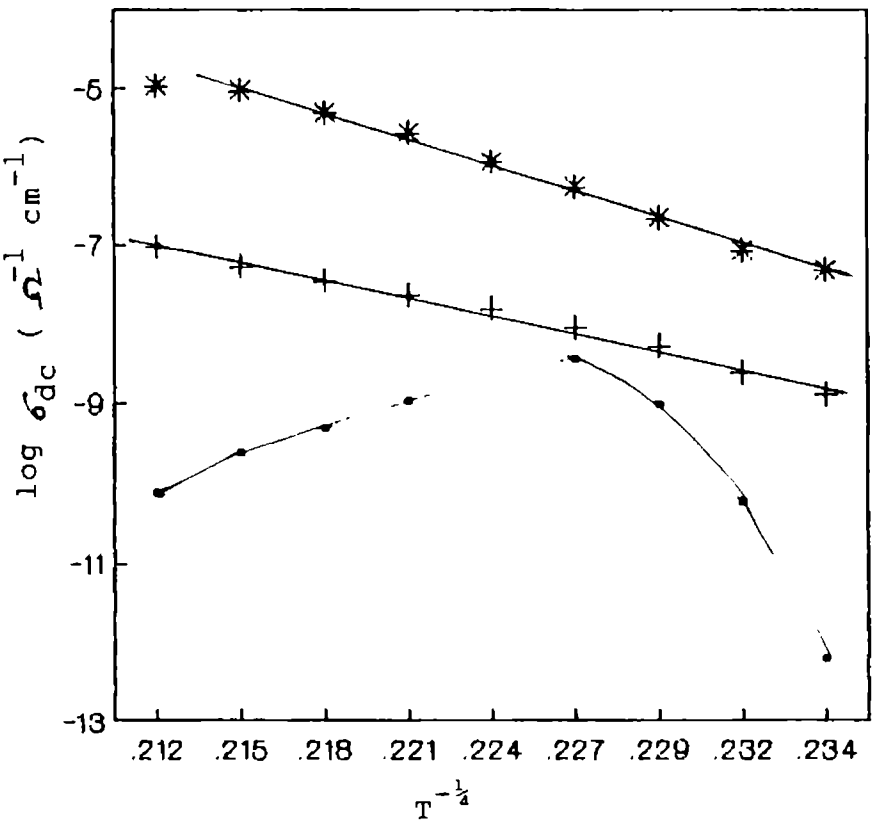

Fig.6.9: Plot of log σ_{dc} versus $T^{-\frac{1}{4}}$ for CuPc and $Cu(Pc)I_x$

a - CuPc b - $Cu(Pc)I_{0.2}$ c - $Cu(Pc)I_{0.4}$

CoPc and NiPc give Arrhenius plots which are almost linear. The activation energy decreases with increasing dopant concentration. Pristine CuPc shows a break in the plot, the nearly straight line arms intersecting at $\sim$ 100°C temperature in air. This has been attributed to the desorption of oxygen.[21] Doping with iodine desorbs oxygen and Cu(Pc)I samples show Arrhenius behaviour. When the dc conductivity data were plotted using the equation corresponding to variable-range-hopping better linear fit is observed, especially, for iodinated samples. This supports the existence of islands of more conductive phase embedded in a less conductive matrix of undoped MPc.[22] This is true of all the three metal phthalocyanines studied. It may also be noted that the dopant concentration was not raised to a level where truly metallic conduction sets in.

The dc conductivity, parameters are presented in Table 6.1. The values show that activation energy decreases with increase in dopant concentration in the case of Ni(Pc)I and Co(Pc)I whereas the activation energy increases with dopant concentration for Cu(Pc)I. The lower conductivity observed at higher dopant levels for Cu(Pc)I may be due to the effect of residual oxygen present in Cu(Pc)I.

Table 6.1 DC conductivity parameters of pristine and iodine-doped phthalocyanine.

Material	σ_{dc} (300 K) Ω^{-1} cm^{-1}	E_a eV
NiPc	3.4×10^{-13}	0.63
$Ni(Pc)I_{0.2}$	5.7×10^{-10}	0.57
$Ni(Pc)I_{0.4}$	7.0×10^{-7}	0.38
CoPc	9.8×10^{-12}	0.69
$Co(Pc)I_{0.2}$	4.7×10^{-9}	0.54
$Co(Pc)I_{0.4}$	3.2×10^{-7}	0.42
CuPc	2.0×10^{-13}	
$Cu(Pc)I_{0.2}$	9.0×10^{-9}	0.36
$Cu(Pc)I_{0.4}$	3.4×10^{-8}	0.54

6.6 AC CONDUCTIVITY STUDIES

The ac conductivity of any sample is a combination of two contributions, namely σ_{ac} of the resistor and the ac admittance of the capacitive component. The contribution of the capacitive component depends on the dielectric properties of the material. Any change in the character of the material affecting its polarizability will be exhibited in σ_{ac} measurements.

6.6.1 Results and discussion

The ac conductivity of pristine and iodine-doped samples of Ni, Co and CuPc was studied in the frequency range 10 kHz to 1 MHz. The results of ac conductivity measured as a function of frequency at 28 ± 2°C are presented in Fig.6.10 to 6.12. In all the cases it is seen that with pristine samples broad humps are observed in the frequency range studied. This is not due to the moisture effect since the samples were annealed at 100°C in nitrogen atmosphere before measurement. Ni(Pc)I is unique in that at higher doping level the plot correspond to truly metallic conduction.

The plot of log σ_{ac} vs. 1/T yield some very interesting results. The variation of σ_{ac} with T at selected frequencies for NiPc and Ni(Pc)I is illustrated in Fig.6.13. At all the three frequencies ie., 40 kHz, 400 kHz and 1 MHz, the pristine samples show only very broad humps due to relaxations. Doping enhances the conductivity and the doped samples show a reproducable hump at a higher frequency. The enhancement of ac conductivity in doped samples may be due to enhanced carrier generation as well as due to capacitive coupling. In the case of CoPc

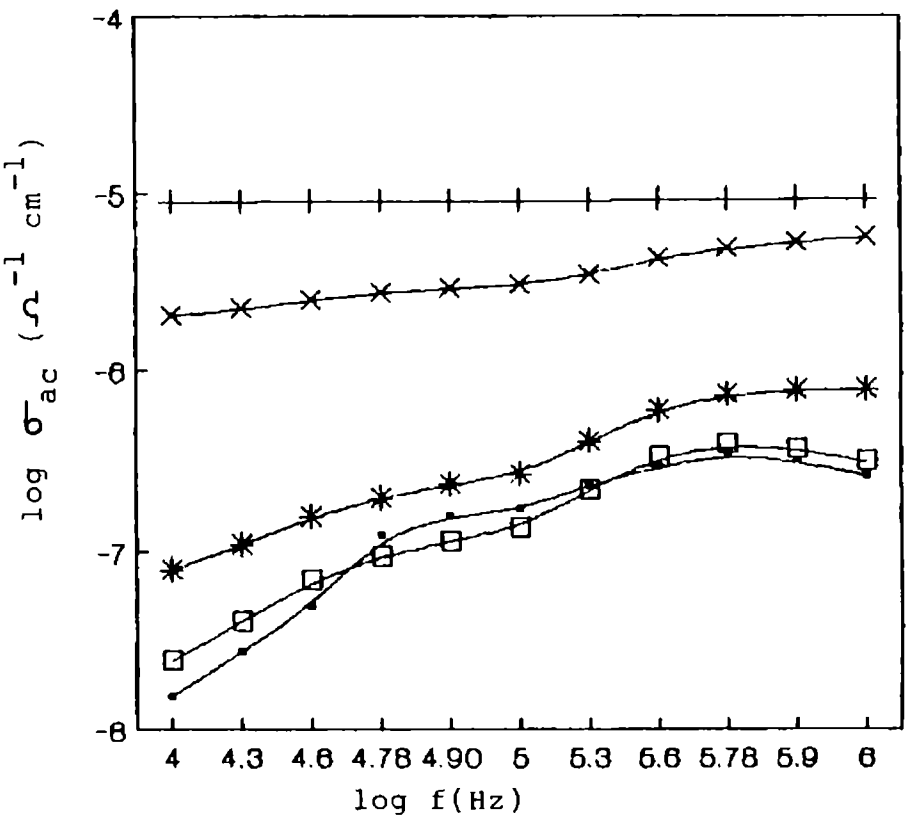

Fig.6.10: Plot of log σ_{ac} versus log f for NiPc and $Ni(Pc)I_x$

NiPc

$Ni(Pc)I_{0.1}$

$Ni(Pc)I_{0.2}$

$Ni(Pc)I_{0.4}$

$Ni(Pc)I_{0.5}$

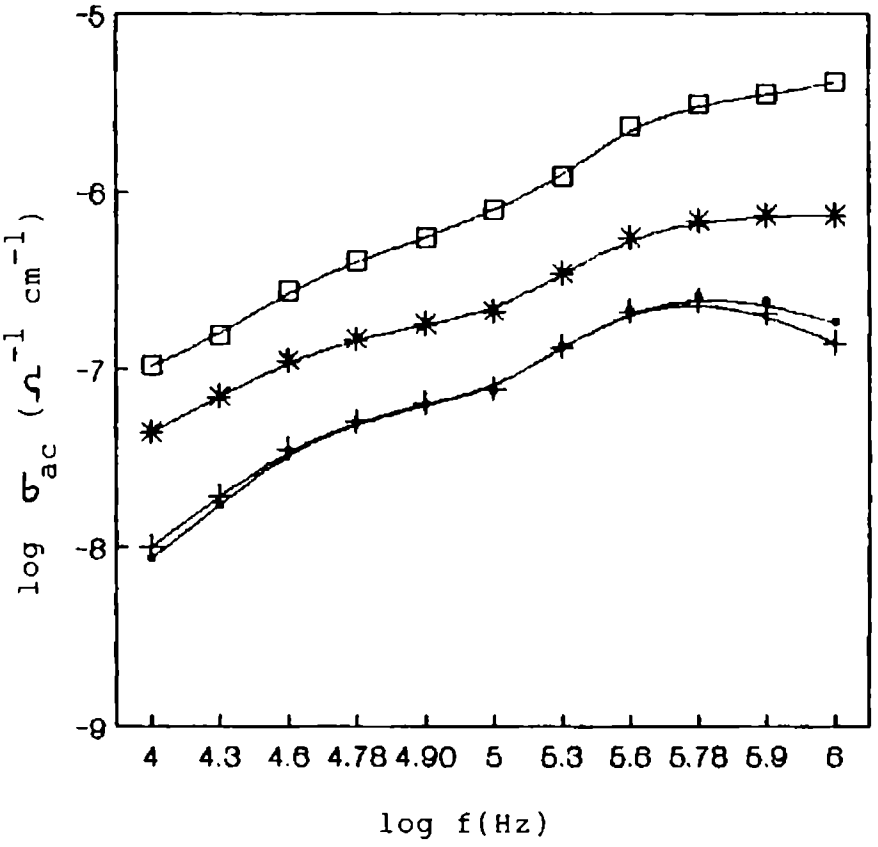

Fig.6.11: Plot of log σ_{ac} versus log f for CoPc and $Co(Pc)I_x$

—•— CoPc —+— $Co(Pc)I_{0.1}$

—×— $Co(Pc)I_{0.2}$ —□— $Co(Pc)I_{0.4}$

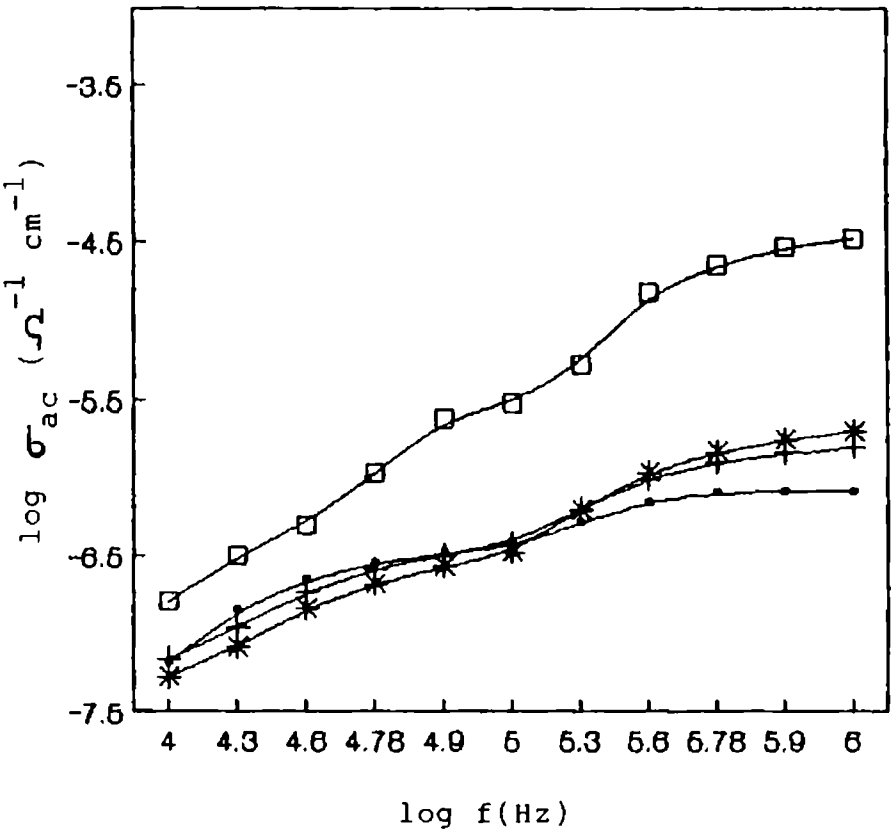

Fig.6.12: Plot of log σ_{ac} versus log f for CuPC and $Cu(Pc)I_x$

CuPc $Cu(Pc)I_{0.1}$

$Cu(Pc)I_{0.2}$ $Cu(Pc)I_{0.4}$

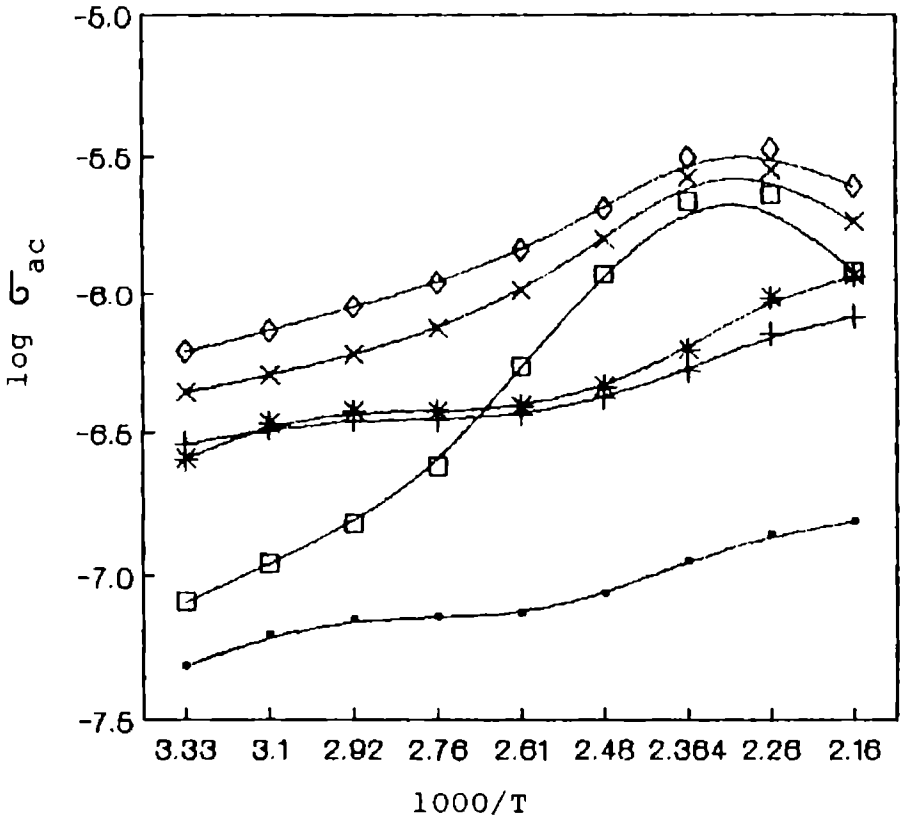

Fig.6.13: Plot of log σ_{ac} versus T^{-1} at different frequencies for NiPc and $Ni(Pc)I_{0.4}$

NiPc 40 kHz — NiPc 400 kHz

NiPc 1 MHz — $Ni(Pc)I_{0.4}$ 40 kHz

$Ni(Pc)I_{0.4}$ 400 kHz — $Ni(Pc)I_{0.4}$ 1 MHz

(Fig.6.14) the plots have a better defined feature. Doping enhances σ_{ac} but the features of the plot remain more or less the same. The most interesting features are observed with CuPc. Fig.6.15 shows that an increase in temperature enhances the conductivity of pristine samples, the conductivity reaches a maximum at around 90 to 110°C and then decreases. The initial increase in conductivity on heating may be due to thermal activation but the decrease is likely to be due to the loss of chemisorbed oxygen. This confirms the observation of Harrison et al.[23] on the chemisorption of oxygen by CuPc. In iodine-doped samples the oxygen effect is weaker probably due to the displacement of adsorbed oxygen upon doping.

6.7 DIELECTRIC CONSTANT

In dielectric constant measurement the sample is sandwiched between two electrodes as a dielectric and the assembly is equivalent to a capacitor. Any dipolar relaxation induced by an ac field contributes to the dielectric constant of the material. Thus dielectric constant measurement is a useful technique to detect the dielectric relaxation taking place in the time scale of the applied frequency. At a fixed frequency the variation of thermally induced dielectric relaxation can be monitored. In quasi-

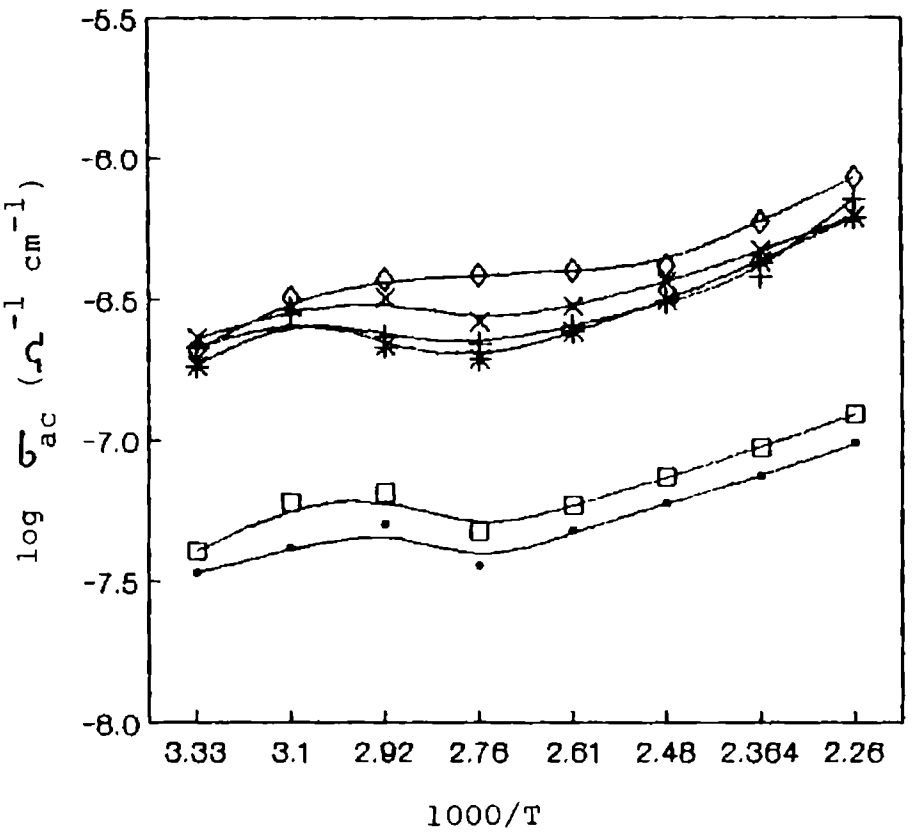

Fig.6.14: Plot of log σ_{ac} versus T^{-1} at different frequencies for CoPc and $Co(Pc)I_{0.4}$.

CoPc 40 kHz — CoPc 400 kHz

CoPc 1 MHz — $Co(Pc)I_{0.4}$ 40 kHz

$Co(Pc)I_{0.4}$ 400 kHz — $Co(Pc)I_{0.4}$ 1 MHz

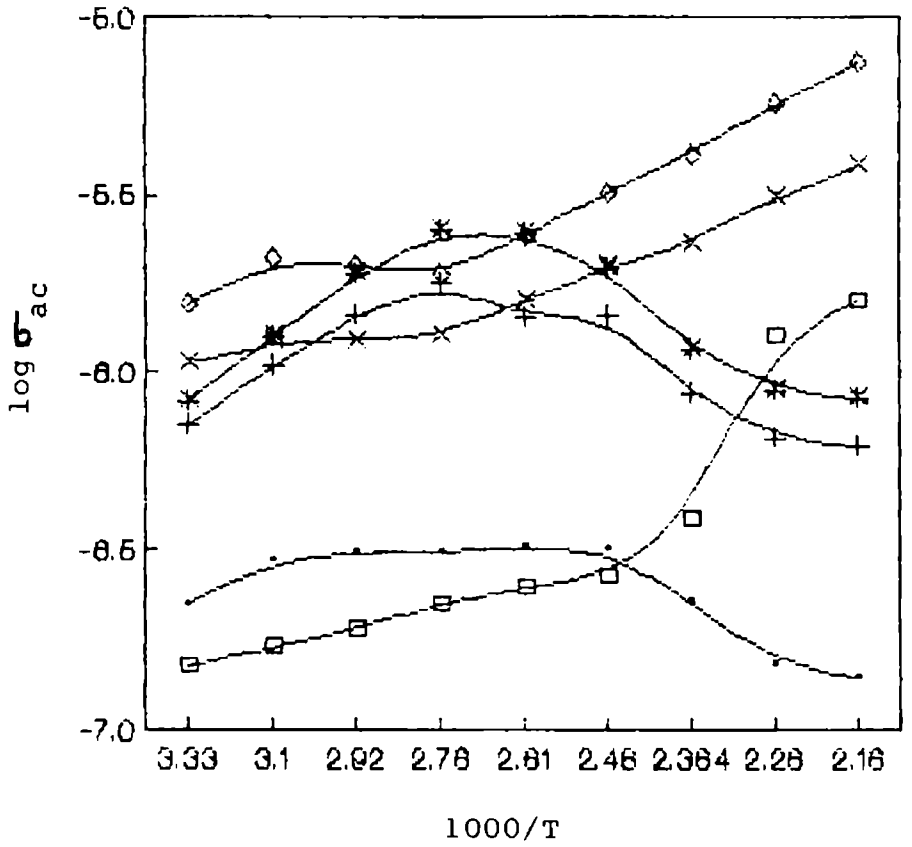

Fig.6.15: Plot of log σ_{ac} versus T^{-1} at different frequencies for CuPc and $Cu(Pc)I_{0.4}$

CuPc 40 kHz
CuPc 400 kHz
CuPc 1 MHz
$Cu(Pc)I_{0.4}$ 40 kHz
$Cu(Pc)I_{0.4}$ 400 kHz
$Cu(Pc)I_{0.4}$ 1 MHz

one-dimensional systems the groups/molecules/ions involved are either massive or are in an unfavourable environment for fast relaxation. Hence the dielectric processes are likely to occur atlow and moderate frequencies.

The plots of dielectric constant as a function of frequency are presented in Figs.6.16-6.18. In all the cases the pristine samples and samples with low dopant concentration have only low values for dielectric constant in the whole frequency range. In the case of NiPc the low frequency contribution to dielectric constant is very large at higher dopant concentration, which is characteristic of the induction of more charge carriers.[24] In the case of CoPc also doping enhances ϵ especially at higher dopant concentration. Here also the low frequency contribution is high, but is much less than that in NiPc. The plots for Cu(Pc)I are unique in the sense that the ratios of the low and high frequency contributions are relatively large. At the same time doping does not appreciably change the nature of the plot. This may be due to the fact that the dopant iodine and chemisorbed dioxygen play nearly the same role as far as CuPc is considered.

The dielectric constant of the materials at different frequencies as a function of temperature are

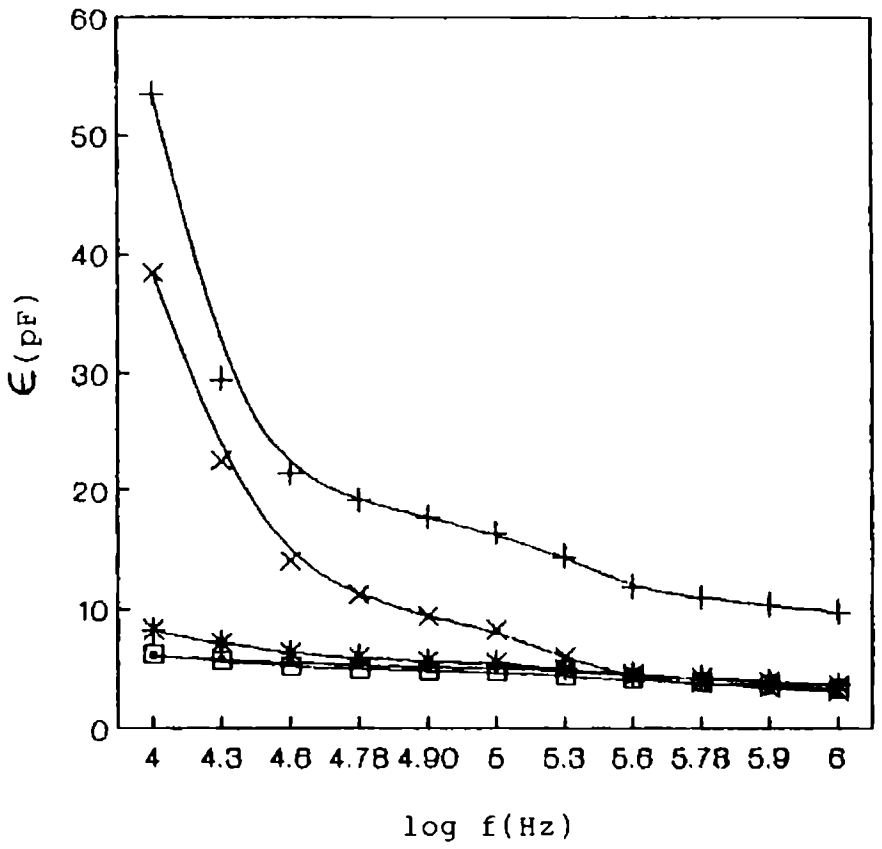

Fig.6.16: Plot of dielectric constant versus log f for NiPc and $Ni(Pc)I_x$

NiPc
$Ni(Pc)I_{0.1}$
$Ni(Pc)I_{0.2}$
$Ni(Pc)I_{0.4}$
$Ni(Pc)I_{0.5}$

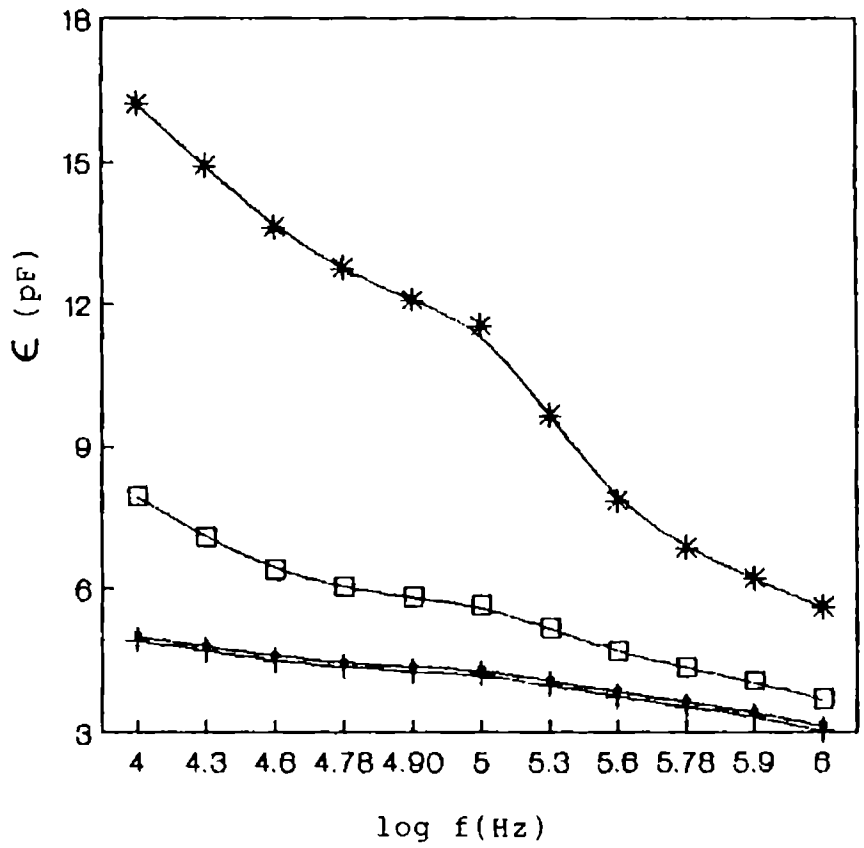

Fig.6.17: Plot of dielectric constant versus log f for CoPc and $Co(Pc)I_x$

CoPc $Co(Pc)I_{0.1}$

$Co(Pc)I_{0.2}$ $Co(Pc)I_{0.4}$

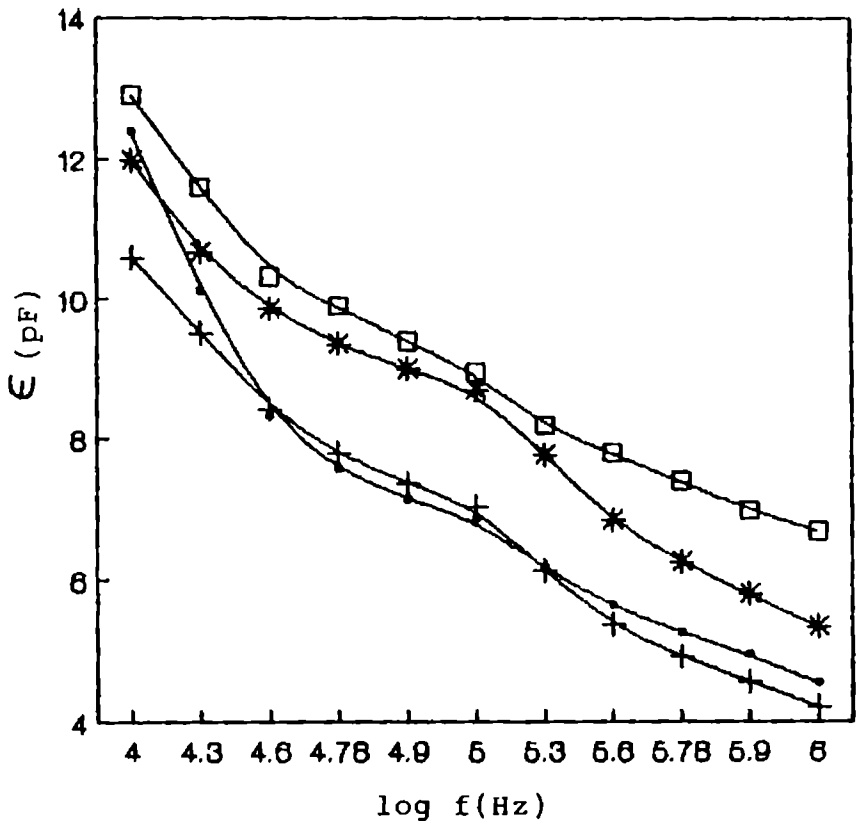

Fig.6.18: Plot of dielectric constant versus log f for CuPc and $Cu(Pc)I_x$

CuPc
$Cu(Pc)I_{0.1}$
$Cu(Pc)I_{0.2}$
$Cu(Pc)I_{0.4}$

presented in Figs.6.19-6.21. In all the cases it is found that the dielectric constant increases with increasing temperature indicating thermal activation of the dielectric processes in the case of CuPc. In the case of CoPc also the behaviour is similar to that of nickel except that the dispersion peak becomes more defined at lower frequencies for the doped samples.

The dielectric constant varies as a function of temperature for CuPc and has a very distinct feature. Pristine CuPc shows a dielectric peak (40 kHz) around 90-110°C which disappear on doping. It is a very clear case of the influence of iodine on the displacement chemisorbed dioxygen. These results show that measurement of dielectric constant at low frequencies is a useful probe to detect the presence of dioxygen in CuPc.

6.8 CONCLUSION

The dc and ac conductivity and dielectric constant measurements with pristine Ni, Co and CuPc and their iodine-doped forms show distinct features. All the three measurements clearly make out the influence of oxygen on the electrical properties of CuPc. Doping with iodine

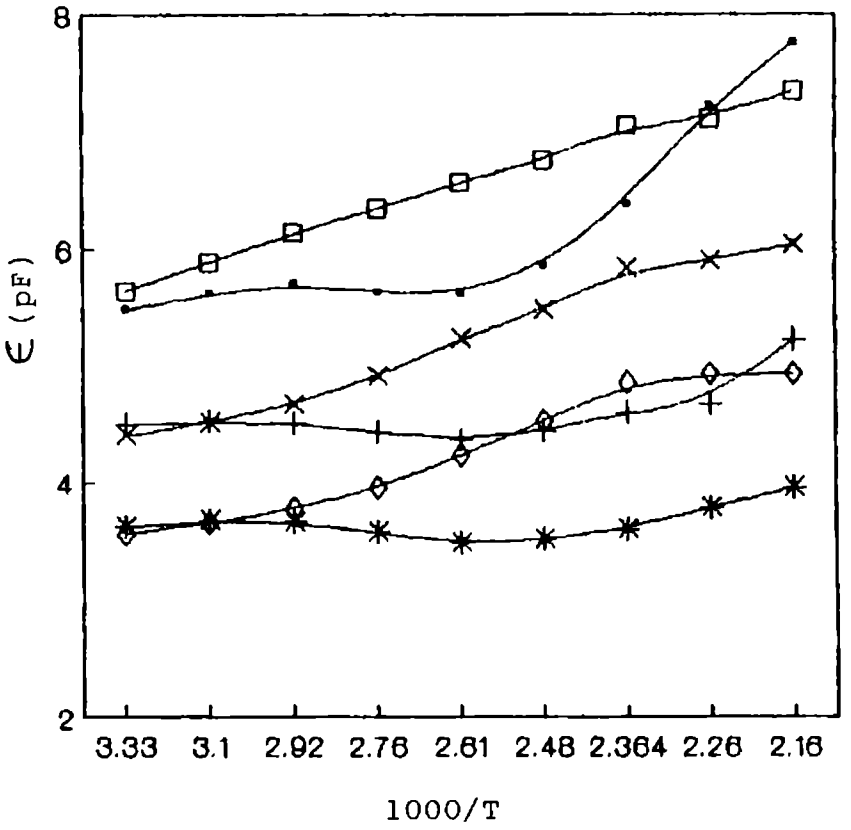

Fig.6.19: Plot of dielectric constant versus T^{-1} for NiPc and $Ni(Pc)I_{0.4}$ at different frequencies.

NiPc 40 kHz
NiPc 400 kHz
NiPc 1 MHz
$Ni(Pc)I_{0.4}$ 40 kHz
$Ni(Pc)I_{0.4}$ 400 kHz
$Ni(Pc)I_{0.4}$ 1 MHz

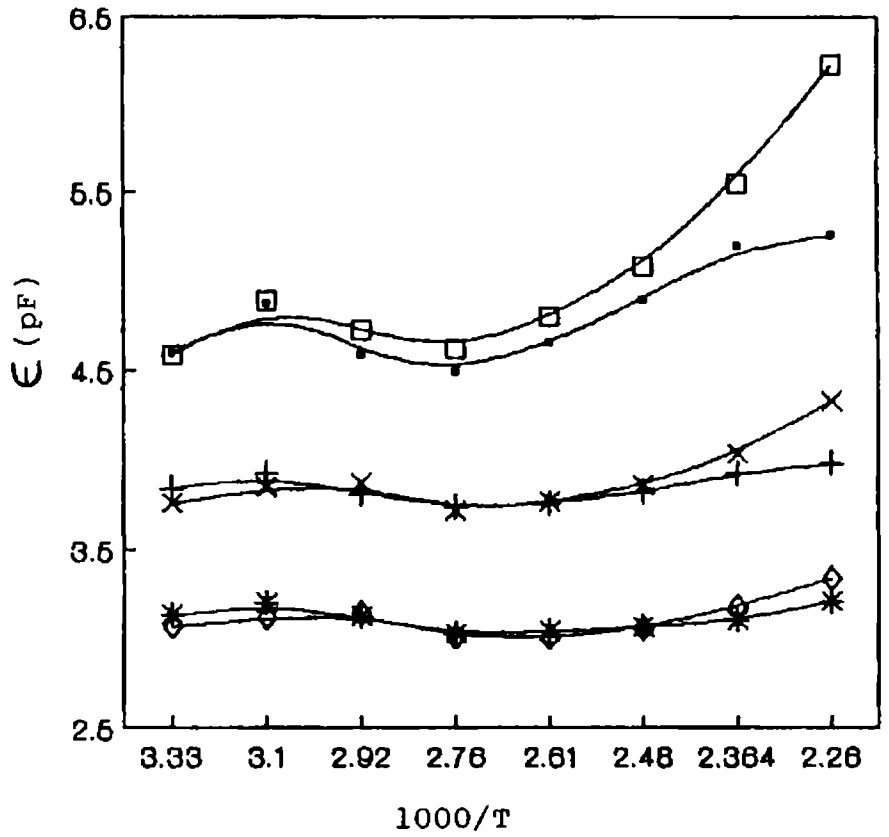

Fig.6.20: Plot of dielectric constant versus T^{-1} for CoPc and $Co(Pc)I_{0.4}$ at different frequencies.

CoPc 40 kHz
CoPc 400 kHz
CoPc 1 MHz
$Co(Pc)I_{0.4}$ 40 kHz
$Co(Pc)I_{0.4}$ 400 kHz
$Co(Pc)I_{0.4}$ 1 MHz

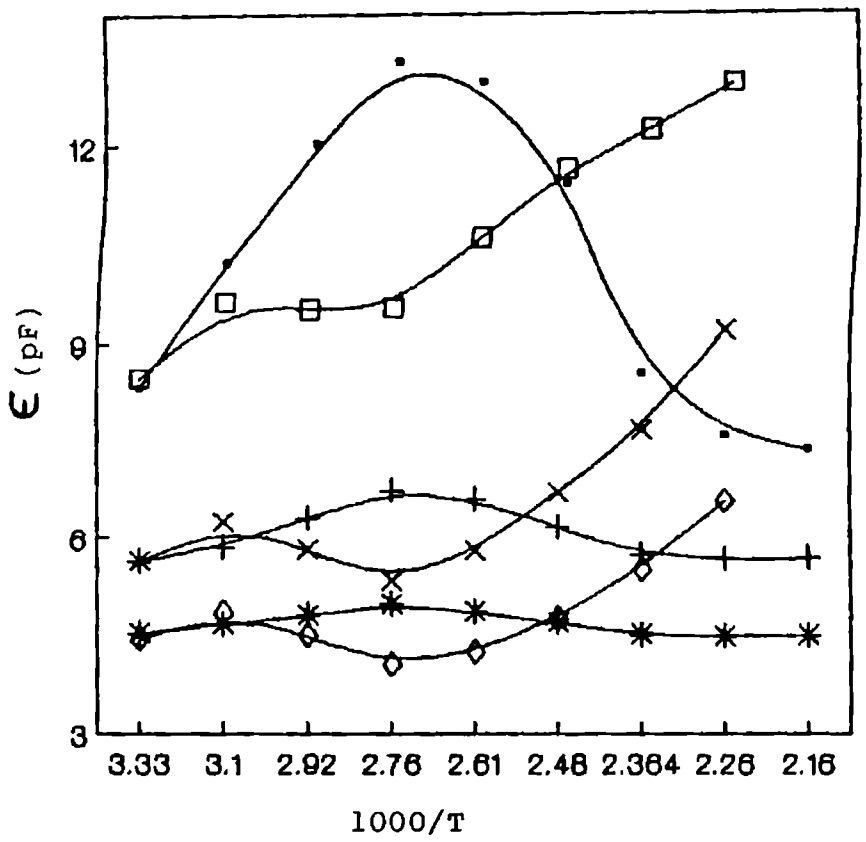

Fig.6.21: Plot of dielectric constant versus T^{-1} for CuPc and $Cu(Pc)I_{0.4}$ at different frequencies.

CuPc 40 kHz — CuPc 400 kHz

CuPc 1 MHz — $Cu(Pc)I_{0.4}$ 40 kHz

$Cu(Pc)I_{0.4}$ 400 kHz — $Cu(Pc)I_{0.4}$ 1 MHz

alleviate the influence of adsorbed oxygen on CuPc. With NiPc and CoPc dioxygen does not influence the measurements. In all the cases doping with iodine enhances the dielectric constant and conductivity. Only in the case of NiPc, iodine doping gives rise to metallic behaviour as indicated by ac measurements. However, dc measurements indicate a mechanism of charge-transport involving variable-range-hopping of charge carriers.

REFERENCES

1. Vartanyan, A.T. Zh. fiz. Kleimei 1948, 22, 769.

2. Vartanyan, A.T.; Karpovich, I.A. DAN SSSR 1956, 111, 561.

3. Vartanyan, A.T. DAN SSSR, Seriya fiz. 1956, 1541.

4. Vartanyan, A.T. DAN SSSR, 1963, 153, 70.

5. Terenin, A.N. Zhurnal VKhO in D.I. Mendeleeva 1960, 5, 498.

6. Arnold, V., McLeigh, E. in Structure and Functions of Photosynthetic Apparatus, IL Publishers, Moscow, 1962, 9.

7. Skotheim, T.A., Ed. Marcel Dekker, Handbook of Conducting Polymers, INC, New York, 1986.

8. Shorin, V.A.; Meshkova, G.N.; Vartanyan, A.T.; Pribytkova, N.N., Alyanov, M.I.; Borodkin, V.F. Izv. vuzou. Khimiya i khim. tekhnol. 1973, 16, 1904.

9. Martynenko, A.P., Shorin, V.A.; Borodkin, V.F.; Alyanov, M.A. Izv. vuzov khimiya i khim, tekhnol. 1973, 16, 1904.

10. Hamann, C. Phys. Status Solidi 1967, 20, 481.

11. Felmayer, W.; Wolf, J. J. Electrochem. Soc. 1958, 105, 141.

12. Danzig, M.; Liang, C.; Passaglia, E. J. Am. Chem. Soc. 1963, 85, 668.

13. Koifman, O.I.; Zemlyanaya, N.G.; Alyanov, M.I.; Larionov, V. Izv. vuzov. khimiya i khim. tekhnol. 1975, 18, 1644.

14. Linstead, R.P.; Robertson, J.M. J. Chim. Soc. 1936, 1195 and 1636.

15. Wihksue, K.; Newkirk, A.E. J. Chem. Phys. 1961, 34, 2184.

16. Fielding, P.E.; Gutman, F. J. Chem. Phys. 1957, 26, 411.

17. Pelletier, S.W.; Parthasarathy, P.C. J. Am. Chem. Soc. 1965, 87, 777.

18. Martinsen, J.; Stanton; Greene, R.L.; Tanaka, J.; Hoffman, B.M.; Ibers, J.A.; J. Am. Chem. Soc., 1985, 107, 6915.

19. Drago, S.R. Physical Methods in Chemistry, W.B. Saunders Company, London, 119.

20. Mott, N.F., Davis E.A. Electronic Processes in Non-Crystalline Materials, Clarendon Press, Oxford, 1979.

21. Boreskov, G.K.; Keier, N.P.; Rubstsova, L.F.; Rukhadze, E.G. Dokl. Akad. Nauk SSSR, 1962, 144, 1069.

22. Springett, B.E. Phys. Rev. Lett. 1973, 31, 1463.

23. Harrison, S.E.; Landewig, K.H. J. Chem. Phys. 1966, 45, 343.

24. Grant, P.M.; Krounbi, M. Solid State Commun. 1980, 36, 291.

CHAPTER -VII

SUMMARY AND CONCLUSION

Metal phthalocyanines have some unique optical properties which are exploited for dyeing fibers and films used in applications like dye lasing and optical information storage. Aggregation of dye molecules modifies their absorption and emission spectra with concomitant degradation in their energy transfer characteristics. MPcs as such have poor processability and are seldom used in solid matrices. The finest energy transfer characteristics are shown by the monomers of metal phthalocyanines. In the third chapter of this thesis the studies on two series of metal phthalocyanines are reported. The first one constitutes 4,4',4",4"'-tetrakis(n-dodecanoylamino) derivatives of Ni(II), Co(II) and Cu(II)phthalocyanines. The introduction of n-dodecanoylamido group enhances their solubility in non-polar solvents like $CHCl_3$ and CH_2Cl_2, thus making them easily processable by diffusion from solution or by spin coating of a solution containing a polymer. These derivatives of phthalocyanines are having a melting point in the range 75-80°C. The visible absorption spectra indicate that all the three dodecylamido derivatives of MPcs exist as dimers in $CHCl_3$. The blue-shifting and broadening of the Q band in the spectra of these derivatives indicate H-type aggregation in solution.

Addition of DMF leads to dissociation of dimers to monomers. In DMF/$CHCl_3$ (4% v/v) at 28±2°C the dimerization constants are $\sim 10^4$ l mol^{-1}. The central metal atom exerts only a very small influence on dimerization constant.

The n-octadecanoylamido derivatives also form H-type aggregates. However, the melting points are much lower (53-55°C) than those of the corresponding dodecanoyl derivatives. All the octadecylamido derivatives of phthalocyanines reported here exist as dimers in $CHCl_3$/DMF solution. The tendency of the octadecanoyl derivative of CoPc(CoOAPc) to form monomer on the addition of DMF may be due to the axial coordination possible for cobalt with DMF. Increasing the length of the substituent alkyl chain leads to suppression of the tendency to exist as monomers. These results indicate that the dodecanoyl derivatives are superior to octadecanoyl derivatives for applications where the existence of the monomer in solution is desirable.

The results of studies carried out on water soluble phthalocyanines are presented in chapter 4. The only class of phthalocyanines that has found wide spread application in aqueous medium is the tetrasulfonato derivatives which are known to exist as dimer in aqueous

medium. Three types of soluble CoPc derivatives have been synthesized and investigated by incorporating the groups, $-SO_2NHCH_2CH_2NH_2$, $-SO_2NHC_6H_4SO_3H$ and $-NH_2$, $-SO_3H$. Only the properties of the derivatives of CoPc have been investigated as a typical case. All the three derivatives establish a measurable monomer-dimer equilibrium in ethanol/water (20% v/v). Conversion of the dimer to monomer is complete when ethanol concentration exceeds 30% v/v. The aminosulfonato derivative show some interesting features. Dilution or ethanol addition does not affect the spectrum of this derivative. Also dilution over a wide range does not affect the adherence to Beer-Lamberts law. These indicate that the aminosulfonato derivative exists only as a monomer probably by zwitter ion formation between the amino and sulfonic acid groups. The strong solvation of the zwitter ion may hinder the formation of an H-type dimer normally observed in phthalocyanines. Thus it is found that diffusion of the above CoPc derivative from an aqueous-ethanolic medium or of the aminosulfonic acid derivative from aqueous medium is favourable for the incorporation of its monomer into various matrices. When these derivatives are incorporated into PVA from an aqueous solution and cast into films

crosslinked with glutaraldehyde, only the dimer form of the dye is present as indicated by the absorption spectra.

Iodine-doped MPcs show enhanced electrical conductivity. In iodinated MPcs iodine is irreversibly bound to the Pc stacks. The identity of the iodine molecule is more complex than that in a simple CT complex. Studies have indicated that oxidation of metal or phthalocyanine ring can take place with iodine in such adducts. In an effort to exploit the processability, conductivity and charge storage properties of iodinated MPcs, electrochemical characteristics of an all-solid galvanic cell of the configuration Ag/AgI/M(Pc)I was studied. The cell shows an open circuit voltage of 600 mV. With discharge current density less than about 0.3 A/cm^2 the cell gives a steady closed circuit voltage of 500 mV and a discharge of 80 coulombs per gram of M(Pc)I. The low limiting discharge current density may be due to the low mobility of Ag^+ ions in the AgI phase used and the consequent concentration polarization. Such cells find application in supporting the memory of computers.

Iodinated MPcs are found to give interesting electrical properties as well. The electrical properties

of iodinated Ni, Co and CuPc have been investigated for different dopant concentrations as a function of temperature as well as frequency. The conductivity of Ni(Pc)I reaches the metallic regime though with a lower magnitude than true metals. In all the cases the conductivity increases with increasing dopant concentration. Co(Pc)I is a metal spine conductor, whereas in Ni(Pc)I and Cu(Pc)I conduction occurs through the charge carriers generated by the partial oxidation of phthalocyanine ring. In all the cases it is reasonable to conclude that the oxidized Pc moieties are embedded in the less conductive non-oxidised phase and a thermally activated conduction occurs with variable-range-hopping mechanism. The frequency dependent variation of conductivity of Ni(Pc)I indicates that this material is more "metallic" than the other two materials.

A part of the work presented in this thesis has been published in journals/presented in conferences/ communicated in the following forms:

1. Cyclic voltammetric studies on plasma treated cobalt phthalocyanine, P.S.Harikumar, P.Narayanan and V.N.Sivasankara Pillai, Journal of Material Science Letters, 8(8), 969 (1989).

2. Synthesis and aggregation of nickel 4,4',4",4"'-tetrakis (n-dodecanoylamino)phthalocyanine, P.Narayanan and V.N.Sivasankara Pillai, Seminar on Photochemistry, Laser Chemistry and Photobiology, 7-9 January, 1991, Madras.

3. Electrical conductivity of quinoxaline-bridged metal phthalocyanine, P.Narayanan and V.N.Sivasankara Pillai, accepted for presentation, National Seminar on Solid State Chemistry and Allied Areas, January 1991, Nagpur.

4. Cyclic voltammetric studies on plasma treated coblat phthalocyanine, P.S.Harikumar, P.Narayanan and V.N.Sivasankara Pillai, First National Conference on Electrocatalysis, 28-29, January, 1987, Baroda.

5. Fabrication of a cell suitable for electrochemical studies on solids at elevated temperature, P.Narayanan and V.N.Sivasankara Pillai, National Symposium on Instrumentation, 26-29 November, 1991, Cochin.

6. Synthesis and aggregation of 4,4',4",4"'-tetra(1-aminoethyl sulfonamido)phthalocyanine Co(II), P.Narayanan, V.N.Sivasankara Pillai, (Communicated to Indian Journal of Technology).

7. Electrical properties of iodine-doped Co(II), Ni(II) and Cu(II)phthalocyanines, P.Narayanan and V.N.Sivasankara Pillai, (Communicated to Journal of Material Science Letters).

8. Performance of iodine-doped Co(II), Ni(II) and Cu(II) phthalocyanine as cathode material in solid state galvanic cell, P.Narayanan and V.N.Sivasankara Pillai, (Communicated to Bulletin of Electrochemistry).